COMMITTEE CERTIFICATION OF APPROVED VERSION

The committee for Tahani Khulaif Alshammari certifies that this is the approved version of the following dissertation:

DISRUPTION OF THE HIPPOCAMPAL GABAERGIC SYSTEM IN THE *Fgf14*$^{-/-}$ MOUSE MODEL

COMMITTEE:

_____

Fernanda Laezza, MD, Ph.D.
Supervisor

_____

Kenneth M. Johnson, Ph.D.

_____

Filippo Tempia, MD, Ph.D.

_____

Maria Micci, Ph.D.

_____

Thomas A. Green, Ph.D.

_____

David Niesel, Ph.D.
Dean, Texas Graduate School of Biomedical Sciences

DISRUPTION OF THE HIPPOCAMPAL GABAERGIC SYSTEM IN THE *Fgf14*$^{-/-}$ MOUSE MODEL

by

Tahani Khulaif Alshammari
Department of Pharmacology and Toxicology Graduate Program
University of Texas, Galveston Texas

Dissertation
Presented to the Faculty of The University of Texas Graduate School of Biomedical Sciences at Galveston
in Partial Fulfillment of the Requirements
for the Degree of

Doctor of Philosophy

Approved by the Supervisory Committee

Fernanda Laezza, MD, Ph.D.
Kenneth M. Johnson, Ph.D.
Filippo Tempia, MD/PhD
Maria Micci, Ph.D.
Thomas A. Green, Ph.D.

March, 2016
Galveston, Texas

© Copyright by Tahani Khulaif Alshammari, 2016
All Rights Reserved

DISRUPTION OF THE HIPPOCAMPAL GABAERGIC SYSTEM IN THE *Fgf14*$^{-/-}$MOUSE MODEL

Tahani Khulaif Alshammari

Department of Pharmacology and Toxicology Graduate Program
University of Texas, Galveston Texas

ABSTRACT

In CNS, cognitive function is greatly dependent on the functional integrity of gamma-amino-butyric acid (GABA) interneurons. These inhibitory interneurons modulate synaptic plasticity and intrinsic excitability of principal neurons balancing the excitatory/inhibitory ratio in the brain. Reduction in parvalbumin interneurons (PVIs) and GABAergic synapses function lead to desynchronized neuronal circuits associated with cognitive deficit across many neuropsychiatric diseases, such as schizophrenia. Yet, the mechanisms underlying the loss in PVIs and E/I imbalance are not completely understood. Here, I demonstrate that the genetic ablation of the intracellular fibroblast growth factor 14 (FGF14), a molecule required for proper neuronal development, excitability, synaptic plasticity and cognitive function, leads to a reduction in PVIs in the hippocampal CA1 area, accompanied by declined expression of GABAergic presynaptic components, the glutamic acid decarboxylase 67 (GAD67) and the vesicular GABA transporter (VGAT). In addition, the CA1 GABAergic inhibitory transmission is disrupted. These cellular phenotypes coincide with reduced *in vivo* oscillations at gamma wave, and spatial working memory deficit. Also, the bioinformatics studies of schizophrenia transcriptomics indicated a functional co-clustering of GABAergic genes and FGF14 with correlative decreased expression of *FGF14*, *PVALB*, *GAD67* and *VGAT*.

Next, I expand these studies to examine GABAergic postsynaptic proteins that are relevant

to cognitive impairment such as gephyrin, GABAA alpha-1, and alpha-2 receptor subunits. Interestingly, the results indicate genetic deletion of *Fgf14* exhibit fewer effects on GABAergic postsynaptic components. Suggesting a potential role of FGF14 in regulating the GABAergic pre and postsynaptic components.

Several lines of evidence support a neurodevelopmental hypothesis of schizophrenia. Although the neurodevelopmental model theory is fully appreciated, it is not well understood. So far, our studies suggest that *Fgf14*$^{-/-}$exhibits some of the aspects of schizophrenia. Thus, to provide a better understanding of putative developmental changes in *Fgf14*$^{-/-}$, I quantified the age-related changes in PV expression in the hippocampus. Our results indicate that genetic deletion of *Fgf14* might impairs the maturation of PVIs.

These findings suggest that *Fgf14*$^{-/-}$ mice exhibit molecular, cellular, functional, and developmental features associated with psychiatric disorders, and the loss of FGF14 function might be linked to the etiology of cognitive impairment and complex psychiatric disorders such as schizophrenia.

CONTENTS

LIST OF FIGURES

LIST OF TABLES

COMMITTEE

Fernanda Laezza, MD/Ph.D.
Associate Professor
Department of Pharmacology & Toxicology
Mitchell Center for Neurodegenerative Diseases
Graduate School of Biomedical Sciences
University of Texas Medical Branch

Kenneth M. Johnson, Ph.D.
Professor
Department of Pharmacology & Toxicology
Graduate Program Director
University of Texas Medical Branch

Filippo Tempia, MD/Ph.D.
Professor
Department of Neuroscience,
University of Torino

Maria Micci, Ph.D.
Associate Professor
Department of Anesthesiology
Graduate School of Biomedical Sciences
University of Texas Medical Branch

Thomas A. Green, Ph.D.
Assistant Professor
Department of Pharmacology & Toxicology
Center for Addiction Research
Graduate School of Biomedical Sciences
University of Texas Medical Branch

ACKNOWLEDGEMENTS

First and foremost, I want to express my gratitude to Allah for providing me the support, strength, and blessing to finish this work. I am grateful to him for giving me the opportunity to be here and do this work that hopefully will help people who suffer from brain disorders.

I want to express my appreciation to my parents for their continuous support and motivation. Although they never had the chance to pursue high degrees, they always believed in science, and they encouraged me to work hard and achieve my goals. I am also deeply grateful to my husband (Musaad) for his patience, cooperation, and understanding and for all the help he gave me throughout my Ph.D. studies. Furthermore, I want to express my sincere appreciation to my mother-in-law and father-in-law and to my brothers and sisters, as well as my brothers-in-law and sisters-in-law for their love, support, guidance, and encouragement throughout my Ph.D. studies.

My deepest acknowledgment goes to my children (Hazza and Malika) for being the coolest and the craziest partners in this journey.

I extend my sincere appreciation to my mentor, Dr. Fernanda Laezza. In the summer of 2012, I joined Dr. Laezza's laboratory with minimal skills and research background. In her multidisciplinary lab, I learned how to design an experiment, prepare an experimental plan, and be patient with troubleshooting. I also like to thank Dr. Filippo Tempia for his support, guidance, and help in this project.

I am deeply grateful to my committee members, Dr. Fernanda Laezza, Dr. Kenneth M. Johnson, Dr. Filippo Tempia, Dr. Maria-Adelaide Micci, and Dr. Thomas A. Green, for their feedback and cooperation.

I warmly thank my current and former labmates, Alexander Shavkunov, Neli Panova-Elektronova, Miroslav Nenov, Federico Scala, Thomas James, Jim Hsu, Syed Ali, and Aditya Singh.

I like to extend my gratitude to my collaborators who contributed to the scientific materials and helped me in this project. I am deeply grateful for the electrophysiological recordings that Dr. Miroslav Nenov performed. I would like to thank Dr. Eriola Hoxha, Dr. Andrea Marcinno and Dr. Filippo Tempia for conducting and analyzing the behavioral experiments. I appreciate the

beautiful EEG recordings that Dr. Marco Cambiaghi and Dr. Benedetto Sacchetti conducted. I would acknowledge Dr. Demetrio Labate and Dr. Pankaj Singh for sharing the fancy neuropil analysis. I owe my thanks to Dr. Jiang Li and Dr. Herbert Y. Meltzer for sharing the bioinformatics analysis.

I want to acknowledge the Pharmacology and Toxicology Graduate Program coordinators, formerly Penny Welsh and currently Nicole Reynolds.

Finally, I thank the Saudi Arabian Cultural Mission and King Saud University for the financial support.

ABBREVIATIONS

ACSF: artificial cerebrospinal fluid
AIS: axon initial segment
AP: action-potential.
CA1: Cornu Ammonis 1
CA3: Cornu Ammonis 3
CaCl2: Calcium chloride
CNS: Central nervous system
DG: dentate gyrus
DLPFC: dorsolateral prefrontal cortex
EEG: electroencephalogram extracellular field potentials
EGTA: ethylene glycol tetraacetic acid
FGF14: fibroblast growth factor 14
GABA: gamma aminobutyric acid
GAD1: glutamate decarboxylase 67 encoding gene
GAD67: glutamate decarboxylase 67
GEO: Gene Expression Omnibus
GO: Gene Ontology
GWAS: genome-wide association studies
HEPES: 4-(2-hydroxyethyl)-1-piperazineethanesulfonic acid (buffering agent)
Hil: hilus
iDG: immature dentate gyrus
KCl: potassium chloride
KEGG: Kyoto Encyclopedia of Genes and Genomes
LFP: local field potential
Limma: Linear Models for Microarray
LTD: long-term depression
LTP: long-term potentiation
M: mask
MgATP: magnesium salt of Adenosine triphosphate
MgCl2: Magnesium Chloride
mIPSC: miniature inhibitory postsynaptic current
MO: month
NaGTP: Guanosine 5′-triphosphate sodium salt hydrate
NaH2PO4: Monosodium phosphate
NaHCO3: Sodium bicarbonate
Nav: voltage gated sodium channel
NCBI: The National Center for Biotechnology Information
NeuN: Neuronal Nuclei
NGS: normal goat serum
PBS: Phosphate-buffered saline
PCR: Polymerase chain reaction
PFA: paraformaldehyde
PVALB: parvalbumin encoding gene.
PVBcs: PV Basket cells
PVChcs: PV chandelier cells / axo-axonic
PVIs: parvalbumin interneurons
QX-314: N-Ethyllidocaine (Na+ channel blocker)
SCA27: Spinocerebellar ataxia type 27
SEEK: Search-Based Exploration of Expression Compendium
sIPSC: spontaneous inhibitory postsynaptic current
SNPs: Single nucleotide polymorphisms
SO: striatum oriens
SP: striatum pyramidalis
SR: striatum radiatum
SVM: support vector machines
TBST: Tris-Buffered Saline with Tween 20
TTX: tetrodotoxin
VGAT: vesicular GABA transporter

Chapter 1: **Background**

1.1 E/I Imbalance

Brain connectivity is complex, and maintaining normal function depends primarily on the delicate balance between excitatory and inhibitory networks. The neuropathology of brain diseases, especially psychiatric disorders, is still poorly understood, but the disruption of the excitatory-inhibitory circuitry balance is an emerging hypothesis (Brambilla et al., 2003). Within the cortical regions, disruption in this global balance may underlie many neurological and neurodevelopmental disorders characterized by cognitive deficits. Such disorders include epilepsy, autism spectrum disorders, bipolar disorder, schizophrenia, and Tourette's syndrome (Baraban and Tallent, 2004;Belmonte et al., 2004;Cossart et al., 2005;Dani et al., 2005;Kalanithi et al., 2005;Lewis et al., 2005;Woo and Lu, 2006). Cognitive impairment includes alterations in learning, memory, attention, planning, and other executive functions (Marder, 2006).

Cognition is considered to be the brain's ultimate function. The core of the majority of neuropsychiatric disorders is cognition. Growing evidence suggests that cognitive elements influence hallucination and delusions (Robbins, 2011). Despite these facts, there is a lack of neurocognition treatment, measurement (Marder, 2006), and pre-clinical models. There is also a dearth of biomarkers (Saunders Iv, 2012). In multiple brain disorders, cognitive impairment precedes neurological and psychological symptoms. In schizophrenia, it is considered a sign in the evaluation of patient functionality (Van Dam et al., 2003;Lewis et al., 2004;Van Raamsdonk et al., 2005;Vorstman et al., 2015). So far, there is no effective treatment for cognitive impairment. Thus, the researchers shifted to a new drug screening approach; they sought to understand the

neurological basis of cognitive deficits, which would help develop treatments, rather than focusing on disease-based screening (Insel and Sahakian, 2012;Robbins et al., 2012).

Multiple physiological pathways have been linked to cognitive deficits, and one of them is the GABAergic inhibitory system (Lewis and Moghaddam, 2006). Some of the most consistent findings in postmortem studies concerning different neurological disorders are: 1) reductions in PV cell number, content and/or overall activity in the hippocampal region and the prefrontal region (Arai et al., 1987;Konradi et al., 2011;Wang et al., 2011a;Jiang et al., 2013); 2) reduction in GAD67 expression (Guidotti et al., 2000;Woo et al., 2004;Fatemi et al., 2005;Thompson Ray et al., 2011); 3) reduction in VGAT expression (Buzzi et al., 2012;Hoftman et al., 2015). Moreover, the loss of other GABAergic markers (including gephyrin, GABA alpha subunits, and neuroligin) is considered the hallmark of schizophrenia and other psychiatric disorders (Enoch et al., 2012;Lewis et al., 2012;Lionel et al., 2013;Sindi et al., 2014).

The advances and breakthroughs in multiple approaches have been used to generate neuropsychiatric animal models, such as genetic, pharmacological, environmental, and electrical simulations (Nestler and Hyman, 2010). However, major challenges face these models. Of particular interest is the lack of an animal model that captures all complex features of any CNS disease (Markou et al., 2009). Despite this, the GABAergic hypofunction hypothesis has been validated in multiple animal models of brain disorder (Chao et al., 2010;Galanopoulou, 2010;Verret et al., 2012;Benham et al., 2014;Colciaghi et al., 2014;Falco et al., 2014). Until now, the exact molecular and cellular mechanisms that control and regulate the GABAergic inhibitory system are not well understood. Therefore, we need to understand these mechanisms in order to shed light on the etiology of the aforementioned disorders and develop better therapeutic innervations for them (Table 1:1).

Disorder	Animal model/description	Alterations in the inhibitory system	Reference
Rett syndrome	MeCP2 knockout. (methyl-CpG- binding protein 2, a transcription repressor)	Reduction in GABA synaptic transporters (GAT-1, and Vgat)	(Kang et al., 2014)
		Reduced GAD67/65	(Chao et al., 2010)
		Decreased in GABAergic inhibitory transmission	(Medrihan et al., 2008)
			(Zhang et al., 2008)
Autism	CNTNAP2 knockout (member of neurexin superfamily, important for neuronal development and K+ channels clustering)	Reduced PVIs and GAD67	(Penagarikano et al., 2011)
	Cadps2 knockout (Ca^{2+}-dependent activator protein for secretion, regulates synaptic exocytosis)		(Penagarikano et al., 2011)
	Shank3 mutant mice (postsynaptic density protein critical for recruitment of PSD component)	Decreased in inhibitory synaptic transmission	(Lee et al., 2015)
	Prenatal valproate treatment (embryonic chemical insult) and Neuroligin-3 mutant animal model.	Reduced PVIs	(Gogolla et al., 2009)
Schizophrenia	MAM treated rats (methylazoxymethanol acetate)	Reduced PVIs	(Lodge et al., 2009)
	ketamine treated mice		(Koh et al., 2016)
	DISC1 mutant mice		(Hikida et al., 2007)
	Shn-2 knockout (Schnurri-2, a nuclear factor-κB site-binding protein)	Reduction in PVIs and GAD67	(Takao et al., 2013)
Epilepsy	GFRα1 knockout mice	Reduction in PVIs	(Canty et al., 2009)
	PV knockout mice treated with epileptogenic (Pentylenetetrazole)	Genetic deletion of PV causes defects in the cortical inhibitory circuitry compared to the PV wild type treated with epileptogenic.	(Schwaller et al., 2004)
	pilocarpine-treated rats	Loss in PVIs	(Dinocourt et al., 2003)
	Selenoproteins knockout mice (regulates the cellular calcium homeostasis and membrane proteins folding and degradation)	Loss in PVIs	(Wirth et al., 2010)
	Scn1a mutant mice (NaV1.1 encoding gene)	Defects in inhibitory circuitry	(Ogiwara et al., 2007)

Table 1:1 Alterations in GABAergic system in multiple brain disorders that are linked to (E/I) dysregulations

1.2 The Hippocampus

1.2.1 The Structure

The hippocampus is the special brain structure located in the temporal lobes of the cortex, with two U-shaped structures located in the left and right brain hemispheres. The hippocampal formation is divided into the hippocampus proper, the dentate gyrus, the entorhinal cortex, and the subiculum (Freund and Buzsaki, 1996;Forster et al., 2006;Per Andersen, 2006). In mammals, the general buildup of the hippocampus is well conserved. The hippocampus proper structure is composed of three main regions: CA3, CA2, and CA1. Unlike the neocortical regions, where the principal cell bodies exist within the six layers, in the hippocampus, the excitatory cell bodies are localized to one heavily packed layer. This single architectural layer of excitatory cells (SP in the CA and granular cell layers in the DG) mediates unidirectional excitatory pathways. The majority of the hippocampus cells are excitatory, mediating glutamatergic input. The remaining 15% of neuronal populations mediate inhibitory input by releasing GABA. As a structure, the hippocampus is well laminated into non-overlapping layers. The assembly, simplicity, and functional implications of the hippocampus in multiple disorders render it one of the most extensively studied brain regions in the field of neuroscience (Per Andersen, 2006;Winterer, 2012).

1.2.2 The Hippocampal Circuitry

Information processing in the hippocampal circuitry is predominantly unidirectional. It is known as the trisynaptic circuit. Within the trisynaptic loop, three main stages occur (Andersen et al., 1971). The DG is the first element in this circuitry. The entorhinal cortex cells project to the DG and excite the granular cells of the DG molecular layer. The entorhinal inputs carry the sensory information (Perforant path input) from the layer II of the cortex to the granular cells dendrites. Specifically, the outer and middle third of granule cells dendrites receive an axonal projection from

the entorhinal cortex neurons. The DG principal cells' axons, which are called mossy fibers, contain two forms of terminals: mossy terminals and filopodia. Structurally and functionally, they are different. For instance, mossy terminals are larger in size, fewer in number, and innervated by principal cells. On the other hand, filopodia are smaller, numerous, and innervated by interneurons. The DG mossy neurons from the hilar region have a powerful projection to the CA3 principal cells that are located in the SP sublayer. Once they contact the CA3 neuronal dendrites, the trisynaptic loop reaches the second stage. The mossy fibres axons projects to the CA3 proximal and apical dendrites. The filopodia synapse with CA3 GABAergic interneurons and the CA3 principal neurons generate excitatory inputs in both SO and SR. The Schaffer collaterals constitute the third element of the trisynaptic circuitry. In this stage, the CA3 principal cells project to the CA1, SO, and SR. The CA3 Schaffer collaterals send a strong excitation into the CA1 cells' proximal dendrites. The CA1 principal neurons direct the hippocampal circuitry output to the subiculum and the entorhinal cortex. Thus, DG-CA3-CA1 fine tuning hippocampal circuitry provides efficient, delicate and unique information processing that are critical for higher cognitive tasks (Lawrence and McBain, 2003;Neves et al., 2008;Chevaleyre and Siegelbaum, 2010;Papp, 2013) as illustrated in Figure 1:1.

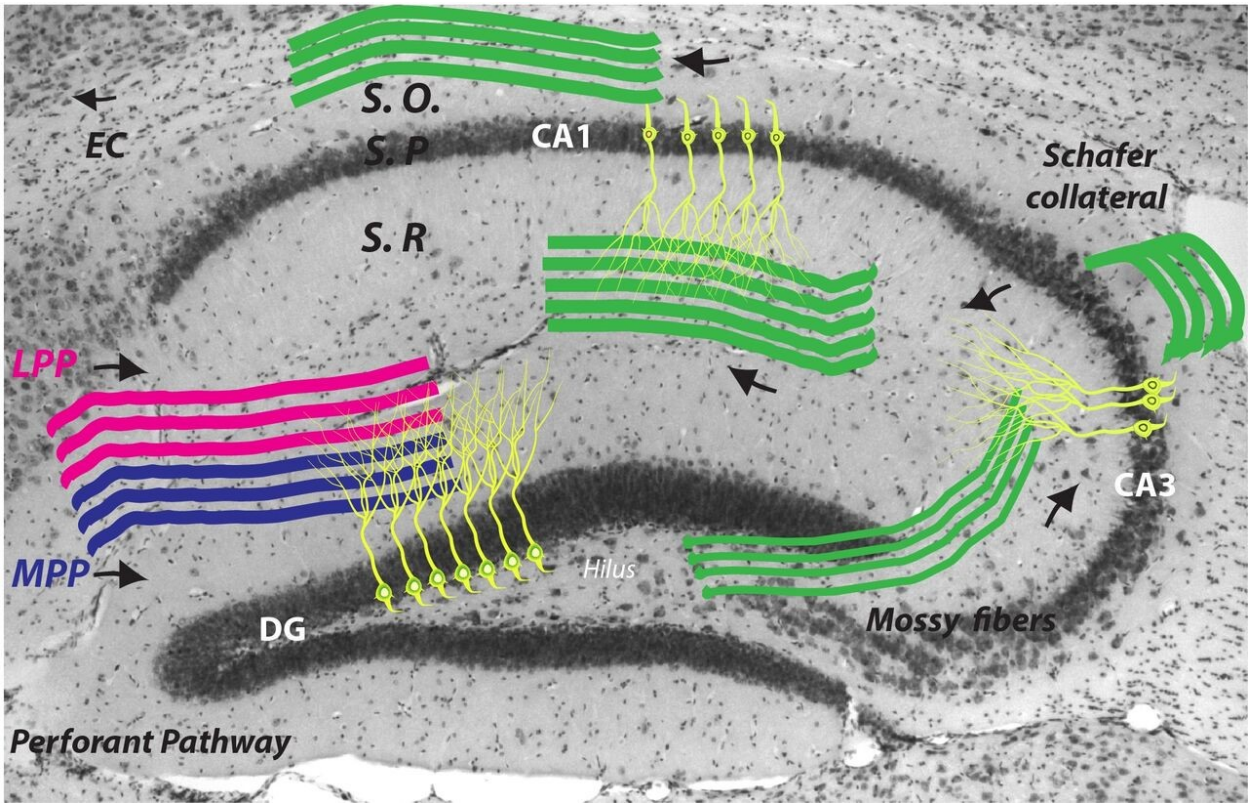

Figure 1:1 Hippocampal structure and circuitry (the tri-synaptic loop).

An illustration of hippocampal basic structure using classical cresyl violet staining. The deep color represent the hippocampal excitatory cells condensed in single layer (SP in the CA1 and CA3, and granular cell layer in the DG). Arrows dictate The tri-synaptic loop unidirectional path. Stage 1: hippocampal DG granular cells' dendrites receive input carrying sensory information from the perforant pathway. Stage 2 (Schafer collateral) take place at the CA3 region. The DG neuronal axons project to the CA3 dendrites. Stage 3 occur at the CA1 region. The CA1 dendrites collect information from the CA3 circuitry input. CA1 collect the hippocampal output to the subiculum and entorhinal cortex. DG: dentate gyrus, CA: cornu ammonis, Sub: subiculum, EC: entorhinal cortex, S.O.: stratum oriens, S.P.: striatum pyramidalis, SR: striatum radiatum, LPP: lateral perforant pathway, MPP: medial perforant pathway. Adapted by permission from Macmillan Publishers *Ltd*: [Nature Reviews Neuroscience] (Deng et al., 2010), copyright (2010).

1.2.3 Inhibitory Interneurons in the Hippocampus

While the excitatory cells have stereotyped properties, the GABAergic inhibitory interneurons composed of diverse and highly heterogeneous groups Figure 1:2. These populations can be distinguished by their neurochemical, anatomical and electrophysiological properties. Based on their anatomical characters, they can basket, chandelier and bistratified cells. According

to their neurochemical expression they can be classified based on their calcium-binding protein content (parvalbumin, calbindin, and calretinin). Moreover, they can be classified according to their neuropeptides contents into neuropeptide Y and somatostatin. The most extensively studied subtype is the calcium-binding protein group, Particularly PVIs (Klausberger and Somogyi, 2008;Tepper et al., 2010).

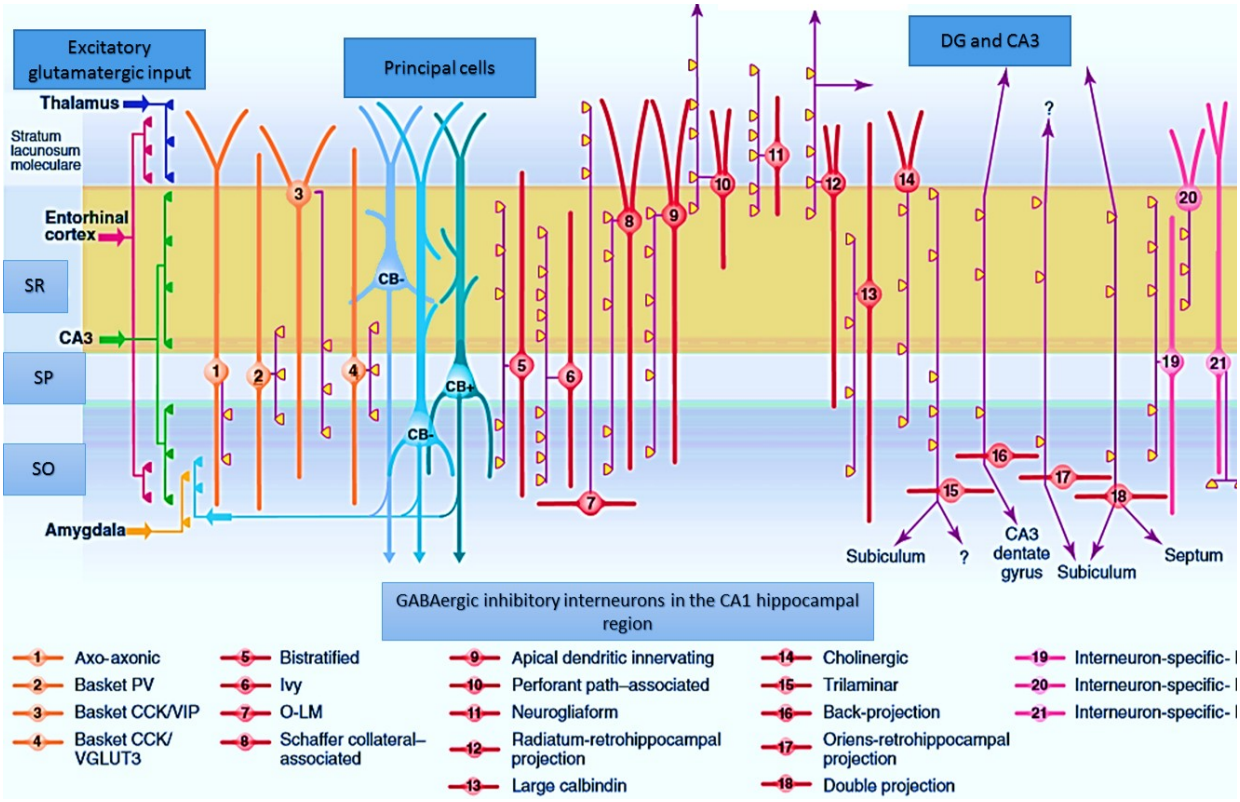

Figure 1:2 The heterogeneity of GABAergic inhibitory in the hippocampal CA1 region.

Klausberger and Somogyi characterized multiple types of interneurons in the CA1 area.
The blue represents the principal cells. The orange indicates the perisomatic and the somato-dendritic innervations. Interneurons-interneurons innervations are shown in pink. The purple represents the axons. The yellow indicates the main synaptic terminations. The excitatory glutamatergic inputs are shown on the left. The Schaffer collateral and the perforant pathway are shown on right. DG: dentate gyrus, CA: cornu ammonis, Sub: subiculum, EC: entorhinal cortex, S.O.: stratum oriens, S.P.: striatum pyramidalis, SR: striatum radiatum; O-LM, oriens lacunosum moleculare; VGluT, vesicular glutamate transporter; VIP, vasoactive intestinal polypeptide. Adapted with permission from The American Association for the Advancement of Science Publishers *Ltd*: [Science](Klausberger and Somogyi, 2008), copyright (2008).

The GABAergic inhibitory populations, particularly PVIs, connect to the principal cells in two forms: perisomatic and dendrodendritic (Szentagothai and Arbib, 1974). The perisomatic innervations are the most intensively studied. When the inhibitory cell axons lie close to the excitatory cell somata, they mediate perisomatic inhibition, which is one of the most abundant forms of inhibition (Szabadics et al., 2006;Glickfeld et al., 2009). Within the hippocampal CA1 region, the perisomatic inhibitory cells can be basket or axo-axonic cells **Figure 1:2**. The basket cells can be PV (PVBcs) or CCK positive cells. Each one of them has distinct physiological properties. For instance, CCK positive cells synapse with excitatory cells in an asynchronous form. They also fire regular spikes and exhibit high input resistance. However, perisomatic PVIs displays synchronous innervations and connectivity with principal cells. They fire fast spikes, and they have lower input resistance (Freund, 2003;Winterer, 2012). PVBcs offer powerful and reliable clockwork that maintains synchronized network oscillations (Freund and Katona, 2007). A single perisomatic inhibitory cell has the ability to synchronize principal cells output at different frequencies, for instance, theta and gamma waves. Physiologically, they are essential for multiple cognitive functions (Freund and Buzsaki, 1996;Freund, 2003).

The axo-axonic inhibitory cells (PVChcs) innervate the excitatory cells' axons. They form a number of boutons on the AIS, securing adequate control over the excitatory output (Somogyi, 1977). So far, only PVIs have been characterized to form this connection with principal cells (Kosaka et al., 1987). Within the dendrodendritic connections, the inhibitory neurons, mainly bistratified, contact the principal' cells dendrites in the SR and SO (Winterer, 2012). They can be parvalbumin, Neuropeptide-Y, or somatostatin positive cells. This type of interneuronal connectivity is still under examination, and the list of the cells' immunoreactivity and characterization is expanding. So far, it includes more than ten well-described members (Klausberger and Somogyi, 2008).

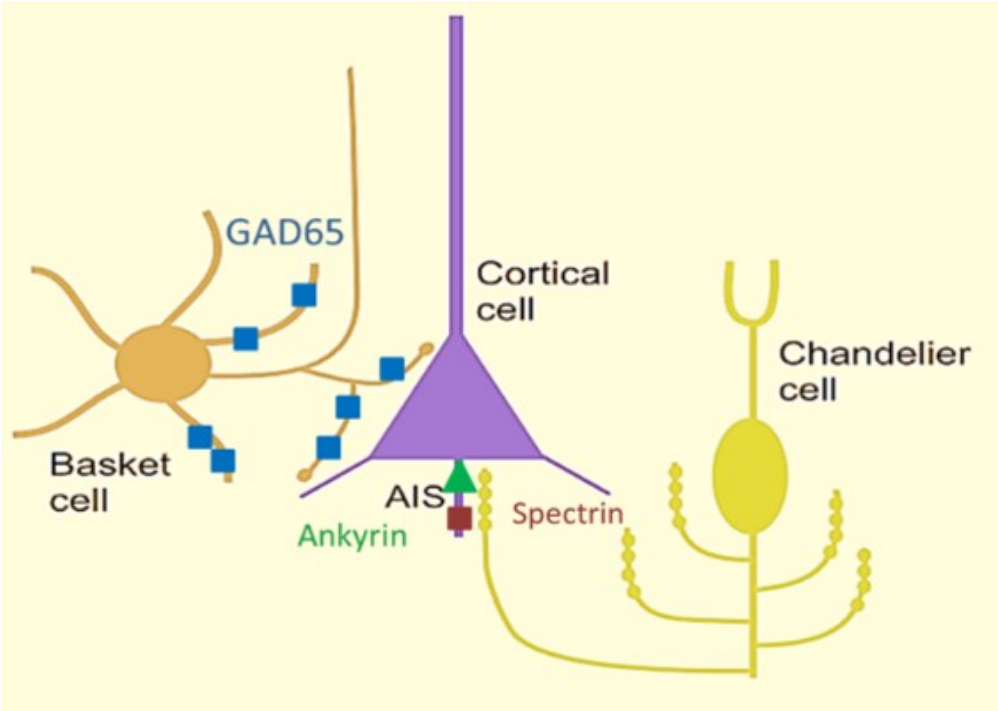

Figure 1:3 PVIs perisomatic inhibitory innervation, parvalbumin basket and parvalbumin axo-axonic cells.
The basket cells innervate the principal cells (purple) soma and dendrites. Structurally this type of cells expresses GAD65 in their dendrites. On the other hand, parvalbumin chandelier cells innervate the principal cells AIS. Ankyrin-G and spectrin are AIS cytoskeletal proteins. Structurally, their dendrites express characteristics buttons. Adapted from (Woo and Lu, 2006).

1.3 GABAergic inhibitory system

1.3.1 The Synapses

In the mammalian CNS, the GABAergic system is composed of GABAergic interneurons and synapses. At the presynaptic site, the synthesis of the inhibitory neurotransmitter GABA is achieved by 2 isoforms of decarboxylase enzyme (GAD67 and GAD65). Both isoforms show a distinct pattern of interneuronal localization, expression during development, and regulatory mechanism (Chattopadhyaya et al., 2007). GAD67 is responsible for the synthesis of the majority of GABA in the brain. In fact, knocking down the GAD1 gene (GAD67 encoding gene) would be lethal. Due to its critical role, alterations in GAD1 are linked to multiple psychiatric diseases

(Uchida et al., 2014 Yanagawa, & Fukuda, 2014). Reduction in GAD1, which leads to a decrease in the GABA level, is one of the consistent findings in schizophrenic postmortem studies (Lewis et al., 2012). Following GABA synthesis, vesicular GABA transporter (VGAT) loads the neurotransmitter into presynaptic vesicles. VGAT is a critical component of the GABAergic presynaptic site as it controls GABA dynamic release in a pH-dependent, precise, and accurate manner (Liu and Edwards, 1997). Conditional $VGAT^{-/-}$ mice exhibit ataxia (disrupted motor coordination) and cognitive impairment similar to *Fgf14*$^{-/-}$ mice (Kayakabe et al., 2014). An electrical signal triggers GABA release (Saunders et al., 2015); the GABA diffuses to the postsynaptic sites, where it binds to GABA receptors and hyperpolarizes the postsynaptic sites of principal cells.

1.4 The inhibitory interneurons

1.4.1 Overview

GABAergic inhibitory interneurons represent ~20% of all neurons in the cortex, yet they project axons over a large population of excitatory cells and exert dominant control on brain excitatory activity. The activity of interneurons is required for proper excitability, output, and the synaptic plasticity of excitatory cells (Ting et al., 2011). They exert their effects by the following means: i) feed-back and feed-forward inhibition, ii) regulating synaptic plasticity – LTP and LTD (Castillo, 2012), and iii) maintaining the network oscillations (Dupret et al., 2008).

Interneurons are highly heterogeneous and extraordinarily diverse. They can be classified into chandelier, bistratified, and basket cells, depending on the shapes and organization of their somata and dendrites. Biochemically, they are classified based on their Ca^{2+} binding protein content, for instance, PV, calretinin (CR), and calbindin (CB). All these interneurons have distinct physiological properties, with regular, clustered, or irregular firing patterns (Krook-Magnuson et

al., 2012). The unifying feature of the interneurons is their ability to release GABA, which is an inhibitory neurotransmitter in the adult brain.

Given these highly specialized functions and the powerful influence that interneurons have over many excitatory cells, it is not surprising that the disruption of several components of the GABAergic system has been linked to cognitive deficits in psychiatric disorders and neurodegenerative diseases (Bernard et al., 1998). Of particular interest where brain disorders are concerned are PVIs (Jiang et al., 2013). Dysfunctional PVIs have been strongly implicated in multiple neurological disorders, including epilepsy, Tourette's syndrome, autism, and schizophrenia (Hill, 2004;Verte et al., 2005;Waltz and Gold, 2007;Campbell et al., 2008;Sebe and Baraban, 2011).

1.4.2 The PVIs

PV protein is a slow Ca^{+2} buffer. By reducing the presynaptic Ca^{+2} level, it helps to prevent the accumulation of Ca^{+2} presynaptically, thus protecting the cell from potential toxicity. Furthermore, buffering ability allows PVIs to regulate other Ca^{+2} dependent cellular functions, such as short-term synaptic plasticity. Since they prevent cumulative facilitation, PVIs maintain synaptic strength in an almost resting state (Chard et al., 1993;Caillard et al., 2000). Physiologically, PVIs fire unique fast spikes, which enable them to be dynamically involved in neuronal input and output circuitry signals (Connors and Gutnick, 1990;Erisir et al., 1999). PVIs' firing properties render them powerful in the regulation of neural transmission in the brain (Woodruff et al., 2010). The sustained high-frequency trains of action potentials that PVIs generate synchronize large-scale oscillations, including gamma oscillations. Multiple *in vivo* studies demonstrate that PVIs are essential for generating gamma oscillations (Hashimoto et al., 2003;Cardin et al., 2009;Sohal et al., 2009 & Deisseroth, 2009).

Voltage-gated sodium channels (Navs) play a vital role in action potential generation and propagation. They regulate neuronal excitability at the cellular and network levels (Meisler and Kearney, 2005). The Nav1.1 subunit is expressed primarily in PVIs (Ogiwara et al., 2007;Wang et al., 2011b). Alteration in the Nav1.1 encoding gene (SCN1A) gives rise to neuronal network asynchrony in epilepsy (Yu et al., 2006;Ogiwara et al., 2007). Nav1.1 haploinsufficiency leads to severe myoclonic epilepsy of infancy, a progressive age-dependent manifestation. During the first year of life, patients with this condition develop status epilepticus. Later, they experience ataxia, autistic-like behaviors, and cognitive deficits (Yu et al., 2006;Kalume et al., 2007;Cheah et al., 2012;Rubinstein et al., 2015). In an Alzheimer's mouse model, the cell-specific depletion of Nav1.1 impaired the network oscillations and the cognitive capacity (Huang and Mucke, 2012;Verret et al., 2012). In human postmortem studies of schizophrenia, the impact of PVIs on pathology in cortical networks is probably more attributable to the changes in their firing properties than to the reductions in their counts (Gonzalez-Burgos et al., 2015). This suggests that Nav1.1 mediates inhibition by inhibitory cells, thus influencing neuronal synchrony and emphasizing the role of PVIs in AP regulation for proper brain wave activity.

1.4.3 The Gamma Oscillations

Gamma oscillations are brain waves detected at 30–100 Hz. They are critical for fundamental cognitive tasks, including perception, information processing, learning, and memory. They reflect dynamic and extreme delicate interactions between excitation and inhibition circuitries. Thus, they constitute a useful diagnostic tool for cognitive capacity. Moreover, they are utilized as an endophenotype for brain disorders (Porjesz and Rangaswamy, 2007). Multiple studies have reported that dysfunction in the auditory-evoked gamma wave response is associated

with working memory deficit in schizophrenic patients (Liu and Edwards, 1997;Light et al., 2006;Teale et al., 2008).

Within the cortex, gamma oscillations are the result of delicately synchronized principal cells spiking (generating AP) (Kann, 2015). PVIs are expressed in the cortex, cerebellum, and hippocampus (Seto-Ohshima et al., 1989). In the hippocampal CA1 region, they represent more than 70% of interneuronal populations (Szilagyi et al., 2011). One of the pathophysiological scenarios in brain disorders is based on alterations in PVIs that lead to dysfunctional fast spikes and impaired gamma oscillations (Kann, 2015). PVIs have been found to be reduced in multiple animal models of neurological and neurodevelopmental disorders such as Alzheimer's disease, autism, bipolar disorder, and schizophrenia.

It is believed that impaired cognition and reduced gamma oscillations in schizophrenia and other psychiatric disorders are the basis for reduced executive function (Lewis and Moghaddam, 2006) and are caused by a specific loss in PVI function (Lewis et al., 2012).

1.5 The Current Status

So far, we know that the CNS will not function properly if there is an imbalance between excitation and inhibition (Yizhar et al., 2011). Alterations in the GABAergic system are linked to abnormal information processing and cognitive impairment in a broad range of neurodevelopmental disorders (Smith-Hicks, 2013). PVIs play a critical role in generating the gamma oscillations that are essential for cognitive capacity. Proper Nav1.1 currents in PVIs are indispensable for cognitive function (Yu et al., 2006;Cheah et al., 2012;Han et al., 2012). Currently, there is a lack of knowledge regarding the molecules that modulate PVI structure, expression, development and function. Therefore, we need to identify the molecules that regulate PVIs in the normal brain and the diseased brain.

1.6 FGF14

1.6.1 overview

FGF14 is an intracellular growth factor that belongs to the fibroblast growth factor (FGF) family. FGFs are classified into two groups: secretory FGFs and intracellular FGFs. Moreover, their structure and amino acid sequence are highly conserved. Secretory FGFs bind tyrosine kinase FGF receptors and mediate multiple functions such as neuronal growth, differentiation, and survival. Four FGF family members (FGF11-14) lack tyrosine kinase binding residues and are called intracellular growth factors. However, they bind the alpha subunit carboxy terminus of the voltage-gated sodium channel and modulate neuronal voltage-dependent activities (Yan et al., 2013;Ornitz and Itoh, 2015). FGF14 has been found to be involved in multiple neuronal events, such as neuronal excitability (Laezza et al., 2007;Shakkottai et al., 2009), glycogen synthase kinase 3 signaling (Shavkunov et al., 2013;Leterrier and Dargent, 2014), synaptic transmission (Yan et al., 2013;Xiao et al., 2007), presynaptic Ca^{+2} currents, the recycling of presynaptic vesicles (Yan et al., 2013), the maintenance/loading of glutamatergic synaptic vesicles (Tempia et al., 2015), and adult neuronal stem cell maturation.

In humans, multiple forms of alteration in the FGF14 encoding gene have resulted in its being reported an emerging disease gene. For example, the *Fgf14* missense mutation is a leading cause of spinocerebellar ataxia type 27 (SCA27). SCA27 is a progressive neurodegenerative disorder characterized by motor dysfunction and cognitive impairment (Wang et al., 2002;Brusse et al., 2006;Hsu et al., 2014). Other SCA27 genetic studies have revealed abnormalities in the FGF14 encoding gene, for instance frameshift mutations (Dalski et al., 2005), microdeletion (Megan E Tucker, 2013), and nonsense mutations (Misceo et al., 2009). Genome-wide studies reported the occurrence of SNPs in the FGF14 encoding gene in major depressive disorders,

bipolar disorder, and schizophrenia (Wang et al., 2002;Goldfarb, 2005;Laezza et al., 2007;Laezza et al., 2009;Terwisscha van Scheltinga et al., 2010;Shavkunov et al., 2013;Hsu et al., 2014). This suggests that FGF14 is an emerging brain disease risk gene and might be a good candidate for the identification of a biomarker or potential therapeutic target in brain disorders characterized by cognitive impairment.

1.6.2 Rationale

Four critical facts have influenced this project. First is the fact that the genetic deletion of *Fgf14* causes cognitive impairment and locomotor dysfunction, including ataxia and paroxysmal dyskinesia. These phenotypes were explained by an imbalance between the dopaminergic inhibition pathway (D1 receptor) and dopaminergic excitation signals (D2 receptor) in the basal ganglia (Wang et al., 2002). Growing evidence suggested that the impaired dopaminergic tone in the basal ganglia was strongly influenced by an imbalance in the hippocampal circuitry (Taepavarapruk et al., 2000;Floresco et al., 2001;Floresco et al., 2003;Shah and Lodge, 2013;Boley et al., 2014). Second is the fact that alterations in neuronal excitability are highly implicated in PVIs dysfunction in neuropsychological disorders (Gonzalez-Burgos et al., 2015). Third is the importance of FGFs in the regulation of the neuronal plasticity and functions attributed to learning and memory (Wozniak et al., 2007;Need et al., 2009;Xiao et al., 2007).

The fourth fact is related to adult neurogenesis, which is a physiological process that occurs in two brain regions: the olfactory bulb and hippocampal DG. In each neurogenesis cycle, the neuronal stem cells proliferate, differentiae, migrate, and then become fully mature cells, at which point they integrate into the circuitry (Johnson et al., 2009;Sun et al., 2011;Tye et al., 2011). Functionally, adult neurogenesis is essential for multiple cognitive processes. Subtle changes in this physiological course's stages have been linked to the cognitive deficits of neurological

disorders, including Huntington's disease, Alzheimer's disease, depression, and schizophrenia (Ming and Song, 2005;Taupin, 2008;Jun et al., 2012).

One form of the abnormal alterations in adult neurogenesis is known as immature DG (iDG). We recently found that the genetic deletion of FGF14 resulted in iDG (Alshammari et al., 2015). The elevation in immature neuronal markers and accompanying reduction in mature markers are hallmarks of pathophysiological alterations of DG, named iDG. Multiple psychiatric animal models exhibit iDG phenotypes, including genetically modified strains such as α-CaMKII heterozygous mice, SNAP-25 knock-in, Schnurri-2 knockout, and region-specific calcineurin knockout mice. In these animal modes, the neuronal immaturity during adulthood is accompanied by cognitive impairments, which mostly comprise working memory deficits. The cellular and molecular iDG phenotypes have been identified in schizophrenic and bipolar human patients using both immunohistochemical analysis and gene expression profiling. Recently, iDG has been considered as an endophenotype for brain disorders (Yamasaki et al., 2008;Hagihara et al., 2013).

These facts ***prompted me to hypothesize*** that *Fgf14* expression might play a role in maintaining the PVIs and regulating GABAergic synapses, which are the basis for cognitive deficits in brain disorders Figure 1:4**.**

To validate this hypothesis, I chose the hippocampal CA1 region. Compared to other cortical regions, it is one of the most intensively studied area. The structural simplicity allowed the cellular morphological and functional examination. Moreover, the CA1 directs the largest hippocampal output to the cortex (Insausti and Munoz, 2001;Klausberger and Somogyi, 2008). In schizophrenia, anatomical abnormalities in CA1 area considered as a disease severity and a treatment evaluation index (Zierhut et al., 2013).

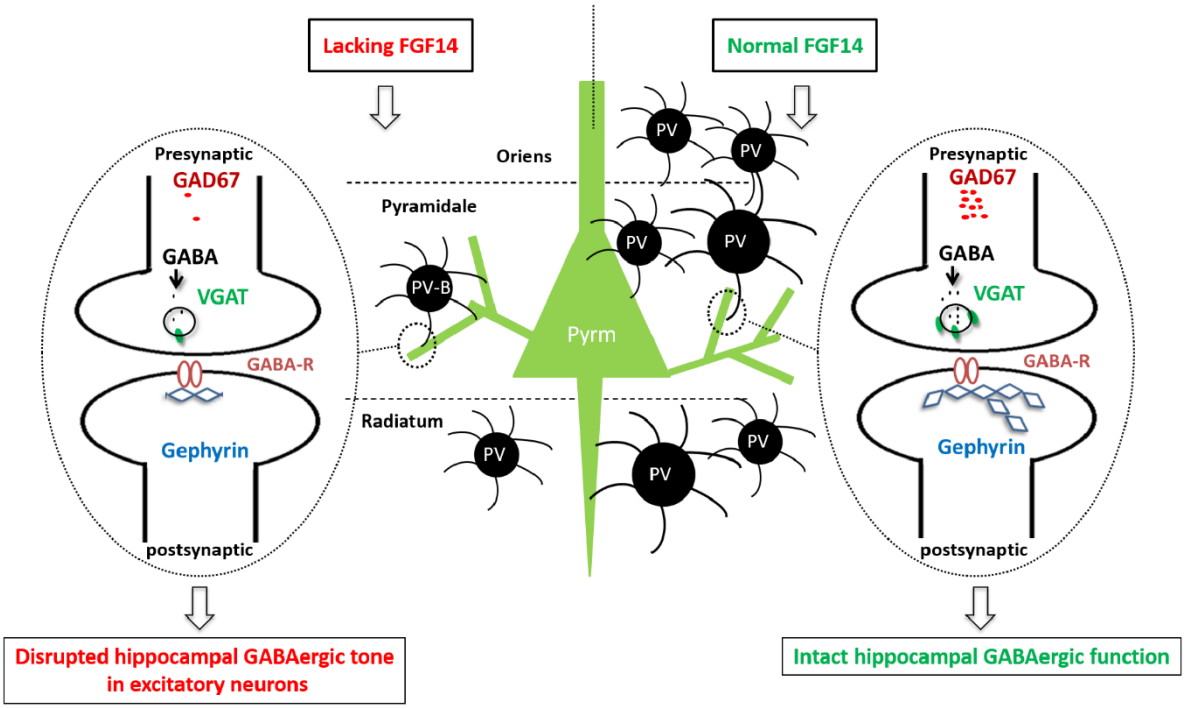

Figure 1:4 Schematic representation of my hypothesis.
Phenotypes observed in *Fgf14*$^{-/-}$ reveal a possible reduction in parvalbumin interneurons (PV) in specific sub-field of the CA1 region. Also, in both pre- and postsynaptic inhibitory synapses, lack of *Fgf14* might result in decrease in GAD67and VGAT expression accompanied alterations in gephyrin expression, a postsynaptic inhibitory marker. Designed by Alshammari, Tahani.

1.7 The Goal of this Study

My first goal was to determine the role of FGF14 in regulating the expression of PVIs and GABAergic synapse composition in the hippocampal CA1 region. I started this study by counting the total PVI population, which is presented in chapter three. We found selective cell loss in the CA1 region. To understand whether this reduction was global or specific, we quantified: 1) the total PV protein content per soma, 2) the neuropil density, and 3) the total neuronal populations. The results indicated that the reduction in PVIs was selective to the SO and SP. This suggested that the perisomatic inhibition and axo-axonic inhibition were altered in *Fgf14*$^{-/-}$. Next, we examined the GABA synthesis and transporting machineries (GAD67 and VGAT respectively).

Furthermore, we sought to determine whether functional consequences accompanied these structural alterations at the cellular, circuitry, and behavioral levels. To address these questions, we examined the inhibitory circuitry using the whole-cell patch clamp (sIPSC and mIPSC). We conducted an *in vivo* gamma oscillation recording and examined the spatial working memory. Then, for added translational value, we conducted a computational analysis using postmortem transcriptomic data sets.

In chapter four, I expand our study to the GABAergic postsynaptic compositions that are relevant to cognitive impairment in brain disorders. In order to understand whether FGF14 influences the GABAergic postsynaptic integrity and function, we examined the gephyrin, $GABA_A$ alpha-1, and alpha-2 subunits. We then characterized these proteins using immunohistochemical studies and puncta analysis.

After characterizing the role of FGF14 in regulating PVIs, I wanted to understand the mechanisms of PVIs loss in *Fgf14*$^{-/-}$ mice. In chapter five, I conducted developmental studies to quantify the total number of PVIs in three age groups. Then, I ask whether this reduction was due to the activation of the apoptotic machinery (capsase-3). In the last set of experiments, I examined the AIS structure. To provide a link between lacking FGF14 and the loss in PVIs that could be due to dysfunctional circuitry.

1.8 Significance

Most mental disorders, including neurodevelopmental, degenerative, and psychiatric disorders, are incurable long-term diseases. Cognitive impairment is common among these disorders, and, so far, there is no effective treatment for the cognitive deficit (Green, 2007;Duinen et al., 2015). The disability and the distress represent an expensive burden to the patients, the family caregivers, and the system. Thus, the cost is growing. These life-long conditions impact the

productivity of the patients and their families. This indicates the importance of identifying better therapeutic interventions for neuropsychiatric disorders, particularly for cognitive impairment (McGovern-Institute;Okura and Langa, 2011;Sahakian et al., 2015).

This project is innovative because the molecular and cellular mechanisms underlying the role of FGF14 in regulating GABAergic system have not been explored yet. Furthermore, the project has the goal of identifying new target mechanisms that maintain GABAergic fidelity and cognitive capacity. This work is significant because it helps to fill the gaps in our knowledge, providing a better understanding of the GABAergic system in animal model of schizophrenia and other neuropsychiatric disorders in conveying a potential therapeutic targets for disease treatment.

Chapter 2: **Materials and Methods**[1]

The following chapter illustrates the experimental procedures used in this work.

2.1 Animals

Fgf14$^{-/-}$ mice were maintained on an inbred C57/BL6J background (greater than ten generations of backcrossing to C57/BL6J) Animals were bred in the UTMB animal care facility by mating either heterozygous *Fgf14*$^{+/-}$ males and females or homozygotes *Fgf14*$^{-/-}$ males with *Fgf14*$^{+/-}$ females. The University of Texas Medical Branch operates in compliance with the United States Department of Agriculture Animal Welfare Act, the Guide for the Care and Use of Laboratory Animals, and IACUC approved protocols. Mice were housed, n≤5 per cage, with food and water *ad libitum*. All genotypes described were confirmed by in house PCR analysis, Charles River Laboratories International, Inc. (San Diego, CA), or conducted at Transnetyx Inc. (Cordova, TN).

2.2 Genotyping

Genotyping was described previously in (Wang et al., 2002). Typically, protocols started with DNA extraction from a mouse tail biopsies using a Puregene Core Kit-A (QIAGEN, Valencia, CA) according to the manufacturer's protocol, followed by PCR targets amplification. The targets of genotyping to detect the *Fgf14*$^{-/-}$ constructs and the wild type alleles were custom-designed and purchased from Integrated DNA Technologies (Coraville, IA) of mouse Fibroblast Growth Factor 14 (*Fgf14*) wildtype (primers: forward, 5'-CTA GTT TCA TGA AAT CCC TAT TTC-3'; reverse, 5'-GCC TTG CCT GCA ATA TAA CCT GGT CAC-3'), together with mouse *Fgf14* knockout

[1] **Parts of chapter are published in Frontiers cellular neuroscience (Alshammari et al., 2016), and parts are accepted for publications in Translational Psychiatry (March 2016).**

allele (primer: reverse 5'-CGC TAT TAC GCC AGC TGG CGA AAG-3'). Amplification cycles of PCR (30) were performed and cycling temperatures and times were as follows: 95°C for 2 minutes (initial denaturation), followed by 30 cycles of: 95 °C for 30s (denaturation), 55°C for 1 min (annealing), 72°C for 1 min (extension) followed by 3 min at 72°C (final extension). Finally, Southern Blotting analysis were used to locate a particular target bands. The wildtype bands detected at 255 bp and the *Fgf14*$^{-/-}$ band detected at 350 bp **Figure 2:5**. Bands were visualized using FluorChem® HD2 System.

2.3 Paraformaldehyde Fixation

2.3.1 Rationale.

In neuroscience research, one of the most routinely used techniques is Immunohistochemistry. This approach allows detection, tracking, and quantification of proteins via fluorescence microscopy. Basically, it provides descriptions of the pattern and the level of proteins expression in cell type and tissue-specific context.

Optimal results depend mainly on two criteria: well-preserved tissue and ideal fixation. For conventional immunohistochemistry, regular 4% PFA intracardial perfusion process was effective in providing well-preserved tissue, sharp detectable immunoreactivity and as a consequences easily quantifiable signals. One of the most recognized drawbacks of PFA fixation is masking antigenicity. Especially in visualizations the delicate sub-cellular structures such as AIS, which requires brief or almost non-fixative treated tissue in order to be detected.

This generate a technical barrier because the core question here was whether FGF14 is a component of PVIs or not? To answer this question, we needed to conduct FGF14, PV and AIS marker- such as Ankyrin or spectrin- a triple staining experiment. As shown in **Figure 2:1**, snap frozen sections are ideal for AIS proteins including FGF14, and PanNav. The same condition

results in undetectable signals of PV (data not shown). However, when I treated the sections with methanol, I observed a weak detected PV signals in the soma and almost non-detected immunosignals in the dendrites.

In order to improve the available choices and combine the advantages of both approaches, the brief, and the strong fixation, I designed a study composed of three tissue preparations (snap-freezing, fixed sections, and freshly prepared living tissue). Using up to ten experimental conditions, the variable was either fixative material, concertation, fixation time, and washing buffers. **Our goals** were: 1) to obtain sharp AIS signals; 2) to get well-preserved tissue 3) to be able to detect cell type markers, such as NeuN, calbindin, and PV.

The results demonstrated two optimal experimental conditions. The first condition is based on using mixed fixative, i.e. 1% formaldehyde mixed with 0.5% methanol. We used a commercially available product from (diluted at 37% in 1X PBS, MasterTech Scientific, catalog number fxfor37gal). As shown in **Figure 2:2** this condition is ideal for detection FGF14 immunoreactivity and cell-type markers (NeuN) in multiple brain regions including the cerebellum, hippocampus, and the cortex. The second condition is permeabilizing the 4%PFA fixed tissue with cold acetone at -20 for 7 minutes. I chose the second condition because it is the best suited to our work routine. This condition has been tested with multiple markers and in different brain regions **Figure 2:3** and tested and in *Fgf14*$^{-/-}$ mice as a control **Figure 2:4** (Alshammari et al., 2016).

2.3.2 Intracardial fixation with 4%PFA

Age- and gender- matched *Fgf14*$^{+/+}$ and *Fgf14*$^{-/-}$ mice were first deeply anesthetized with 2,2,2-tribromoethanol 250 mg/kg intraperitoneal injection (Sigma-Aldrich, Saint Louis, MO). Then we perfused them intracardially with 1% phosphate buffer (PBS), followed by 1% or 4%

paraformaldehyde (MasterTech Scientific, Lodi, CA; Sigma-Aldrich) solution freshly prepared. To ensure complete tissue fixation, the brains were removed carefully and transferred into either 1% paraformaldehyde for 30min to 1hr, or 4% paraformaldehyde 24h-48hr at 4°C and then cryopreserved in 30% sucrose/PBS in preparation for sectioning.

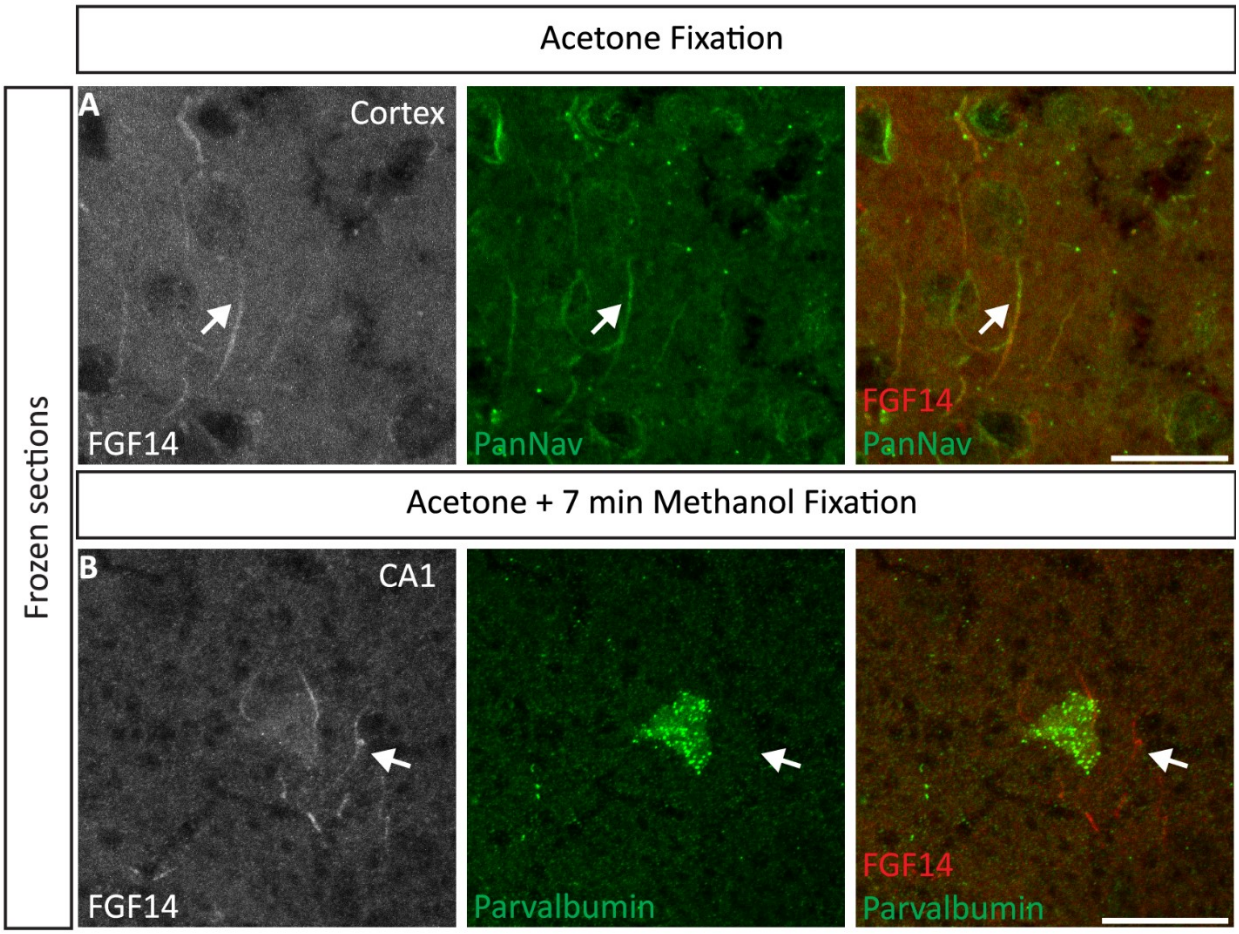

Figure 2:1 Representative examples of The challenges that Faced staining of cell-type markers in sections prepared by snap-freezing (an ideal experimental option for AIS components detection).

A. The detection of FGF14 immunoreactivity at the AIS (arrow) colocalized with PanNav (an AIS resident protein) in mouse cortical region using snap-frozen tissue that is treated with cold acetone. **B**. Confocal images represent FGF14 signals (gray/red) and weak PV (green) immunosignals in the CA1 hippocampal region using snap-frozen tissue that has been incubated with methanol. Scale bars represent 20 µm.

Fixation and Cutting Procedures																		
Tissue		Fixed Sections						Fresh-Frozen Sections								Living Tissue		
		Fixed Brain						Freezing sections								Acute Slices		
Animals perfusion	Fixation Type/ conc.	1% PFA	1% Formaldeh-yde + 0.5% MeOH	4% PFA	Optimal fix*	4% PFA immersion		1% PFA	Acetone	Acetone	4% PFA	2% PFA+ 0.2% Glutar-aldehyde				30 min 1% Formaldehyde + 0.5% MeOH		
	Perfusion Time	10 min	10 min	10 min	10 min	-		5-10 min	7 min	7 min	15 min	10 min				30 min		
Post-fixation/ Permeabilizing		30 min - 1 hour	30 min - 1 hour	1 hour	1 hour	30 min 4% PFA immersion		Acetone	Methanol	None	Acetone	Acetone				Acetone		
				24 hours														
Cutting Procedures 10-25 µm Thickness		Adhered	Adhered	free-floating	free-floating/ Adhered	free-floating		Adhered	Adhered	Adhered	Adhered	Adhered				Adhered		

Table 2-1 Study design of the three experimental conditions.

The study includes three general tissue preparations, the fresh-frozen, the perfusion-fixed, and the freshly prepared acute brain slices tissue preparations. Using up to ten experimental conditions, including variable fixation process, type of fixative, post-fixation material and/or time.

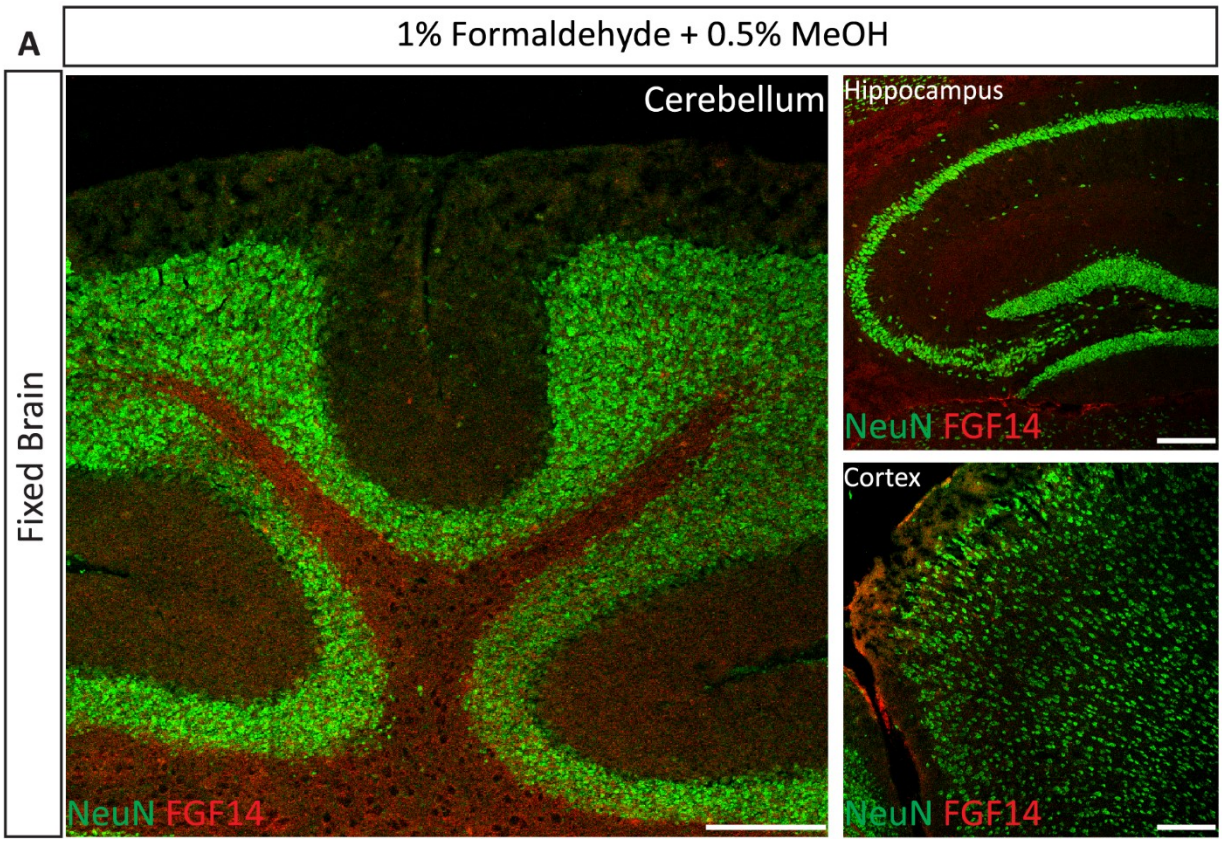

Figure 2:2 Confocal images of FGF14 immunosignals detection in combination with NeuN using 1% formaldehyde + 0.5 methanol fixation.

A. The red channels represent FGF14 immunosignals and NeuN signals represented by the green channel, in the cerebellum, hippocampus and the cortex. Scale bars represent 200 μm.

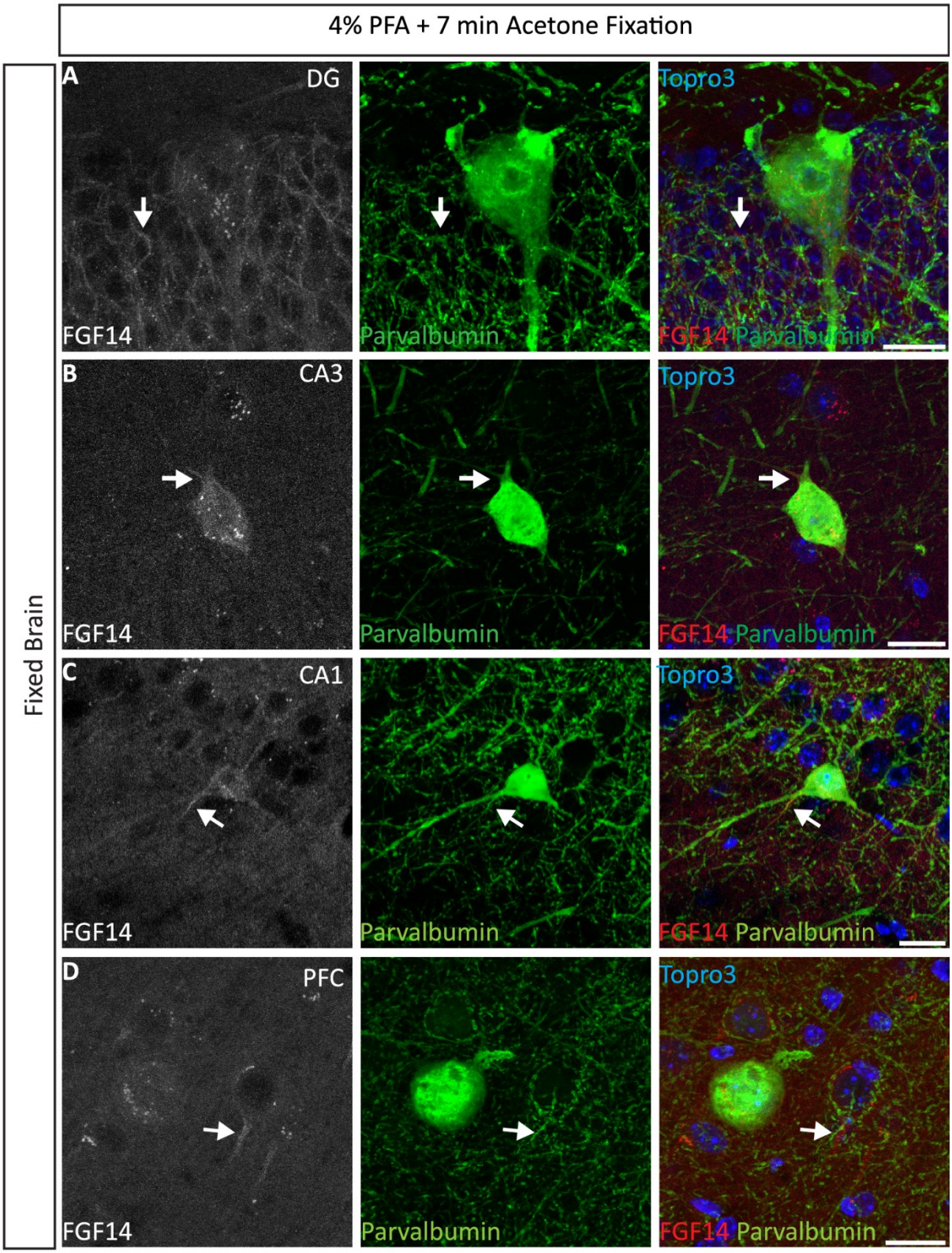

Figure 2:3 Confocal images of AIS detection in PVIs using 4% PFA perfused section treated with cold acetone.

The gray/red channels represent FGF14 immunosignals, the green channel represents

parvalbumin immunoreactivity, and the blue channel represents the nuclei staining Topro-3 in the **A.** hippocampal DG, **B.** hippocampal CA3, **C.** CA1, and **D.** PFC. The arrows indicate FGF14 immunosignals at the AIS. Scale bars represent 20 µm.

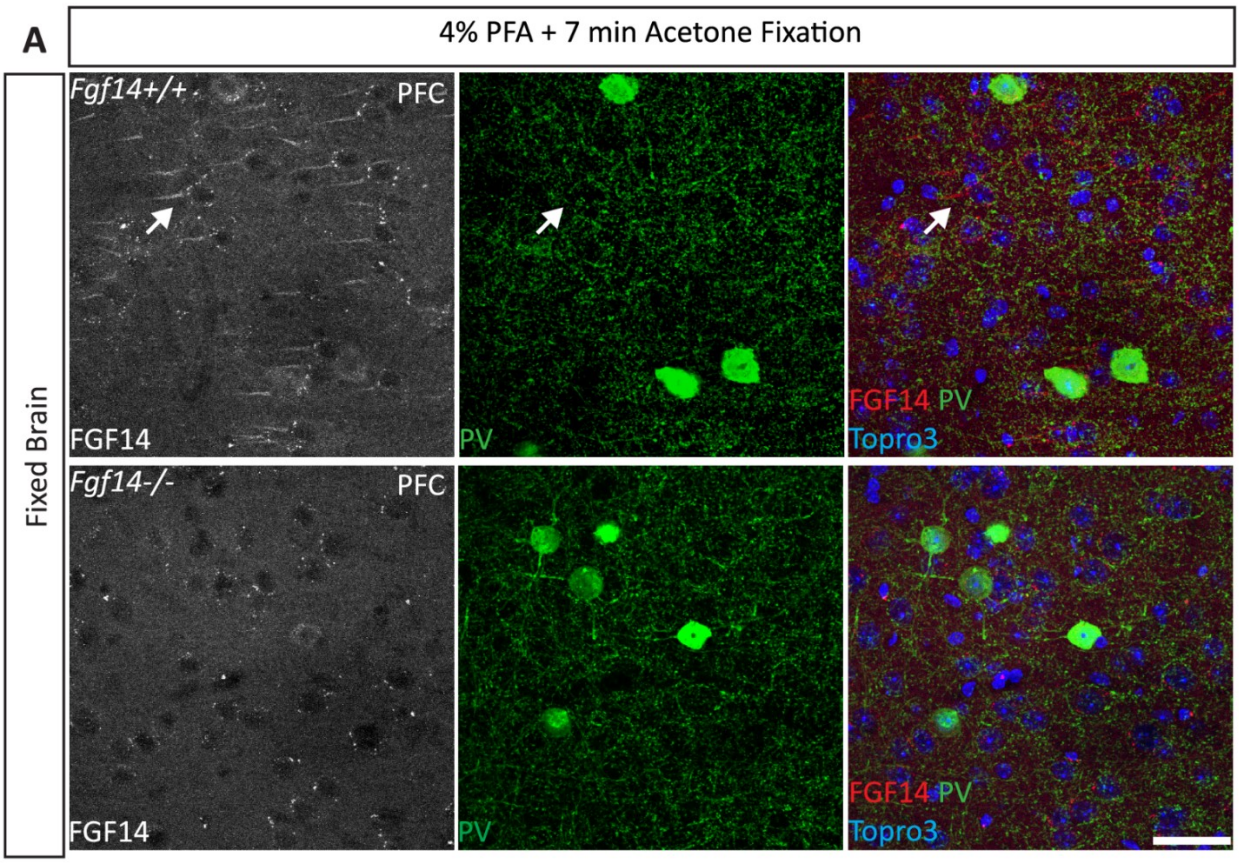

Figure 2:4 Validation the detection of FGF14 axonal signals using Fgf14$^{+/+}$ and Fgf14$^{-/-}$ mouse tissue in 4% PFA fixed tissue treated with cold acetone.
A. Representative images of the sagittal sections, illustrating the immunofluorescent signals of parvalbumin (green), FGF14 (gray and red), and Topro3 (blue), in the prefrontal cortex from *Fgf14*$^{+/+}$ and *Fgf14*$^{-/-}$ mice. The arrows indicate FGF14 immunosignals at the AIS in *Fgf14*$^{+/+}$, but not *Fgf14*$^{-/-}$ tissue. Scale bars represent 20 µm.

2.4 Tissue preparations

2.4.1 Fixed brain preparations.

Brains were allowed to completely sink to the bottom of the container before sectioning. Mouse brain were embedded in Tissue-Tek® medium, then sectioned sagittally into medium thickness slices

(15-25 µm) using a Leica CM1850 cryostat (at -18°C to -20°C). The sections stored in 24 wells-plate, as a free floating slices in a cryoprotectant solution at -20°C. This solution composed of equal amounts of ethylene glycol, glycerol and water, plus some sodium phosphate buffer.

2.4.2 Fresh frozen preparations.

In order to obtain Fgf14 AIS detection at the CA1 region fresh Frozen tissue preparations were used. After anesthetizing the mice by using isoflurane (Baxter, Deerfield, IL), the brain was extracted, allowed to freeze in liquid nitrogen and stored at -80 °C. until use Once needed, the brains embedded in an optimum cutting temperature medium (Tissue-Tek® compound, Ted Pella, Inc, Redding, CA), which allow the brain cryosectioning at a convenient matrix. Using a Leica CM1850 cryostat (Leica Microsystems, Buffalo Grove, IL) we prepared thin sagittal sequential brain sections (10-15 µm). next, we mounted these sections on glass microscope slides (Fisherbrand® Superfrost Plus, Fisher Scientific, Pittsburgh, PA). After that sections were allowed to dry overnight at room temperature. The following day, the slides were stored at -80 °C until use.

2.5 Cresyl violet

To choose an anatomically matched sections **Figure 2:5**, we performed Cresyl violet staining. Two sagittal brain sections (25 µm) adhered to a positively charged slides (Poly-Prep Slides, Sigma-Aldrich, product number P0425) and kept at room temperature overnight to dry. Then, the slides were washed with water, followed by immersion in 100% xylene, for 3o min in three different wells, to allow tissue defatting. Next, the tissue undergoes alcohol rehydration. Followed by submerging the slides in cresyl violet (Sigma-Aldrich) for 30 min before another alcohol dehydration. Images were acquired using a Zeiss SteREO Discovery.V20 microscope along with AxioCam MRc5 and AxioVision Imaging System 4.8 software. Data were analyzed with ImageJ US NIH (http://imagej.nih.gov/ij).

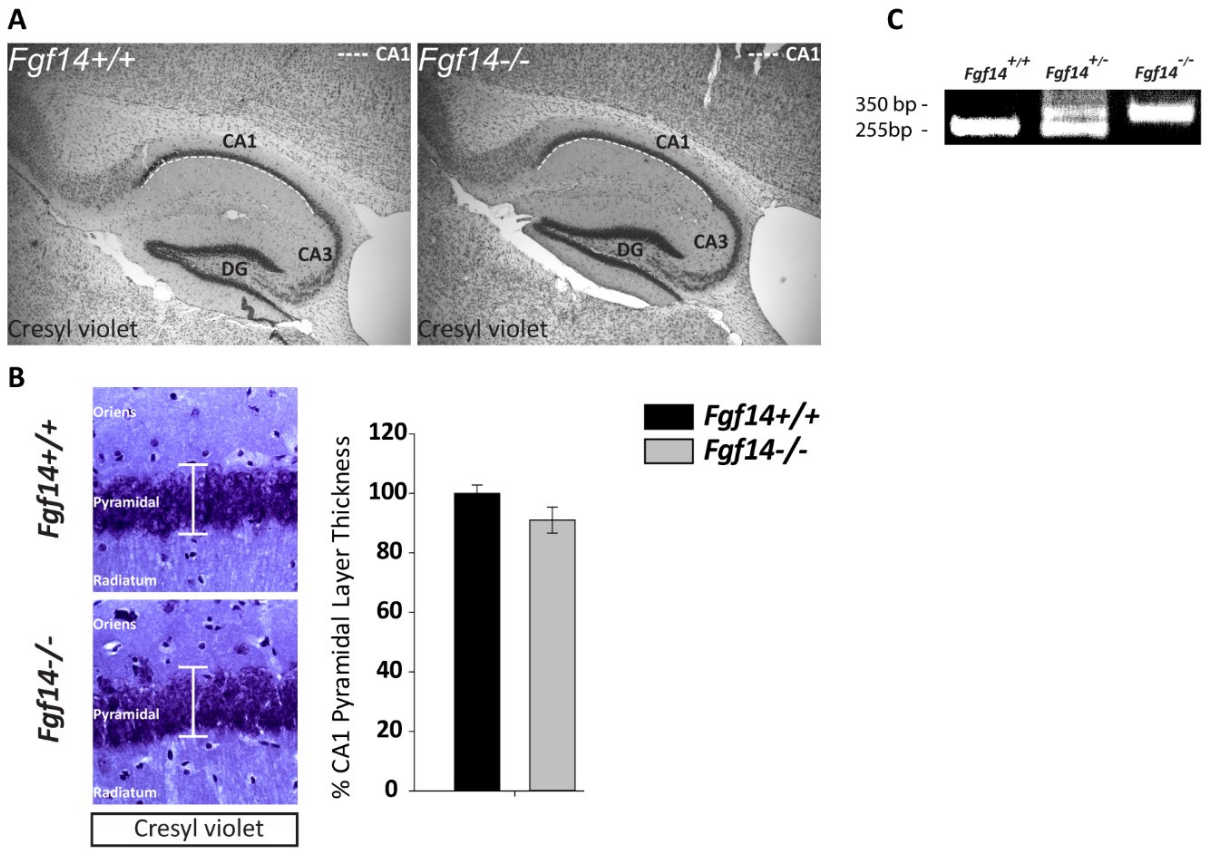

Figure 2:5 The gross morphology of hippocampus in *Fgf14*$^{-/-}$ mice.
A. Representative images of the entire hippocampal sagittal sections using Cresyl violet staining. **B.** Zoomed images of CA1 region, and the volumetric quantifications of the CA1 layer thickness. **C.** Example of *Fgf14*$^{+/+}$ and *Fgf14*$^{-/-}$ bands detection by PCR.

2.6 Immunofluorescence

As described in (Alshammari et al., 2016) *Fgf14*$^{-/-}$ and *Fgf14*$^{+/+}$ age matched mice were transcardially perfused with PBS followed by 4% paraformaldehyde. For studies in chapter three we used 4-5 month old male mice and from each animal we used four issue sections. Brains were removed from the skull, post-fixed in 4% paraformaldehyde overnight, and soaked in 20% sucrose. For FGF14 staining in CA1, whole brains were removed, frozen in liquid nitrogen vapor, and stored at -80 °C until sectioning. 14 and 25-µm-thick sagittal sequential brain sections prepared using Leica CM1850 cryostat. Free floating sections pre-incubated with permeabilizing agent (1% triton, 0.5% tween in PBS or acetone), then incubated with a blocking buffer (10% NGS

in TBST) for 1 h followed by overnight incubation at 4 °C with a primary antibody diluted in the blocking buffer. Primary antibodies are listed

Table 2:2. After five washes in 1% PBS the sections were incubated with appropriate secondary antibodies (Vector Laboratories). Counter staining using To-pro-3 (1:3000). Finally, sections were mounted on Superfrost® glass microscope slides (Fisher Scientific, Waltham, MA) and cover slipped with Prolong Gold anti-fade reagent (Invitrogen).

Antibody	**Source**	**Company**	**Cat #**	**Conc.**
Active Caspase-3	Rabbit	Millipore	AB3623	1/1000
FGF14	Mouse	NeuroMabs	N56/21	1/300
GAD67	Mouse	Millipore	MAB5406	1/500
GABAa Alpha1	Guinea big	Synaptic system	224 204	1/500
GABAa Alpha2	Rabbit	Synaptic system	224 103	1/500
Gephyrin	Rabbit	Abcam	Ab25784	1/400
Nav1.1	Rabbit	Alomone Labs	ASC-001	1/500
NeuN	Mouse	Millipore	MAB377	1/750
NeuN	Guinea pig	Synaptic system	266 004	1/250
PV	Rabbit	Abcam	Ab11427	1/1000
PV	Mouse	Swant	PV235	1/500
Spectrin	Chicken	Gift from Dr. M. Komada, Tokyo Institute of Technology, Japan		1/500
PanNav	Rabbit	Alomone Labs	ASC-003	1/300

Table 2:2 The primary antibodies used in this study.

2.7 Data acquisition and image analysis

Confocal Images acquired using Zeiss LSM-510 META confocal microscope with a Plan-Apochromat (20x/0.75na) objective, a C-Apochromat (40x/1.2 W Corr) objective, and Plan-Apochromat (63x/1.46 oil) objective, with consistent gain and offset settings as well as number of

confocal images Z-stacks. Multitrack acquisition was performed with excitation lines at 488 nm for Alexa 488, 543 nm for Alexa 568, and 633 nm for A647. Z-series stack confocal images were taken at different intervals: 1 µm for 20x, 0.6 µm for 40x objective and 0.4 µm for 63x objective with a same pinhole setting for all three channels. With a frame size of 1024 X 1024 pixels (for cell counting) and 512 X 512 pixels (for PV, GAD67 and VGAT fluorescence intensity analysis). All confocal images were analyzed with software ImageJ US NIH version 1.483 (http://imagej.nih.gov/ij).

PV total neuronal populations cell counting.

Z-stack of confocal images (6 stacks per image) of PV interneurons and total neuronal population were quantified using an integrated Cell Counter plugin (ImageJ software, cell_counter.jar) and automated cell counting macro after applying the same threshold. For inclusion/exclusion criteria A well-defined somatic signal was counted as a cell.

PV, GAD67 and VGAT fluorescence intensity in PV soma and PV soma size.

Z-stack confocal images (8-10 stacks per image) were sum-projected with ImageJ and mean of gray value, and soma size quantified using automatic macro allow to highlight ROI of well-defined PV soma co-labeled with either GAD67 or VGAT.

GAD67 and VGAT positive perisomatic puncta analysis.

In CA1 SP sublayer 8-10 stacks of confocal images were acquired in an area negative to PV cell body using a 63x/1.46 oil objective (1.4 zoom lens). Where puncta fluorescence intensity, number, and size were quantified using automatic macro allow to highlight ROI of puncta with 0.1-10 µm^2 area size within enclosed area (102.04 x 102.04 µm). For fluorescence intensity measurements in the soma inclusion/exclusion criteria, only cells with a well-defined soma were included in the analysis.

Gephyrin, GABAA alpha-1, and alpha-2 puncta analysis.

The fluorescence quantifications conducted on sum projected confocal images acquired with 63x/1.46 oil objective (0.7 zoom lens). The puncta were quantified using automatic threshold-based macro allows highlighting ROI of puncta with 0.5-10 μm^2 area size within enclosed area (202. 3 x 202. 3 μm) at an image resolution of 512 X 512 pixels.

Caspase-3 activity analysis.

We performed NeuN/caspase-3 double immunolabelling experiments to quantify possible apoptotic activities. Caspase-3 immunoreactivity was quantified using NeuN mask. Confocal images acquired with a 63x/1.46 oil objective. Images converted to a gray scale Then threshold adjusted to create the mask at the NeuN channel. The fluorescence intensity was measured and quantified in all sections.

Nav1.1, ankyrin-G, and spectrin AIS analysis

For the fluorescence intensity quantifications in hippocampal CA1 region, a sum-projected Z-stack confocal images acquired with a 63x/1.46 oil objective (0.7 zoom lens) at a resolution of 512 X 512 pixels. The AIS ROI was highlighted using a threshold-based detection within enclosed area (202. 3 x 202. 3 μm).

2.8 Quantification of the PV positive neuropil

To estimate the density of the PV positive neurite network in the str. oriens and str. radiatum of the CA1 region, we used an *ad hoc* automated algorithm whose main step is an image segmentation routine based on support vector machines (SVM) targeted to vessel-like structures(Jimenez et al., 2014). This segmentation routine was first applied to the blue image channel in combination with a morphological closing operator to identify str. pyramidalis in the CA1 region and compute a corresponding mask M. To capture the neurite network in str. oriens and str. radiatum, located above and below str. pyramidalis, respectively, the mask M was displaced by a fixed vertical distance d (d=2X the average width of the mask M) to produce two

other identical masks M_{so} and M_{sr}. The image segmentation routine was then applied to the green channel image (PV staining) to separate neurites from background. The density of neurites in str. oriens and str. radiatum was then estimated by computing the area occupied by neurites within M_{so} and M_{sr} divided by the total area of the mask. Somas within the strata were excluded from the analysis using a blob detection routine. Figure 3:2 summarizes the steps of the algorithm.

2.9 Western blotting for GAD67 and VGAT expression levels

Western blotting was performed according to a previously described method (Tempia et al., 2015). Briefly, *Fgf14*$^{+/+}$ and *Fgf14*$^{-/-}$ mice (n=4 mice per group) hippocampal tissues were homogenized and lysed in a RIBA buffer on ice (Thermo Fisher Scientific). To prevent proteolysis and maintain protein phosphorylation protease and phosphatase inhibitors were added to the extraction buffer. The protein content was measured using Pierce™ BCA Protein Assay Kit (Thermo Fisher Scientific), then 30µg of the protein samples were mixed with 4x sample buffer SDS containing 50 mM TCEP (tris(2-carboxyethyl) phosphine), denatured 10 min 56ºC and run on 7.5% polyacrylamide gel (Bio-Rad Laboratories, Hercules, CA). Gels are electophoretically transferred into PVDF nitrocellulose membranes (Millipore, Bedford, MA) using a cold pack and pre-chilled transferring buffer contain in final concentration (mM) 20 Tris, 150 Glycine at pH 8 for 1.5–2 hr, 75 V. Membranes were blocked with 2-3% non-fat dry milk in 1X Tris-buffered saline contains 0.1% Tween-20 (TBS-T) for 30 min and then incubated in a blocking buffer containing primary mouse monoclonal anti-GAD67 (1:7500, Millipore); mouse monoclonal anti-VGAT (1:3500, Millipore); mouse β-GAPDH antibody as a loading control (1:5000; Thermo Fisher Scientific) overnight at 4ºC. After three times washing with TBS-T for 30 min, nitrocellulose membranes were then incubated with horseradish-peroxidase conjugated secondary antibodies for 2 hr in TBS-T containing 2-3% non-fat dry milk followed by three more times

washing with TBS-T. Finally, nitrocellulose membrane was treated with ECL select western blotting detection reagent (GE Healthcare, Piscataway, NJ) and protein bands were visualized using FluorChem® HD2 System and analyzed using the publically available ImageJ/Fiji (fiji.sc/) software. Rectangular areas were drawn and overlaid on each band and mean gray intensity values of high resolution. TIFF imaging files were used for quantification.

2.10 Whole-cell patch-clamp electrophysiology

Horizontal hippocampal slices were prepared from *Fgf14*$^{+/+}$ and *Fgf14*$^{-/-}$ mice. Spontaneous and miniature inhibitory postsynaptic currents were recorded at room temperature from CA1 pyramidal neurons, using a Multiclamp 700B amplifier (Molecular Devices, Union City, CA). Recordings were filtered at 2.2 kHz and digitized at 10–20 kHz using a Digidata 1322A analog-to-digital interface and pClamp9 acquisition software (Molecular Devices, Union City, CA). Patch pipettes (~4 MΩ) were prepared from borosilicate glass using a Narishige PC-10 vertical puller. The extracellular bath solution contained (in mM) 130 NaCl, 3.5 KCl, 10 glucose, 2 MgCl2, 2.5 CaCl2, 23 NaHCO3, 1.25 NaH2PO4, osmolarity 300-310, pH 7.4 and the intracellular recording solution contained (in mM) 130 CsCl, NaCl 8, 10 HEPES, 10 EGTA, 4 MgATP, 0.4 NaGTP, and 5 QX314, osmolarity 280-290, pH 7.3. In experiments with miniature inhibitory postsynaptic currents registration 1 μM of tetrodotoxin (TTX) was added. Briefly, after seal formation and membrane rupture, sIPSCs and miniature IPSCs were recorded at holding potential of -80 mV. Both sIPSCs and mIPSCs for each cell were analyzed using MiniAnalysis 6.0 (Synaptosoft, Justin Lee). The threshold amplitude for the detection of an event was adjusted to 5pA (≥2S.D. above noise level).

2.11 *In vivo* EEG

For recording of extracellular field potentials in freely behaving mice, stainless steel wires were implanted in the right hippocampus (CA1). Electrodes were built with a stainless steel wire (∅ 150 μm) connected to a gold pin. Electrodes were stereotaxically implanted in CA1 according to the following coordinates: AP = -2.1, L= 1.5, V= -1.6. A screw connected to a different gold pin over occipital areas served as reference and ground. All implants were secured using dental cement. After surgery, mice were allowed to recover for 7 days before testing. All recordings were performed in a customized Faraday chamber. Local field potentials (LFPs) were recorded and initially digitalized at 4 kHz and stored on a hard drive for offline analysis. Five 2-s epochs were visually examined and power spectra of artifact-free segments were computed using fast Fourier transforms by using the NeuroExplorer software with a 0.25 Hz resolution. Gamma power spectrum was divided into low-gamma (30-65 Hz), and high-gamma (65-100 Hz). Spectrograms were calculated using the NeuroExplorer software. At the end of each experiment, electrode placement was histologically verified with Nissl staining.

2.12 Behavioral test

The eight arm radial maze test was performed in young animals between 2 and 4 months of age. All mice were transported to the testing room and left undisturbed for at least 1 h before beginning any behavioral protocol. At the end of each trial, the apparatus was accurately cleaned with 2% ethanol and water. All behavioral procedures were video-recorded and scored by an individual blind to the genotype of the mouse. The maze consisted of eight identical arms (length: 24 cm, width: 6, 5 cm, height: 15 cm) extending radially from an octagonal central area. At the end of each arm, there was a well (1 cm deep) in which reward (0.1 mL of saccharine solution) was placed. The apparatus was elevated 60 cm above the floor and surrounded by extra-maze cues such as posters and objects, necessary for spatial orientation. Beginning on the day prior

to the adaptation phase, the animals were water deprived for 24 h, and then their access to water was restricted to 2 h per day in their home cages, after the test. Food was freely available during the time of experiments. Mice were trained for four consecutive days, and the test was performed on day five. During the experiment, the maze was maintained in a constant orientation. We performed the 4-8 version of eight-arm radial maze as previously described (Satoh et al., 2007). During the training phase mice were trained once per day for four days. Only four arms were baited (arms 1, 3, 5, 7). Each mouse was placed in the central area of the maze with all arms closed. After 10 s, only the doors of the 4 baited arms were opened and the animal was allowed to explore the baited arms for 10 min while the other four arms were kept closed. The fifth day (the test day) all arms were opened with only four arms baited. Each mouse was placed in the center of the maze with all arm entries closed. After 10 s, the doors were opened and the mouse was permitted to enter any of the eight arms. The same four arms baited in the adaptation phase were baited also in this phase (arms 1, 3, 5, 7). The trial ended after either all the saccharine solution was consumed or after 10 min had elapsed, whatever occurred first. An arm entry was counted when all four paws of the animal crossed the entrance of the arm. The time necessary to consume the saccharine solution in all baited arms was defined as latency. Re-entry in a previously visited arm was considered a working memory error.

2.13 Functional annotation and pathway enrichment of FGF14 co expression gene network

Identifying the FGF14 coexpression gene network in the relevant disease/tissue was conducted by a web-based query engine provided by SEEK (http://seek.princeton.edu/). We used default the value for search options. Dataset aggregation was set up as CV RBP weighted, which was a cross-validated, query-based dataset weighting, followed by a combination of datasets' co-expression scores using the relevance weights; the fraction of query genes in each dataset should

cover at least 50%; the fraction of genome in each dataset should cover at least 50%; the distance measure was set up as Z-score of correlation with gene connectivity correction; the RBP parameter p was set up as 0.99. The refined search in SEEK was conducted by selecting different brain regions relevant to schizophrenia, including PFC, HIP, Caudate nucleus, and Substantia Nigra. As the software described, all the available datasets for each category should be included as long as the expression data for that particular gene we were interested was observed. We provided the co-expressed genes with their RANK, Coexpression Score, and p value. The detail for the calculation was documented in http://seek.princeton.edu/faq.jsp. Since we only reported a list of candidate genes coexpressed with FGF14 in a tissue-specific manner, we did not provide cut-off for RANK and p value.;"an enriched dataset" referred to the dataset weighted the highest based on the weighting algorithm used by SEEK. The detail for the calculation is documented in http://seek.princeton.edu/faq.jsp (No 4 and 5). The enriched datasets represent the dataset weighted highest in each tissue type. Functional annotation and pathway enrichment analysis with GO and KEGG terms were also performed using the built-in advanced analysis tool in SEEK. We selected the top 200 and then extended to 500 coexpressed genes for the subsequent pathway analysis with KEGG or GO Biological process terms. We only reported pathway analysis results from top 500 genes because RBP parameter p was set up as 0.99, indicating the top 1000 correlated genes were considered significantly important. Functional categories related to brain were expected since the top enriched co-expression genes were all expressed in that brain region. However, the purpose to perform the pathway analysis with the built-in analysis tool in SEEK was to identify which brain-related function was mostly enriched to the top in FGF14 coexpression gene network in HIP or PFC. Finally, enriched datasets, with the corresponding accession number, were downloaded from NCBI GEO and the global differential gene expression between control and schizophrenia samples

was further analyzed by R Limma package from quality assessment, data transformation, to linear models with eBayes fit.

R script for LIMMA package was obtained from www.ncbi.nlm.nih.gov/geo/geo2r/with some modification. This script included auto-detect log2 transform which is commonly used for Affymetrix array data as showed below. Value distributions for each sample can be viewed as a box plot for QC purpose. According to GEO database, Submitters were asked to supply normalized data in the VALUE column, so that the samples in data dataset were cross-comparable. The data normalization method was described in the original manuscripts (Iwamoto et al., 2005;Narayan et al., 2008).

Subjects were allocated to schizophrenia and controls based on clinical diagnostic criteria which were described previously. The control group was matched to the schizophrenia group in terms of gender and age in two independent datasets. The covariates such as age, gender, and sample pH were included in the linear model as showed in the following equation for dataset GSE21138 but not for GSE12649 (covariates not available from NCBI GEO database). design <- model.matrix(~ description + ph + AGE +Sex + 0, gset). Linear regression and ANOVA assumed the sample distributed normally. Therefore, we did an initial Leveen test for equality of variance and showed that the dataset for FGF14 did not follow the normal distribution with significant unequal variance particularly in GSE12649. According to the boxplot for the distribution of global gene expression, we identified three subjects having significant decreased median value of global gene expression, suggesting they were systemic outliers. We removed two additional samples because they had a mean >2 SD just like those 3 samples for FGF14. After removing five samples, control and disease groups had equal variance. Other statistical graphics was created by R ggplot or R rmeta package. The final sample size for GSE21138 was 59 (30/29 for SCZ/Control) and that for GSE12649 was 64 (34/30 for SCZ/Control). We did not include any bipolar cases from

GSE12649 and five samples have been removed from the final analysis of GSE12649 due to significant decreased median value of global gene expression according to the boxplot for QC.

2.14 Statistical Analysis

Data were expressed as means ± S.E.M The statistical significance of observed differences among groups was determined by Student's t test or the corresponding nonparametric tests, Mann-Whitney rank sum, based on the distribution of the samples underlying the populations. Patch-clamp electrophysiology data were compared across genotypes with a Kolmogorov-Smirnov probability distribution. For brain weights developmental tracking and PVIs age-related changes we used two-way ANOVA tests and *post hoc* Fisher LSD. A $p< 0.05$ was regarded as statistically significant.

Chapter 3: [2]The effect of *Fgf14* genetic deletion on PVIs, GABAergic presynaptic components, and GABAergic circuitry

Cognitive processing is highly dependent on the functional integrity of gamma-amino-butyric acid (GABA) interneurons in the brain. These cells regulate excitability and synaptic plasticity of principal neurons balancing the excitatory/inhibitory tone of cortical networks. Reduced function of parvalbumin (PV) interneurons and disruption of GABAergic synapses in the cortical circuitry result in desynchronized network activity associated with cognitive impairment across many psychiatric disorders, including schizophrenia. However, the mechanisms underlying these complex phenotypes are still poorly understood. Here, we show that in animal model, genetic deletion of fibroblast growth factor 14 (*Fgf14)*, a regulator of neuronal excitability and synaptic transmission, leads to loss of PV interneurons in the CA1 hippocampal region, a critical area for cognitive function. Strikingly, this cellular phenotype associates with decreased expression of glutamic acid decarboxylase 67 (GAD67) and vesicular GABA transporter (VGAT) and also coincides with disrupted CA1 inhibitory circuitry, reduced *in vivo* gamma frequency oscillations, and impaired working memory. Bioinformatics analysis of schizophrenia transcriptomics revealed functional co-clustering of *FGF14* and genes enriched within the GABAergic pathway along with

---

[2] **This chapter is accepted in Translational Psychiatry (March 2016).**

Part of this chapter was published as conference proceedings paper in American College of Neuropsychopharmacology 54th meeting (December 2015)

correlatively decreased expression of *FGF14*, *PVALB*, *GAD67* and *VGAT* in the disease context. These results indicate that *Fgf14*$^{-/-}$ mice recapitulate salient molecular, cellular, functional and behavioral features associated with human cognitive impairment and *FGF14* loss of function might be linked to biology of complex brain disorders.

3.1 Introduction

Psychiatric diseases such as schizophrenia, depression, and bipolar disorder are associated with cognitive deficits thought to arise from an imbalance between the excitatory and inhibitory (E/I) tone in cortical circuits (Lewis et al., 2012;Nissen et al., 2012). Fast-spiking GABAergic PV interneurons play a fundamental role in maintaining E/I balance, controlling excitability, and shaping the synaptic plasticity of principal neurons (Yizhar et al., 2011). Even though disrupted function of other types of inhibitory neurons has been associated with the etiology of brain disorders, changes in PV neurons are one of the most consistent associations. In animal models, reduced function of PV neurons results in desynchronized network activity, decreased gamma frequency oscillations, and cognitive deficits, phenotypes that mimic clinical presentation and *post-mortem* tissue studies of virtually all human brain disorders associated with disrupted cognition (Lewis et al., 2004;Lewis et al., 2005;Hashimoto et al., 2008;Lewis et al., 2008;Volk and Lewis, 2010;Eggan et al., 2012;Lewis et al., 2012;Curley et al., 2013).

In schizophrenia and bipolar patients, the number of PV interneurons and the expression level of molecular components of GABAergic synapses, such as GAD67, VGAT, are found decreased in *post-mortem* brains leading to the "GABA hypofunction hypothesis" as a potential etiology (Conde et al., 1994;Beasley et al., 2002;Zhang and Reynolds, 2002;Knable et al., 2004;Torrey et al., 2005;Guidotti et al., 2011;Lewis et al., 2012). Yet, the molecular understanding of how such a detrimental loss of the GABAergic system might lead to corrupted cortical networks manifesting in disease remains poorly explored.

Recent large-scale genome-wide association studies (GWAS) identified *FGF14* as a locus of SNPs and as such a potential disease-associated gene for schizophrenia, bipolar disease, depression, epilepsy, and addictive behaviors (Liu et al., 2006;Jungerius et al., 2008;Drgon et al., 2010;Hodgkinson et al., 2010;Brennand et al., 2011;Hu et al., 2011;Verbeek et al., 2012;Hunter et

al., 2013;Spencer et al., 2013;Chen et al., 2014;Olson et al., 2014), corroborating initial reports of missense mutations in *FGF14* as genetic links to the neurodegenerative disorder, spinocerebellar ataxia 27 (Van Swieten et al., 2003;Brusse et al., 2006). These results highlight the possibility of an as yet undiscovered and pivotal role for the *FGF14* gene in psychiatric disorders.

Highly expressed in the CNS, FGF14 is an accessory protein of voltage-gated Na+ (Nav) channels at the axonal initial segment (AIS) (Laezza et al., 2007;Goetz et al., 2009;Laezza et al., 2009;Shavkunov et al., 2012;Shavkunov et al., 2013;Ali et al., 2014;James et al., 2015), a regulator of neuronal excitability (Goldfarb et al., 2007;Laezza et al., 2007;Shakkottai et al., 2009;Bosch et al., 2015), a presynaptic organizer of glutamatergic synapses (Yan et al., 2013;Xiao et al., 2007), a scaffolding molecule for kinase signaling pathways (Shavkunov et al., 2012;Shavkunov et al., 2013;Hsu et al., 2014;Hsu et al., 2015) and a regulator of synaptic plasticity (Wang et al., 2002;Wozniak et al., 2007;Xiao et al., 2007). At the circuitry and behavioral level, genetic deletion of FGF14 in *Fgf14*$^{-/-}$ mice results in presynaptic structural deficits of CA3-CA1 hippocampal synapses, decreased long-term potentiation (LTP), and cognitive deficits, aberrant responses to epileptic agents, and decreased threshold for seizure induction (Wang et al., 2002;Wozniak et al., 2007;Xiao et al., 2007). Furthermore, *Fgf14*$^{-/-}$ mice exhibit abnormal locomotor activity explained by a reduced response to dopamine receptor D2 agonists in the basal ganglia (Wang et al., 2002). Both phenotypes in the hippocampus and the basal ganglia could imply an impaired GABAergic tone supporting the emerging view of a tight correlation between the dopamine and the GABAergic systems (Shah and Lodge, 2013;Boley et al., 2014). Yet, evidence of FGF14 control of GABAergic inhibitory transmission is lacking.

Using a combination of confocal microscopy, patch-clamp electrophysiology, *in vivo* local field potential recordings, and behavioral studies, we discovered that genetic deletion of *Fgf14* in rodents leads to a reduced number of PV interneurons, decreased expression of GAD67 and VGAT,

and reduced GABAergic transmission in CA1 pyramidal neurons associated with impaired gamma oscillations and working memory. Further, bioinformatics analysis of schizophrenia transcriptomics confirms FGF14 functional clustering with GABAergic synaptic signaling and identifies genetic covariance of *FGF14, PVALB*, *GAD67*, and *VGAT* in the disease, supporting *Fgf14*$^{-/-}$ mice as an attractive model to interrogate the biology of complex brain disorders associated with disrupted cognitive circuitry such as schizophrenia.

3.2 Material and Methods

Methods for *Fgf14*$^{-/-}$ colony maintenance, perfusion, tissue preparation and sectioning, Immunofluorescence, image acquiring and analysis, cresyl violet, Western blotting, Whole-cell patch-clamp electrophysiology, *in vivo* EEG, eight-arm radial maze behavioral test, and computational analysis on human transcriptomic studies were outlined previously in this work. A complete description of these techniques is detailed in **Chapter 2**.

3.3 Results

Anatomical abnormalities found in the CA1 hippocampal region of *post-mortem* brains from schizophrenia patients have been identified as an index of the disease severity and treatment responsiveness (Zierhut et al., 2013).These studies along with the reported association between hippocampal PV neurons with cognitive function in the normal brain and in schizophrenia, prompted us to begin our investigations in the CA1 hippocampal region (Zhang and Reynolds, 2002;Torrey et al., 2005;Shah and Lodge, 2013;Zierhut et al., 2013;Boley et al., 2014). Thus, we first asked whether FGF14 was expressed in PV interneurons in the CA1 region. Confocal imaging confirmed that FGF14 is expressed at the AIS of cells across all CA1 sub-layers **Figure 3**:1**A** including PV positive neurons **Figure 3**:1**B**. Therefore, we posited whether genetic ablation of *Fgf14* might have physiological consequences for these inhibitory neurons.

To test this hypothesis, we first examined whether the overall number of PV interneurons in the CA1 area was affected by genetic loss of FGF14. Cell count quantification based on immunofluorescence staining revealed that the total number of PV positive cells was significantly reduced in *Fgf14*$^{-/-}$ mice compared to wild type controls (**Figure 3**:1**C-E** 74.21% ± 5.02, 100% ± 4.89, $p<0.001$), consistent with observations in schizophrenia postmortem tissue analysis(Beasley and Reynolds, 1997;Hashimoto et al., 2005). The most pronounced and significant reduction in the stratum oriens (SO; 71.42% ± 6.96, 100% ± 8.10 $p<0.05$) and in stratum pyramidalis (SP; 77.94% ± 4.96, 100% ± 7.06 $p<0.05$, **Figure 3**:1**F**).

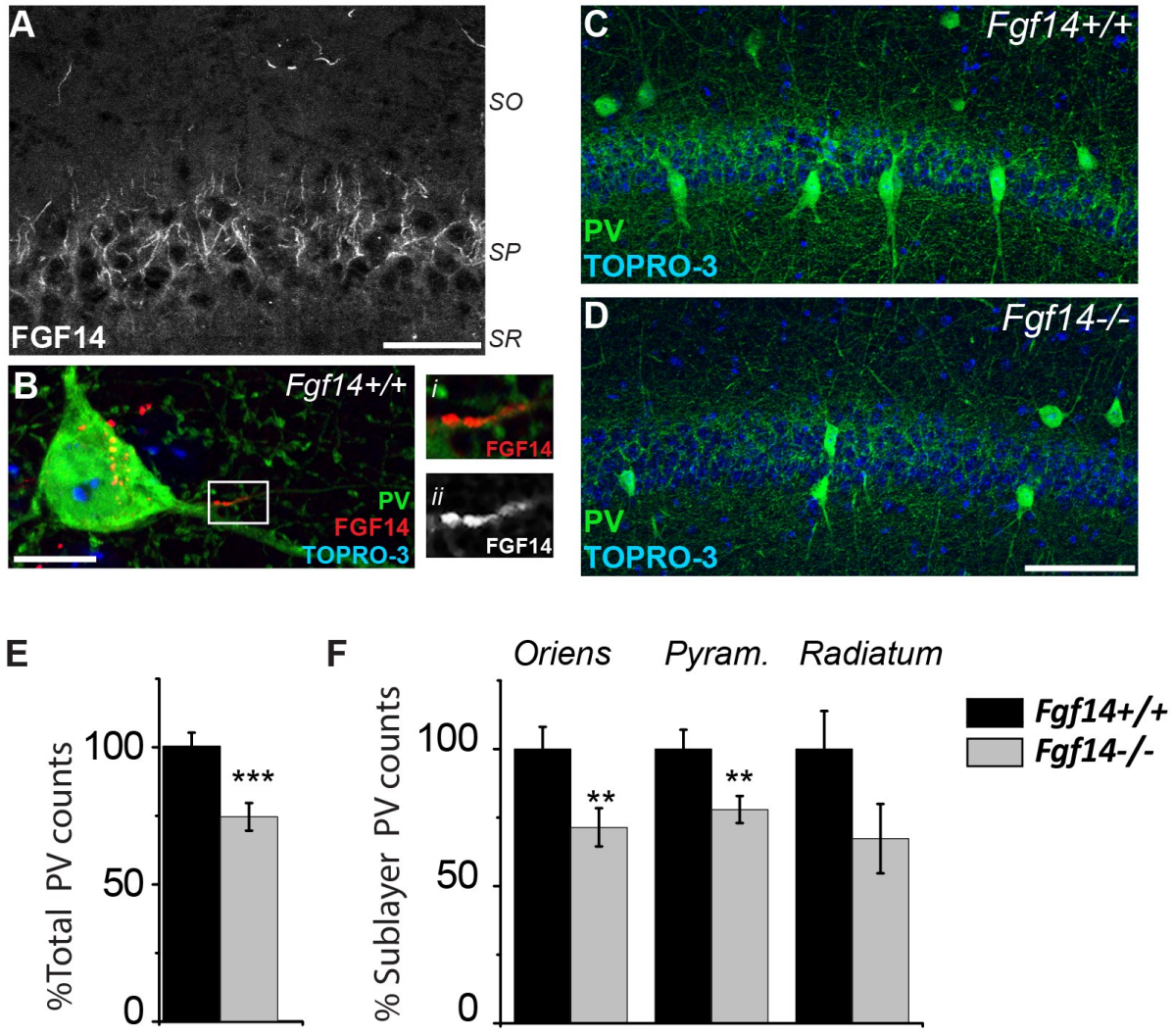

Figure 3:1 Genetic deletion of *Fgf14* results in structural changes in the CA1 PVIs.
A. FGF14 immunoreactivity is detectable at the AIS of cells in CA1. **B.** FGF14 expressed in the soma and AIS of PV interneurons (green), FGF14 (red), **i** and **ii** represent zooms of the boxed area. **C, D.** PV interneurons in the CA1 region of *Fgf14*$^{+/+}$ and *Fgf14*$^{-/-}$ mice and respective higher resolution views of PV somas (**i, ii**). **E, F.** Quantification of total PV interneurons in CA1 (n=4 mice per group, 5-7 sections per mouse), and in specific sub-fields (oriens, pyramidalis, and radiatum). Data represent mean ± SEM, ***$p<0.001$; **$p<0.02$, statistical differences were assessed by Student's t-test or non-parametric Mann-Whitney test. Scale bars: **A**= 40 µm; **B**=10 µm; **D**=100 µm.

Notably, the expression level of PV per cell was not significantly different across groups (p=0.78, n=4 littermate mice **Figure 3**:2 **F-I**); the neuropil composed of PV positive neurites in

either SP or SO was also unaffected by *Fgf14* deletion (p=0.49, p=0.28, **Figure 3**:2 **A-E**). Furthermore, the total number of cells in the CA1 SP, which primarily includes pyramidal neurons, was also unchanged (p= 0.24 **Figure 3**:2 **J-L**). Thus, we concluded that deletion of *Fgf14* leads to a cell- and subfield-specific reduction in the number of PV neurons in the CA1 hippocampal region.

PV interneurons are the primary source of GABAergic synapses in the CA1 region. Reduction in GABA synthesis and its synaptic release machinery accompany loss of PV neurons in schizophrenia and other psychiatric disorders (Hashimoto et al., 2008;Eggan et al., 2012;Curley et al., 2013). Consistent with this, GAD67 mean fluorescence intensity in PV soma, the primary source of the enzyme pool, and in puncta across SP was significantly reduced in *Fgf14*$^{-/-}$ mice compared to littermate control (89.85% ± 3.08, 100% ± 3.96 $p<0.05$, and 91.86% ± 0.10, 100% ± 0.08, $p<0.0001$, respectively, **Figure 3**:4 **A-D** and **Figure 3**:3**A-C**). The area per puncta and total puncta number, though, were unchanged (p=0.10, p=0.88, respectively, **Figure 3**:3**C**).

An additional marker and key regulatory protein at presynaptic GABAergic inputs is VGAT, the vesicular transporter that loads presynaptic vesicles with GABA, another marker associated with brain disorders (Sawada et al., 2002;Sawada et al., 2005;Hoftman et al., 2015). Along with GAD67, the mean fluorescence intensity of VGAT in PV soma and its mean content per puncta in SP were significantly decreased in *Fgf14*$^{-/-}$ mice compared to littermate controls (88.12% ± 3.06, 100% ± 3.18 $p<0.01$, n=4 littermate mice and 91.92% ± 0.14 vs 100% ± 0.135, $p<0.001$, n=3 littermate mice, respectively, **Figure 3**:4 **E-H** and **Figure 3**:3 **D-F**), while puncta area and number were unchanged (p=0.66, p= 0.79, n=3 mice, **Figure 3**:3 **F**). Consistent with these analysis, GAD67 and protein content expression in whole hippocampal cell lysate quantifications revealed reduction to a similar extent compared to the wild type **(Figure 3**:3 **G, H).**

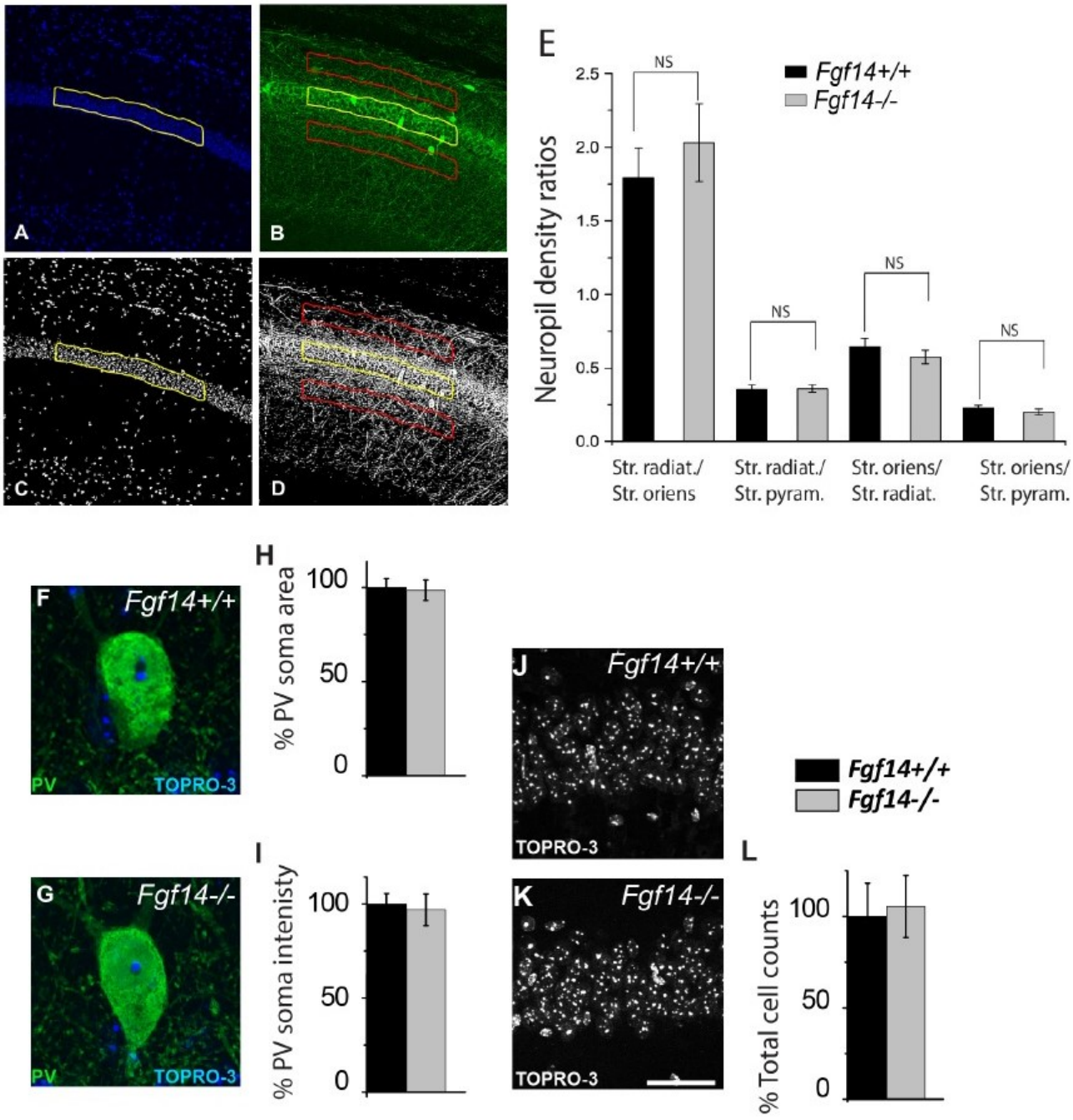

Figure 3:2 PV neuropil density measurement and total neuronal populations quantifications.
A,B. Representative confocal images illustrating Topro-3 (blue channel) and PV staining (green channel) along with overlaying masks in the stratum pyramidalis (yellow), stratum oriens (red, top) and stratum radiatum (red, bottom). **C,D**. Segmented images corresponding to panels A-B. The density of neurites, calculated inside M_{so} and M_{sr} in panel D yields the values 0.2258 and 0.3048, respectively. **E** Bar graph illustrating neuropil density ratios of the CA1 layers. **H**. **H**. Quantification of PV interneuron soma area and PV mean somatic intensity (n=4 mice per group, 5-7 sections per mouse). **J,K**. Total neuronal population in CA1 SP visualized by Topro-3 nuclei staining in *Fgf14*$^{+/+}$ mice and *Fgf14*$^{-/-}$ mice. **l.** Total cell count in CA1(n=3 mice per group, 2-3 sections per mouse).

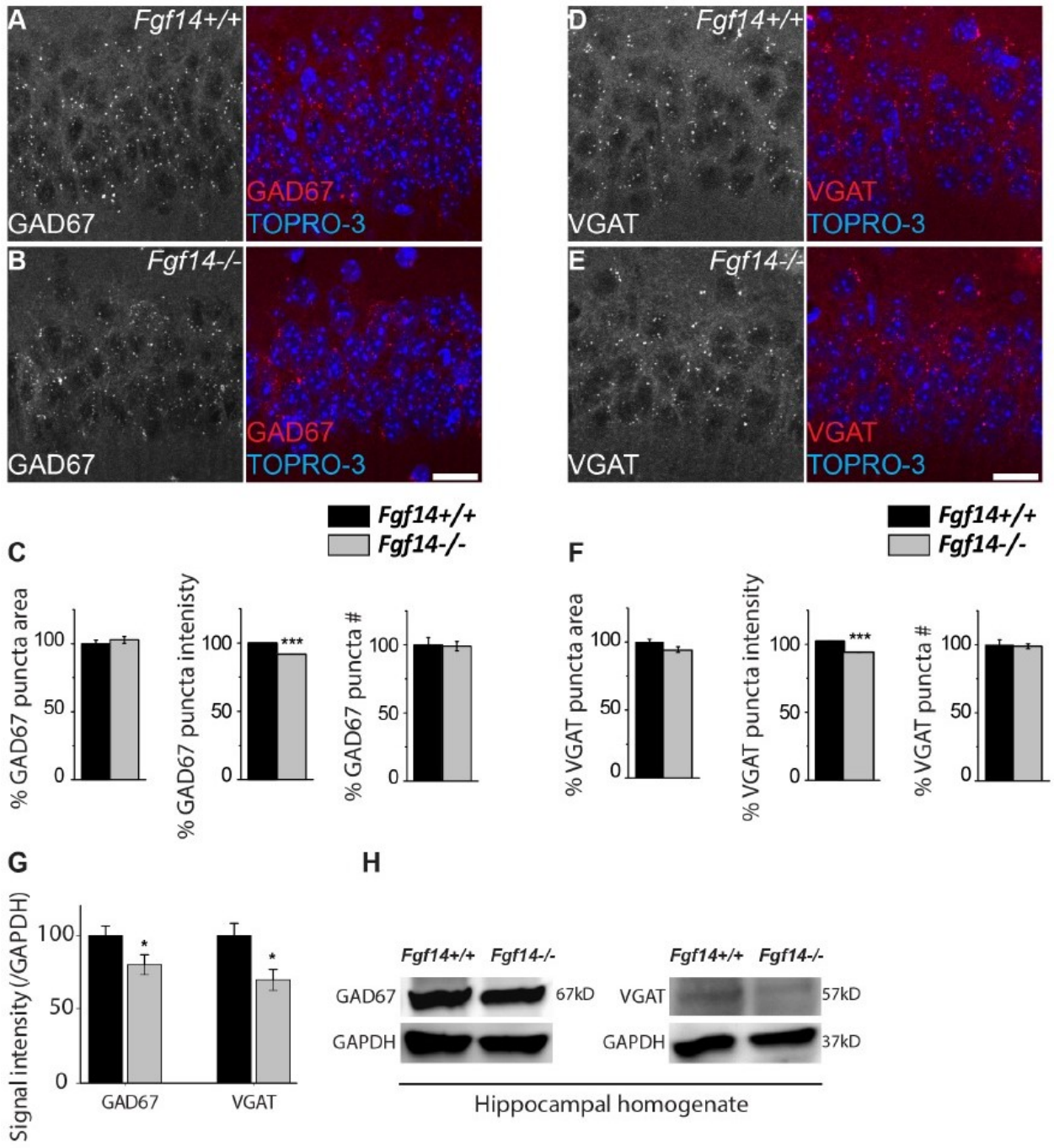

Figure 3:3 The effect of *Fgf14* genetic ablation on GABAergic presynaptic proteins in the hippocampal CA1 region.

A, B. GAD67 representative puncta in CA1 SP at high magnification. **C.** Quantification of GAD67 puncta area, puncta intensity, and puncta number in the indicated genotypes. **D, E.** VGAT representative puncta in CA1 st. pyramidalis at high magnification. **F.** Quantification of VGAT puncta area, puncta intensity and puncta number in the indicated genotypes. For GAD67 and VGAT quantifications (n=4 mice per group, 3-5 sections per mouse**). G.** Quantitative Western blot analysis of GAD67 and VGAT from the hippocampus. **H.** Immunoblot detection of GAD67 and

VGAT in whole hippocampal homogenates from *Fgf14*$^{-/-}$ mice and *Fgf14*$^{+/+}$ controls. Data represent mean ± SEM, ***$p<0.001$; *$p<0.05$ statistical differences were assessed by Student's t-test or non-parametric Mann-Whitney test. Scale bars: **A, D**=20 μm.

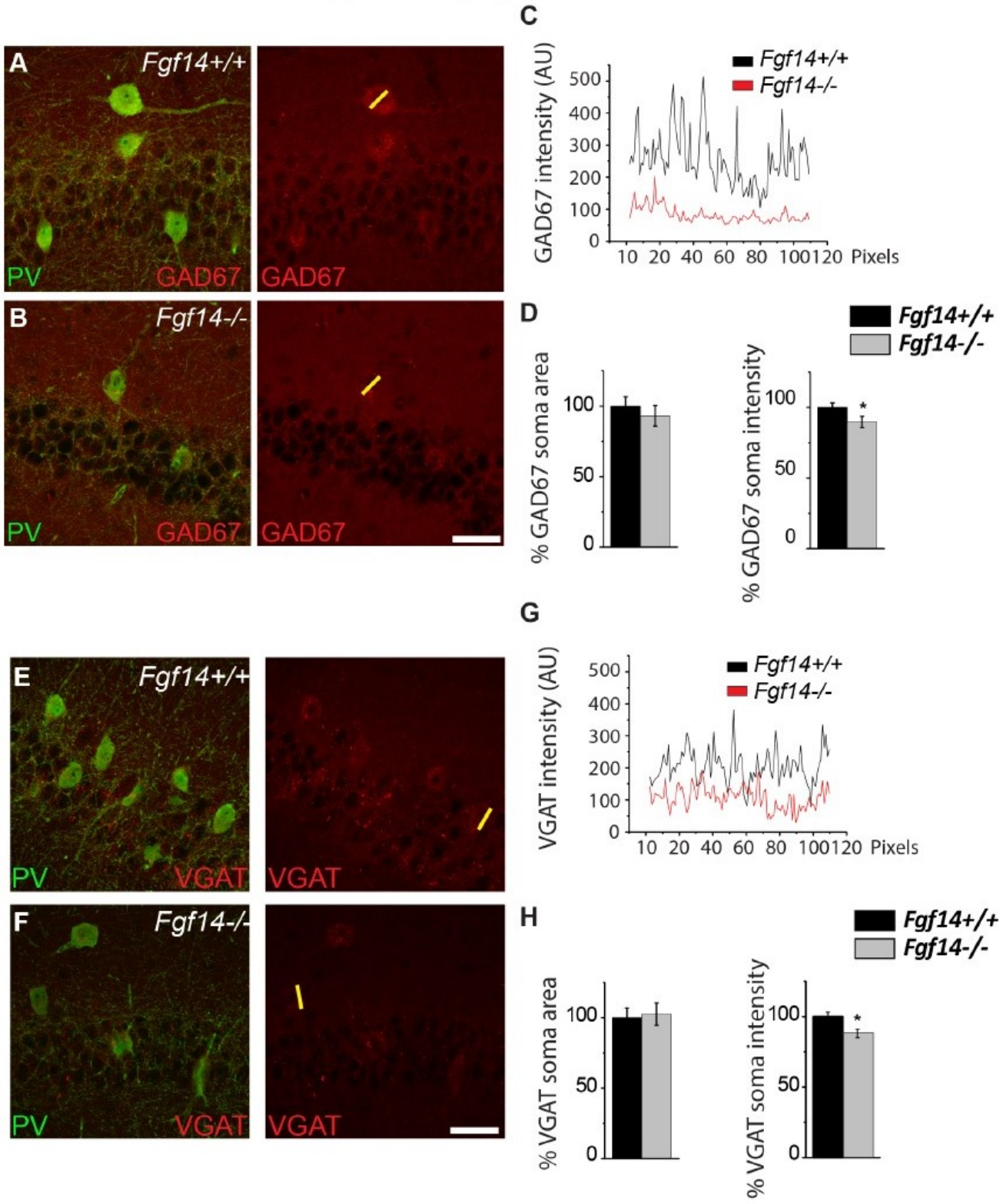

Figure 3:4 Quantifications of GABAergic synaptic components inside PVIs soma.

A, B. GAD67 expression in PV interneurons in CA1, merged image of green channel representing PV expression, and red representing GAD67 expression. **C.** Intensity profile of GAD67 in PV interneuron somas corresponding to the yellow line in **A** and **B**. **D.** Quantification of GAD67 soma area and

fluorescence intensity in PV interneuron somas. **E, F.** VGAT expression in PV interneurons in CA1, merged image of green channel representing PV expression, and red representing VGAT expression. **G.** Intensity profile of VGAT in PV interneuron somas corresponding to the yellow line in **E** and **F**. **H.** Quantification data of VGAT soma area and fluorescence intensity in PV interneuron somas. Data represent mean ± SEM, ***p<0.05* statistical differences were assessed by Student's t-test or non-parametric Mann-Whitney test. Scale bars: **A**, **E**= 40 μm.

PV interneurons contribute greatly to the integrity of the GABAergic circuit in the CA1 region, posing the question of whether *Fgf14* deletion might result in functional consequences for inhibitory transmission. Using patch-clamp electrophysiology, we recorded spontaneous and miniature inhibitory postsynaptic currents (sIPSCs and mIPSCs, respectively) from visually identified CA1 pyramidal neurons in *Fgf14*$^{-/-}$ and wild type control mice (**Figure 3**:5 **A, F**). We found that genetic deletion of *Fgf14* led to a rightward shift in the probability distribution of sIPSCs frequency (apparent loss in the higher frequency domain) accompanied by a reduction in the largest and smallest size synaptic event population (**Figure 3**:5 **C-E**, $p<0.001$, Kolmogorov-Smirnov test). Spontaneous IPSCs are action-potential (AP)-driven synaptic events and as such represent a compound read-out of the firing status of pre-synaptic interneurons and their neurotransmitter release machinery.

To examine GABA release mechanisms independently from interneuron spontaneous firing, we recorded mIPSCs in the presence of TTX and found that, similarly to sIPSCs, the frequency distribution histograms showed lowered probability of short inter-event-intervals in *Fgf14*$^{-/-}$ when compared to wild type control mice (**Figure 3**:5 **F-H** $p<0.001$ with Kolmogorov-Smirnov test). This phenotype was paralleled by a loss of large and small amplitude mIPSCs in *Fgf14*$^{-/-}$ compared to wild type control mice (**Figure 3**:5 **F, I-J**). In both sIPSCs and mIPSCs, the averaged sIPSC frequency and amplitude between the two groups were not significantly different

(**Figure 3**:6) and no changes in rise and decay time were found across synaptic events (both sIPSCs and mIPSCs) of different genetic groups (**Figure 3**:7).

Thus, genetic deletion of *Fgf14* leads to functional changes in the CA1 inhibitory circuitry that support the structural alterations demonstrated in **Figure** 3:1 and **Figure** 3:2. Moreover, it suggests loss of interneuron firing (shift in sIPSCs frequency) and pre- and post-synaptic modifications at GABA synapses (shift in frequency and amplitude distribution of mIPSCs, respectively).

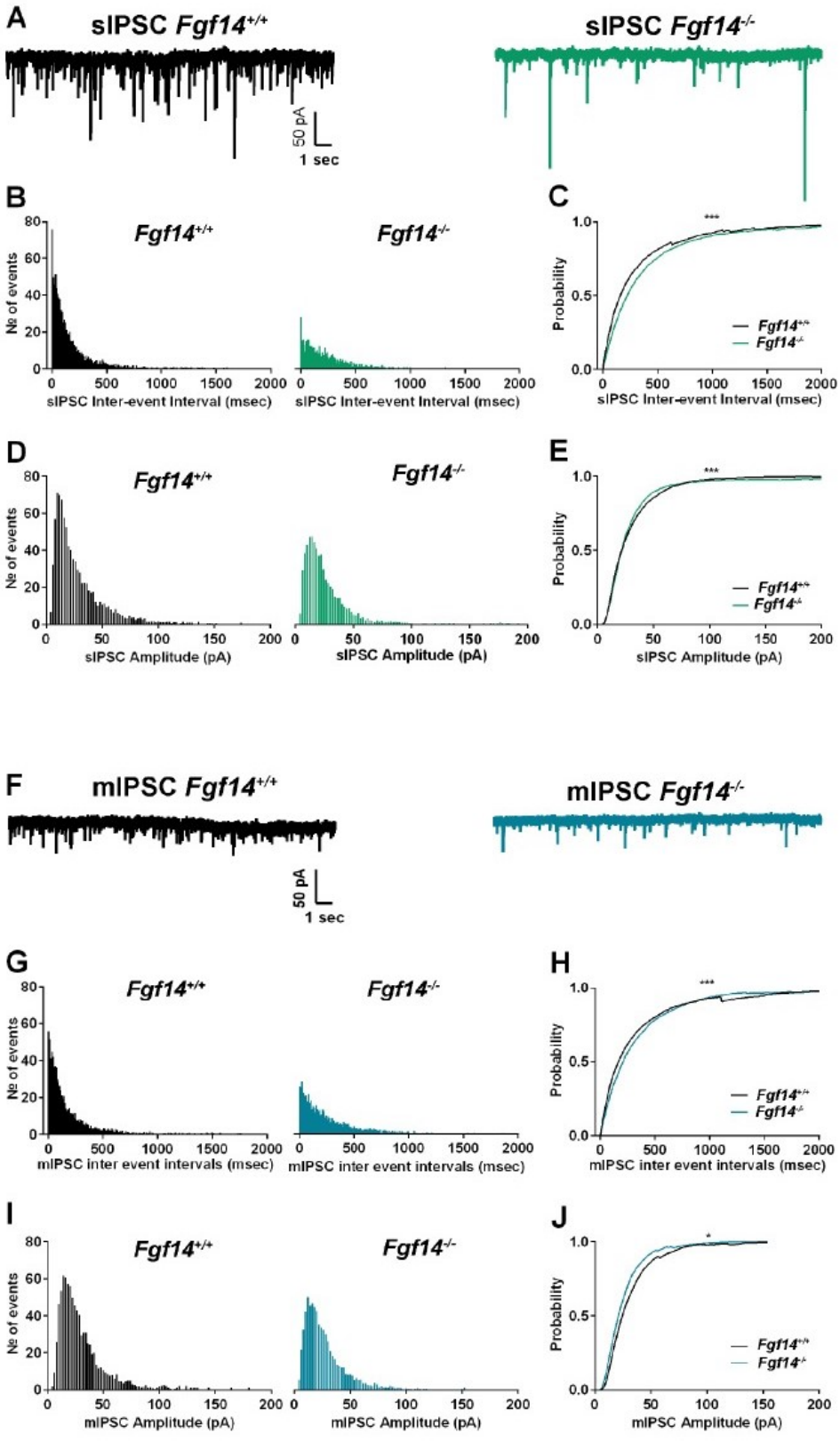
A
sIPSC Fgf14+/+
sIPSC Fgf14-/-
50 pA
1 sec
B
Fgf14+/+
Fgf14-/-
№ of events
sIPSC Inter-event Interval (msec)
C
Probability
***
Fgf14+/+
Fgf14-/-
D
Fgf14+/+
Fgf14-/-
sIPSC Amplitude (pA)
E
F
mIPSC Fgf14+/+
mIPSC Fgf14-/-
G
mIPSC inter event intervals (msec)
H
I
mIPSC Amplitude (pA)
J
*

Figure 3:5 Genetic deletion of *Fgf14* impairs GABAergic transmission in the CA1 region. Representative traces of whole-cell patch-clamp recordings showing effect of *Fgf14* ablation on sIPSCs (**A**) and mIPSCs (**F**). **B.** Inter-event-interval distribution of spontaneous GABAergic events in $Fgf14^{+/+}$ (n=8 cells) and $Fgf14^{-/-}$ (n=10 cells) mice. **C.** Inter-event-interval cumulative distribution plot for $Fgf14^{+/+}$ and $Fgf14^{-/-}$ (sIPSCs; ***p<0.001, Kolmogorov-Smirnov test). **D.** Amplitude distribution of spontaneous GABAergic events in $Fgf14^{+/+}$ (n=8 cells) and $Fgf14^{-/-}$ (n=10 cells) mice. **E.** Amplitude cumulative distribution plot for $Fgf14^{+/+}$ and $Fgf14^{-/-}$ sIPSCs (***p<0.001; Kolmogorov-Smirnov test). **G.** Inter-event-interval distribution of miniature GABAergic events in $Fgf14^{+/+}$ (n=6 cells) and $Fgf14^{-/-}$ (n=7 cells) mice. **H.** Inter-event-interval cumulative distribution plot for $Fgf14^{+/+}$ and $Fgf14^{-/-}$ mIPSCs (***p<0.001 with Kolmogorov-Smirnov test). **I.** Amplitude distribution of miniature GABAergic events in $Fgf14^{+/+}$ (n = 6 cells) and $Fgf14^{-/-}$ (n = 7 cells) mice. **J.** Amplitude cumulative distribution plot for $Fgf14^{+/+}$ and $Fgf14^{-/-}$ sIPSCs (*p<0.05; Kolmogorov-Smirnov test).

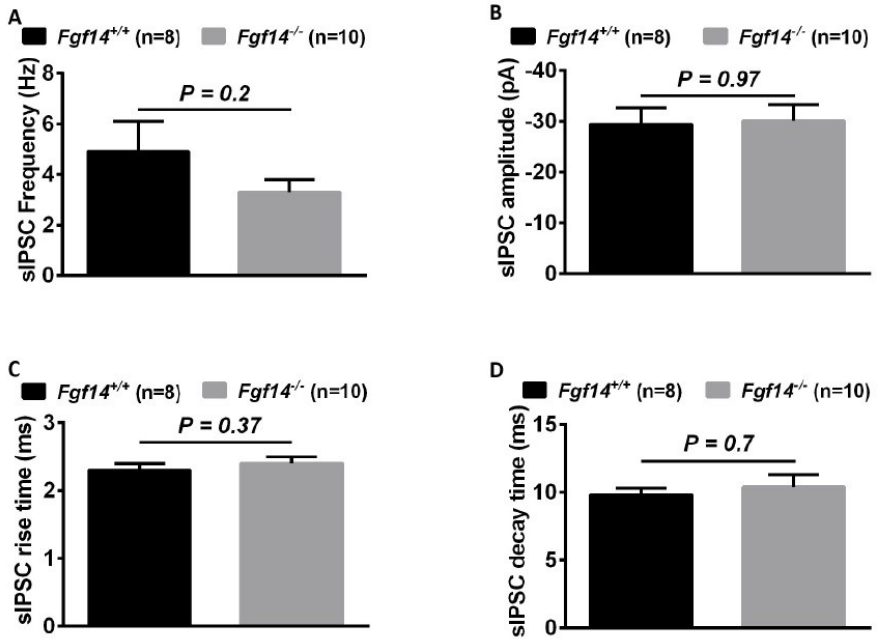

Figure 3:6 Mean values of spontaneous inhibitory postsynaptic currents (sIPSCs). **A.** Mean sIPSC frequency. **B.** Mean sIPSC amplitude. **C.** Mean sIPSC rise time. **D.** Mean sIPSC decay time. Data are mean ± SEM collected from n=8 cells (*Fgf14*$^{+/+}$) and n=10 cells (*Fgf14*$^{-/-}$). *P* values were obtained with Student *t*-test

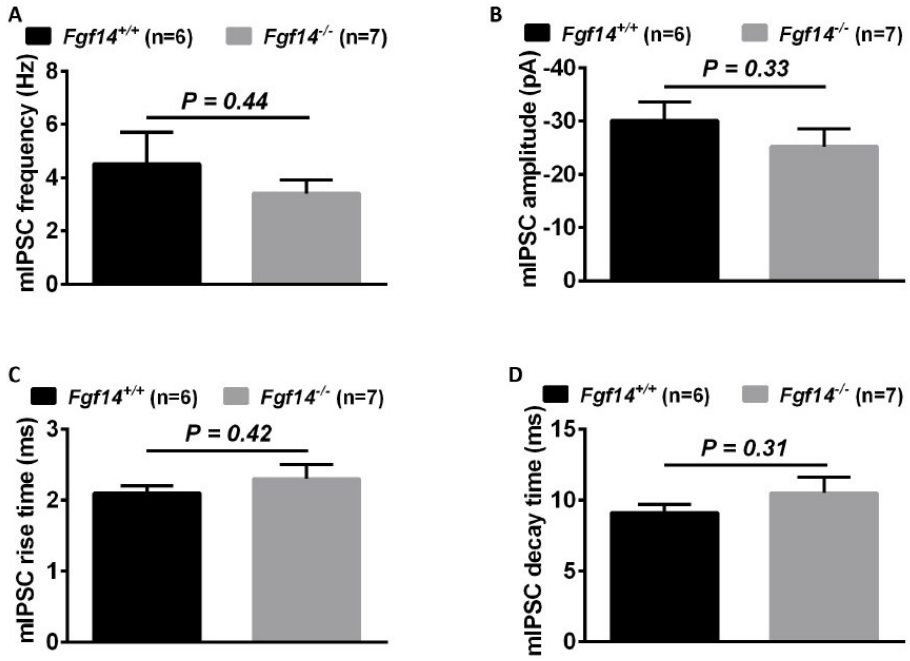

Figure 3:7 Mean values of miniature inhibitory postsynaptic currents (mIPSC).
A. Mean mIPSC frequency. **B.** Mean mIPSC amplitude. **C.** Mean mIPSC rise time. **D.** Mean mIPSC decay time. Data are mean ± SEM collected from n=6 cells (*Fgf14*$^{+/+}$) and n=7 cells (*Fgf14*$^{-/-}$). P values were obtained with Student *t*-test.

Reduced PV neuron function can desynchronize the CA1 network resulting in reduced gamma oscillations and impaired cognition. Thus, we postulated that gamma oscillations might be impaired upon ablation of *Fgf14*. To test this, gamma oscillations were recorded in the CA1 SR layer in *Fgf14*$^{-/-}$ and control mice by *in vivo* local field potential (LFP) (**Figure 3**:8 **A**). Spectral analysis within the 30-100 Hz range revealed that *Fgf14*$^{-/-}$ mice had a strong reduction in gamma oscillation power (2.94 ± 0.11 μV^2 n= 7, compared to 7.92 ± 0.17 μV^2 n= 7 in wild type mice, $p<0.05$; **Figure 3**:8**B, C**) with both slow (low-gamma, 30-65 Hz) and fast (high-gamma, 65-100 Hz) gamma oscillations significantly impaired in *Fgf14*$^{-/-}$ mice compared to wild type (*Fgf14*$^{-/-}$, 2.29 ± 0.85 and 0.65 ±0.25 μV^2; wild type control, 5.97 ± 1.2 and 1.95 ± 0.5 μV^2, respectively

Figure 3:8**D**). Thus, consistent with disrupted GABAergic transmission, spectral analysis confirmed that FGF14 is required for the integrity of the cognitive circuitry.

The combination of phenotypes observed in *Fgf14*$^{-/-}$ mice (**Fig. 1-4**) has been associated with deficits in spatial working memory in animal models and patients afflicted with schizophrenia (Lewis et al., 2012;Dudchenko et al., 2013;Hoftman et al., 2015). Thus, we next evaluated the spatial working memory performance of *Fgf14*$^{-/-}$ mice using the 8-arm maze test. Analysis of the latency to perform the task showed that *Fgf14*$^{-/-}$ mice required a longer time to complete the task than wild-type (n=20 wild-type and n=19, *Fgf14*$^{-/-}$, $p<0.001$, **Figure 3**:8**E**). Furthermore, revisiting errors (**Figure 3**:8**F**), which are directly linked to working memory performance, were more frequent in *Fgf14*$^{-/-}$ mice than in wild types ($p<0.05$), corroborating the cellular and functional phenotypes associated with genetic deletion of *Fgf14*.

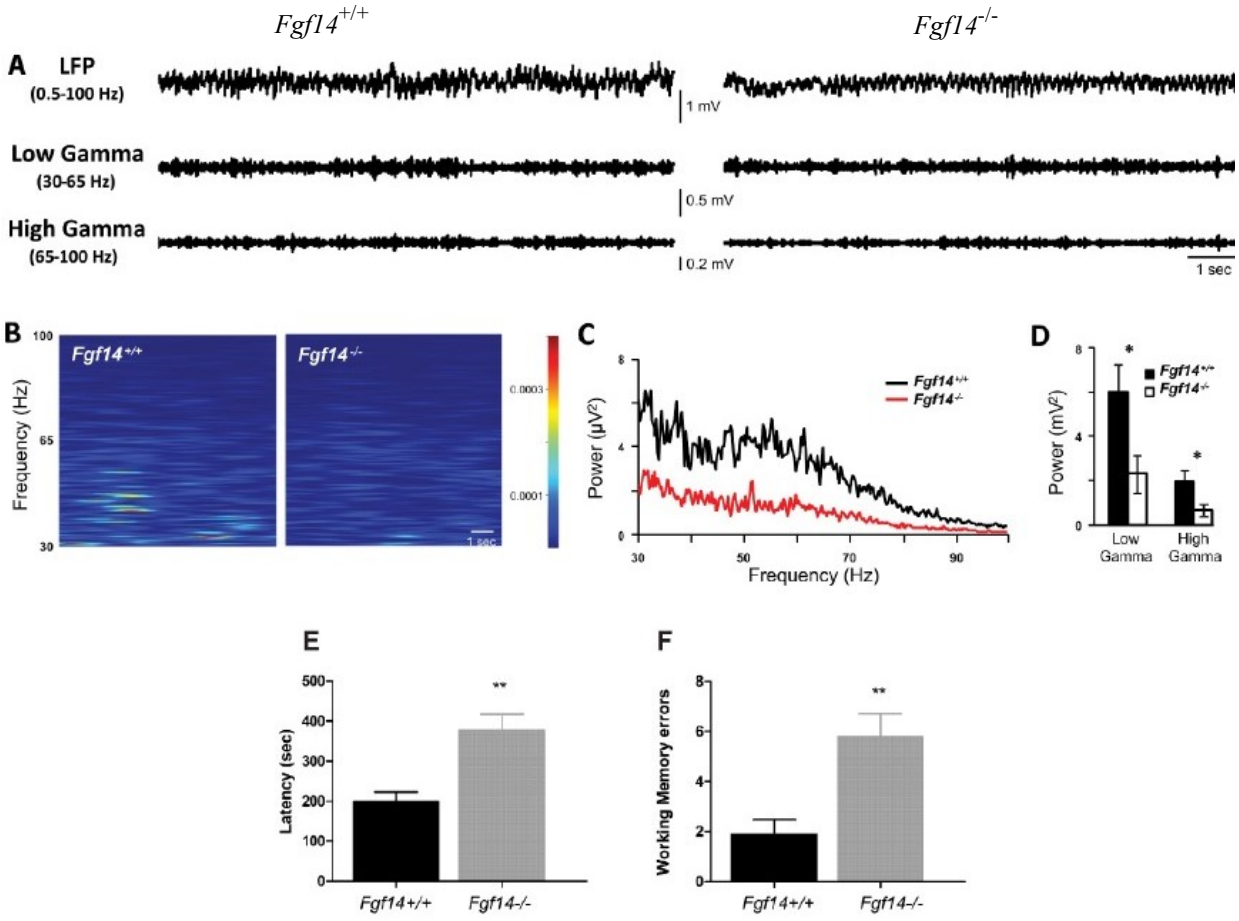

Figure 3:8 Genetic deletion of *Fgf14* reduces gamma frequency and affects working memory.

A. Representative traces of 10 second *in vivo* EEG recordings in the CA1 region of hippocampus (LFP) in *Fgf14*$^{+/+}$ (left) and *Fgf14*$^{-/-}$ mice (right); filtered traces within low- and high-gamma band are also shown. **B**. Spectrogram analysis of the above-mentioned traces in the gamma range (30-100 Hz). **C**. Mean power spectral density of CA1 activity showing a marked decrease in gamma power in *Fgf14*$^{-/-}$ (n=7) with respect to *Fgf14*$^{+/+}$ (n=7) mice, as revealed by power analysis within both low- and high-gamma (**D**). **E.** *Fgf14*$^{-/-}$ mice required a longer time to perform the 8-arm maze test (n=20 wild-type and n=19, *Fgf14*$^{-/-}$; $p<0.001$, t-test). **F**. Analysis of working memory errors committed during the test day showed a significant difference between genotypes ($p<0.05$, t-test). Data are expressed as mean ± SEM (*$p<0.05$).

To provide translational value to our studies, in collaboration with Dr. Herbert Y. Meltzer laboratory, we examined large transcriptomic datasets from schizophrenia *post-mortem* tissues deposited in the NCBI Gene Expression Omnibus (Liu et al., 2006), seeking genes whose

expression might covary with that of *FGF14*. Through the SEEK-based gene co-expression search engine with built-in functional annotation using KEGG orthologue analysis we found that *FGF14* was enriched within the 'GABAergic synapse' pathway **(Table 3:1)**. Since the human studies were collected from different brain region such as PFC, we examined the expression of GAD67 and VGAT in PFC using quantitative Western blot analysis **(Figure 3**:10**A, B**).

We observed a significant reduction in *Fgf14*$^{-/-}$ mice. We subsequently analyzed expression of the *FGF14*, *PVALB**,*** *GAD67* and *VGAT* genes and their correlations in two schizophrenia enriched datasets and matched controls from the dorsal lateral prefrontal cortex (Iwamoto et al., 2005;Narayan et al., 2008). Both datasets showed a significant decreased expression of *FGF14, PVALB, GAD67* and *VGAT* (**Figure 3**:9**A,**) and a highly significant correlation between *FGF14*, *PVALB*, *GAD67* and *VGAT* was found in all samples and in schizophrenia alone with the largest effect size in schizophrenia and controls for *GAD67* (**Figure 3**:9**B**)**.**

A

Study	Gene Name	Affymetrix Probeset_location	Linear Models for data analysis (limma)				Array Platform	Coexpression with FGF14 in all			Coexpression with FGF14 in SCZ		
			adj.P.Val	P.Value	t	β		R.Value*	P value	N	R.Value	P value	N
GSE21138	FGF14	221310_at (Exon)	0.202	0.00742	2.765	-2.448	GPL570	NA	NA	NA	NA	NA	NA
	FGF14	230288_at(3'UTR)	0.380	0.08718	1.737	-4.310	GPL570	0.857	5.16E-18	59	0.884	9.46E-11	30
	GAD67	206670_s_at(Exon)	0.202	0.00641	2.819	-2.332	GPL570	0.777	4.90E-13	59	0.774	5.10E-07	30
	VGAT	240532_at(3'UTR)	0.200	0.00294	3.092	-1.718	GPL570	0.844	5.01E-17	59	0.858	1.32E-09	30
	PVALB	205336_at(Exon)	0.135	0.00492	2.921	-2.125	GPL570	0.818	2.58E-15	59	0.878	1.89E-10	30
GSE12649	FGF14	221310_at(Exon)	0.265	0.02860	2.239	-3.643	GPL96	NA	NA	NA	NA	NA	NA
	GAD67	206670_s_at(Exon)	0.043	0.00018	3.969	-0.674	GPL96	0.659	3.22E-09	64	0.664	1.83E-05	34
	GAD67	205278_at(3'UTR)	0.220	0.01870	2.413	-3.293	GPL96	0.677	8.25E-10	64	0.619	9.63E-05	34
	PVALB	205336_at(Exon)	0.007	7.70E-6	4.866	-3.527	GPL96	0.680	6.39E-10	64	0.723	1.00E-06	34

B

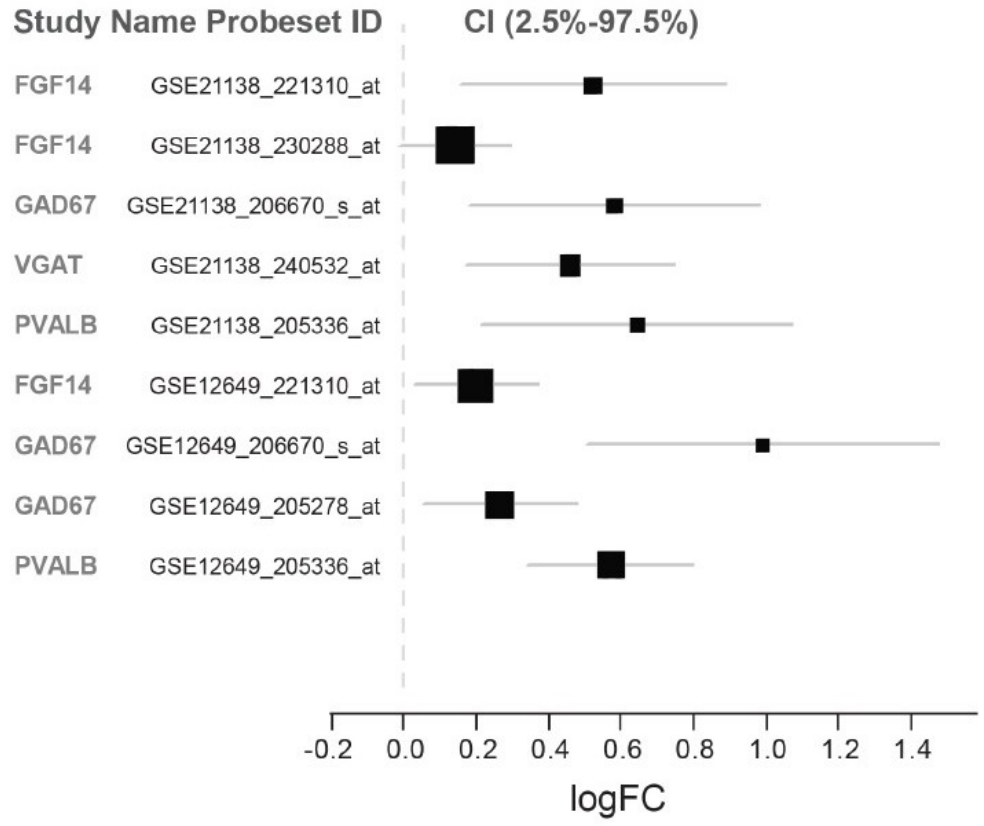

Figure 3:9 Differential gene expression and correlation of *FGF14*, *PVALB, VGAT* and *GAD67* in *post-mortem* control and schizophrenia samples.

A. The GSE21138 and GSE12649 datasets are both derived from previous studies(Iwamoto et al., 2005;Narayan et al., 2008) and deposited in NCBI GEO. Due to significant deviation from the mean (>2SD) in *FGF14* gene expression (221310_at), five samples were removed from the GSE12649 dataset. GPL96 represents Affymetrix Human Genome U133A Array; GPL570 represents Affymetrix Human Genome U133 Plus 2.0 Array. GPL96 had no probeset selected

for VGAT(SLC32A1). The original P.Value was adjusted by Benjamini & Hochberg (False discovery rate). The R.Valuer- represents a Pearson Correlation with significance at the 0.01 level (two-tailed). **B.** Forest plot illustrates the effect size (logFC) of differential gene expression of *FGF14, PVALB, VGAT*, and *GAD67* between controls and schizophrenia patients in post-mortem DLPFC (BA46). Linear model and empirical Bayes method (LIMMA) was applied for assessing the differential gene expression of *FGF14* and its coexpression genes, including *PVALB*, *GAD67* and *VGAT*, in two independent datasets (GSE21138 and GSE12649) deposited in NCBI Gene Expression Omnibus (Liu et al., 2006). LogFC>0 suggest decreased gene expression in patients with schizophrenia. The forest plot was created by R rmeta package.

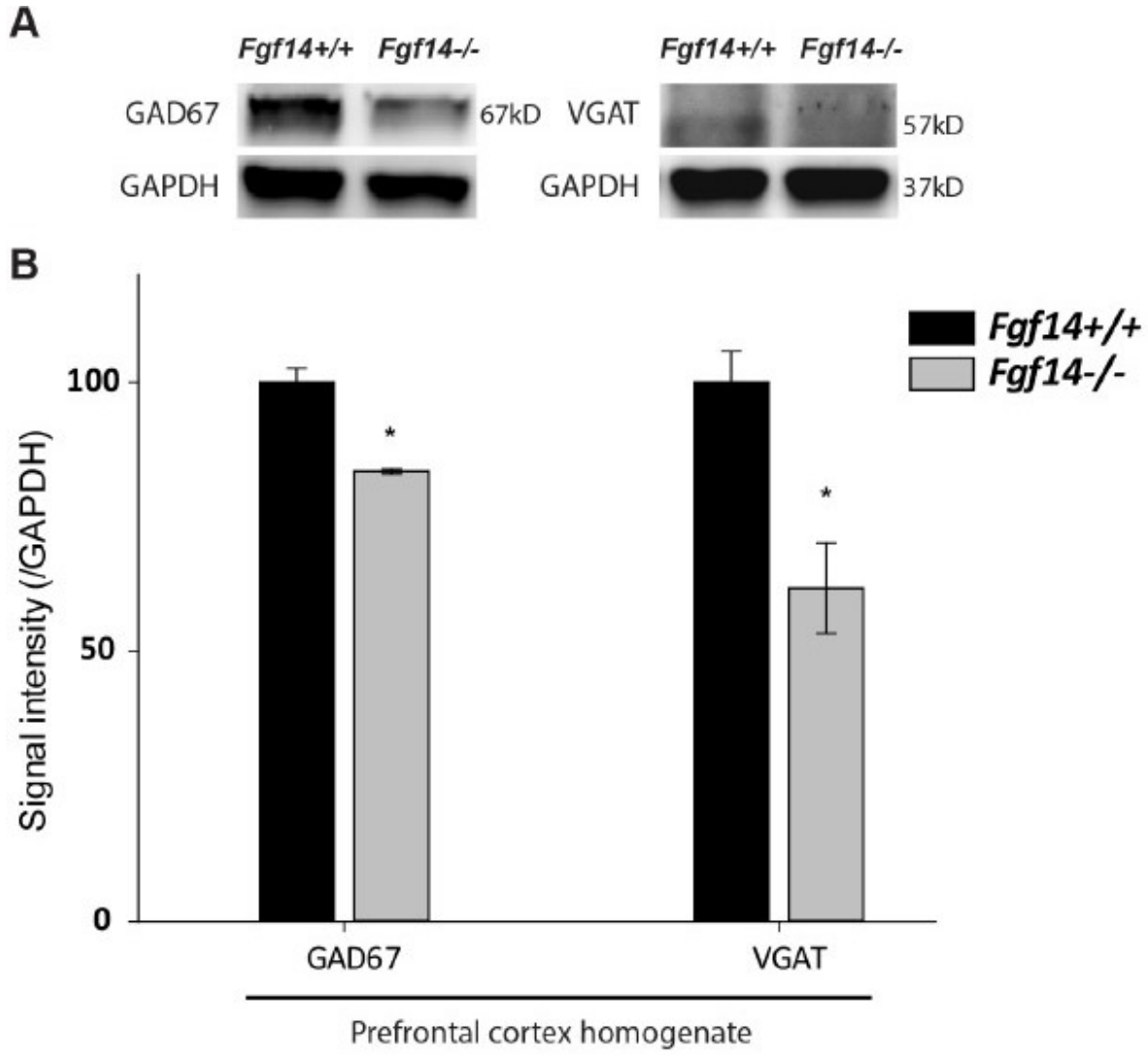

Figure 3:10 Quantitative Western blot analysis of GAD67 and VGAT from the PFC brain region. **A.** Immunoblot detection of GAD67 and VGAT in whole hippocampal and PFC homogenates from *Fgf14*$^{-/-}$ mice and *Fgf14*$^{+/+}$ controls. **B.** Band signal intensity quantification for GAD67 and VGAT in *Fgf14*$^{-/-}$ and *Fgf14*$^{+/+}$. Data represent mean ± SEM, ***p<0.05.* statistical differences were assessed by Student's t-test.

KEGG Term	RANK* (HIP/PFC/SCZ)	p-value	q-value	# of Gene	Gene List
Long term potentiation	1/2/7	8.4E-07	2.99E-06	14	CALM1 CALM2 GRIA2 GRIN2A ITPR1 KRAS MAP2K1 MAPK1 PPP1R12A PPP3CA PPP3CB PPP3R1 PRKACB PRKCB
GABAergic synapse	2/9/5	1.05E-05	2.99E-05	14	GABARAPL1 GABRA1 GABRA4 GABRB2 GABRB3 GABRG2 GAD1 GLS GNB5 GNG3 GPHN NSF PRKACB PRKCB SLC12A5
Oocyte meiosis	3/-/-	0.000028	6.33E-05	15	CALM1 CALM2 CDC27 CUL1 ITPR1 MAP2K1 MAPK1 PPP2CA PPP3CA PPP3CB PPP3R1 PRKACB SKP1 YWHAH YWHAZ
Synaptic vesicle cycle	4/7/14	0.000028	0.000106	11	ATP6V1A ATP6V1B2 ATP6V1C1 ATP6V1D ATP6V1G2 ATP6V1H CLTC DNM3 NSF SNAP25 SYT1
Retrograde endocannabinoid signaling	5/3/1	0.000151	0.000375	13	GABRA1 GABRA4 GABRB2 GABRB3 GABRG2 GNB5 GNG3 GRIA2 ITPR1 MAPK1 MAPK9 PRKACB PRKCB
Alzheimer s disease	6/-/-	0.000496	0.000774	16	ATP2A2 ATP5A1 CALM1 CALM2 GRIN2A ITPR1 MAPK1 NDUFA4 NDUFC2 PPP3CA PPP3CB PPP3R1 SNCA UQCRC2 UQCRFS1 UQCRH
Dopaminergic synapse	7/4/5	0.000496	0.000774	14	ARNTL CALM1 CALM2 GNB5 GNG3 GRIA2 GRIN2A ITPR1 MAPK9 PPP2CA PPP3CA PPP3CB PRKACB PRKCB

Table 3:1 Functional annotation and pathway enrichment based on KEGG Term in hippocampus.
The top significantly enriched categories derived from hippocampus datasets with p-value and gene list were presented in this table. The ranks of the corresponding functional category derived from multiple datasets collected from prefrontal cortex (PFC) and schizophrenia were also listed.

3.4 Discussion

Here, we provide new evidence for FGF14 in maintaining GABAergic activity in the CA1 hippocampal region, an area critical for cognitive function (Godsil et al., 2013). Genetic deletion of *Fgf14* leads to a decrease in the number of PV interneurons and in the expression level of the presynaptic GABAergic markers GAD67 and VGAT. These changes are associated with reduced inhibitory tone of pyramidal neurons, decreased gamma frequency oscillations, and deficits in working memory. Bioinformatics analysis from human transcriptomics identified FGF14 as a component of GABAergic synaptic signaling and revealed a correlated decrease in *FGF14*, *PVALB*, *GAD67*, and *VGAT* gene expression in schizophrenia *post-mortem* tissues compared to

matched controls. These results provide a new mechanistic role for FGF14, an emerging neuropsychiatric disease-associated gene (Liu et al., 2006;Jungerius et al., 2008;Drgon et al., 2010;Hodgkinson et al., 2010;Brennand et al., 2011;Hu et al., 2011;Verbeek et al., 2012;Hunter et al., 2013;Spencer et al., 2013;Chen et al., 2014;Olson et al., 2014) in the context of human brain disorders.

The identification of FGF14 immunoreactivity at the AIS of CA1 PV interneurons suggests this protein contributes to interneuron structural and functional diversity (Chand et al., 2015) and as such might be part of the repertoire of signaling molecules dictating the cell cardinal and definitive specifications of PV neurons in the neural circuitry (Klausberger and Somogyi, 2008;Lewis et al., 2012). The cell type- and sub-layer specific loss of PV neurons observed upon *Fgf14* deletion confirms this hypothesis and supports the notion that FGF14 is indispensable for the development, maintenance, and/or survival of PV interneurons in the CA1 region. Our *post-mortem* human tissue study identifies a significant correlation between the *Fgf14* and *PVALB* genes, which might contribute to the loss of PV interneurons observed in *Fgf14*$^{-/-}$ mice.

We also found that the expression level of GAD67 and VGAT, two well-characterized disease-associated proteins critical for GABA synthesis and differentiation in addition to synaptogenesis of PV neurons (Chattopadhyaya et al., 2004;Chattopadhyaya et al., 2007;Donato et al., 2013) are decreased in PV positive somas and at inhibitory presynaptic terminals in *Fgf14*$^{-/-}$ animals. This phenotype is consistent with a diminished total pool of the two proteins, which might result from covariance of *FGF14, GAD67* and *VGAT* at expression level as suggested by our bioinformatics analysis from schizophrenia samples.

Whether loss of PV neurons and deficits in GABAergic markers in *Fgf14*$^{-/-}$ brains occur through causative loops or are separate coincidental events remains to be determined. Evidence exists for two separate functions of FGF14 as a regulator of intrinsic excitability at the AIS

(Goldfarb et al., 2007;Laezza et al., 2007;Shakkottai et al., 2009;Shavkunov et al., 2012;Shavkunov et al., 2013;Hsu et al., 2014;Hsu et al., 2015) and a presynaptic organizer(Yan et al., 2013;Xiao et al., 2007). Thus, phenotypes observed in *Fgf14*$^{-/-}$ hippocampi might arise from disruption of two independent functions of FGF14: one impairing intrinsic firing of PV neurons, causing cell death, arrested development and/or aberrant circuitry integration, and one disrupting the pre-synaptic GABA machinery (synthesis and loading) via down regulation of selective markers (i.e. GAD67 and VGAT). Convergence of these disrupted functions might have fatal consequences for the final specifications and circuitry integration in PV neurons in the CA1 region. In an *Fgf14* null condition, these uncompensated functions could be aggravated by concomitant loss of excitatory inputs, leading to a global remodeling of PV innervation fields (Chattopadhyaya et al., 2007), shifting cortical networks into a high-PV status with reduced plasticity (Donato et al., 2013).

Given that the majority of GABAergic inputs in the CA1 area arise from PV interneurons, and that GAD67 and VGAT are essential for the synthesis and loading of GABA at presynaptic terminals, we posited that *Fgf14* genetic deletion might impair hippocampal inhibitory transmission. Consistently, the distribution of sIPSCs frequency (and amplitude) in *Fgf14*$^{-/-}$ CA1 pyramidal neurons was found populated by longer inter-event intervals compared to *Fgf14*$^{+/+}$ suggesting that in *Fgf14*$^{-/-}$ mice the remaining inhibitory neurons might fire less than in control animals. sIPSCs are AP-driven synaptic events and as such represent a compound read-out of the firing status of pre-synaptic interneurons and the neurotransmitter release machinery. To examine GABA release mechanisms independent of interneuron spontaneous firing, we isolated mIPSCs. The distributions of frequency and amplitude of mIPSCs in *Fgf14*$^{-/-}$ mice were shifted with loss in short inter-event intervals and in smallest and largest amplitude events, respectively. These results highlight a combination of pre- and postsynaptic deficits in GABAergic transmission possibly

induced by lower quantum content, probability of vesicle release, or reduced number of vesicle, that might arise from structural and/or functional loss of a sub-set of inhibitory terminals. The lack in change of rise and decay time in the *Fgf14*$^{-/-}$ mice argues against significant changes in the mechanism of diffusion of GABA across the synaptic cleft, or in the composition of postsynaptic ionotropic GABA receptors. However, high-resolution structural analysis is required for confirmation.

In cortical areas loss in PV neuron function and changes in GABAergic activity can desynchronize the E/I network leading to reduced gamma oscillations, a phenotype associated with schizophrenia and other psychiatric disorders (Yizhar et al., 2011;Lewis et al., 2012;Craig and McBain, 2015). *In vivo* EEG local field potential (LFP) recordings in the CA1 region revealed that in *Fgf14*$^{-/-}$animals the total, slow and fast, gamma band power was suppressed compared to control mice. These temporally segregated gamma oscillations reflect information carried by CA3 Schaffer collaterals and perforant path inputs, respectively (Csicsvari et al., 2003;Colgin et al., 2009;Yamamoto et al., 2014). Thus, a reduction in both slow and fast gamma implies that both intra- and extra-hippocampal synaptic inputs might be compromised, possibly reflecting more widespread anomalies in *Fgf14*$^{-/-}$ brains, arising from the PFC-thalamic-hippocampal loop (Lisman et al., 2010). At the behavioral level, we show that *Fgf14*$^{-/-}$ animals exhibit impaired spatial working memory, complementing the array of deficits commonly found in psychiatric disorders associated with cognitive impairment (Dudchenko et al., 2013).

Human transcriptomics data confirmed functional clustering of *FGF14* with GABAergic signaling and identified a highly correlated decrease of *FGF14*, *PVALB*, *GAD67*, and *VGAT* in schizophrenia *post-mortem* tissues, indicating possible genetic co-regulation of these genes. Thus, diminished expression of FGF14 in humans might be a risk factor for complex brain diseases associated with cognitive impairment, such as schizophrenia. These findings extend the original

studies linking the dominant negative *FGF14*^{F145S} missense mutation to the inherited, rare disorder SCA27 to a much broader set of human brain diseases. Studies focusing on GABAergic components mRNA and gene expression in *Fgf14*$^{-/-}$ will be the focus of future studies.

3.5 Conclusions

In this chapter we observed a range of phenotypes from molecular to behavioral observed in *Fgf14*$^{-/-}$ mice along with our corroborating human studies lay the groundwork for new mechanistic hypotheses on the biology and potential risk factors of cognitive impairment in schizophrenia and other complex brain disorders associated with E/I tone imbalance and disrupted development and plasticity of GABAergic signaling (Turner et al., 2012).

These findings further strengthen the emerging role of the AIS and its molecular components in the biology of diseases such as schizophrenia, bipolar disorder, and depression (Hsu et al., 2014). Moreover, these observations raised the question whether genetic deletions of *Fgf14* has an impact on the GABAergic postsynaptic components such $GABA_A$ receptor subunits and gephyrin, the scaffold protein that is responsible for $GABA_A$ receptor availability and function (Sassoè-Pognetto and Fritschy, 2001).

This manuscript is accepted for publication in Translational Psychiatry (March, 2016). TA and MA contributed to the design of the work, the acquisition, and interpretation of the data. MA and TA performed tissue sectioning, immunohistochemistry, confocal images, image analysis and Western Blots. MA processed mouse tissue, supervised, maintained, and genotyped the animal colony. M.N.N.: conducted and analyzed electrophysiological experiments. EH, AM and FT conducted and analyzed behavioral experiments. MC and BS conducted and analyzed the EEG recordings.TJ technical assistance. PS and DL analyzed the neuropil density. JL and HM contributed with human transcriptomics studies. FL contributed to the design of the work, provided resources, and intellectual support, and supervised data analysis, acquisition, and interpretation of the manuscript. TA, and FL wrote manuscript.

Chapter 4: **The impact of fibroblast growth factor 14 genetic deletion on GABAergic postsynaptic components**

Efficient synaptic connections require proper communication between the presynaptic and the postsynaptic side. We previously showed that a lack of FGF14 disrupted GABAergic presynaptic components. Though our studies indicated that FGF14 did not impact GAD67 and VGAT puncta number and size, the protein contents reduced significantly upon *Fgf14* genetic ablation. This suggested that the FGF14 modulated inhibitory presynaptic maintenance, recruitment, or degradation. Here, I expand our investigations to the inhibitory postsynaptic terminals, including gephyrin, $GABA_A$ alpha-1, and alpha-2 receptor subunits. These proteins are highly implicated in cognitive disorders. Our studies indicate that the effect of FGf14 on inhibitory postsynaptic components is marginal compared to that on presynaptic proteins. This suggests that FGF14 is a selective presynaptic modulator.

4.1 Introduction

In our previous study, we assessed the expression of GABAergic presynaptic components in FGF14 knocked out mice. Our investigations included the evaluation of the mean number, size and protein contents for each synapse of GAD67 and VGAT. Our results indicated a lack of alterations in the puncta (synapse) size and in the number of both elements. However, the protein contents, which we measured by their fluorescence intensity, were reduced significantly. This suggested that the lack of FGF14 affected GABA synthesis and transport. Moreover, our observations indicated that FGF14 regulated GABAergic presynaptic constituents' recruitment, maintenance, and development or degradation. The functional studies, including the whole-cell

patch clamp, EEG recordings, and behavioral working memory test, suggested that *fgf14* genetic ablation induced lifelong synaptogenic consequences.

The goal of this chapter is to extend these studies and investigate the effect of FGF14 on the structure and function of GABAergic postsynaptic components using immunohistochemical studies and confocal imaging. Our investigations focus on three elements: the scaffold protein gephyrin, and $GABA_A$ alpha-1 and alpha-2 receptor subunits.

Efficient synaptic connections allow proper communication and signal transduction from one neuron to the next, which is required for proper brain function. These connections (contact sites), which are known as synapses, are made of two compartments: the presynaptic and the postsynaptic sides The presynaptic terminals contain vesicles loaded with neurotransmitters and specialized plasma-membrane sites, called active zones, from which neurotransmitter molecules are released; postsynaptic terminals contain receptors, which scaffolding proteins anchor to the membrane, that bind with high affinity to the released neurotransmitter molecules. The binding of the neurotransmitter to its post-synaptic receptor initiates an excitatory or inhibitory electrical signal that is the basis for the electrochemical transmission of signals at synapses (Sassoè-Pognetto and Fritschy, 2001;Terauchi et al., 2010;Panzanelli et al., 2011).

Structurally, synapses can be asymmetric or symmetric. The asymmetric synapse is usually excitatory and contains the postsynaptic density (PSD) protein 95, which is implicated in maintaining and stabilizing the postsynaptic structure integrity by receptor clustering. The other type of synapse (symmetric synapse) is usually inhibitory, and it mediates either GABA or glycine neuronal transmission (Sassoè-Pognetto and Fritschy, 2001;Panzanelli et al., 2011).

The postsynaptic site of GABAergic synapses expresses gephyrin, a protein that stabilizes and clusters postsynaptic $GABA_A$ receptors. Deficits in GABAergic synapse regulations have been

linked to multiple neurodevelopmental diseases, mood disorders, and mental retardation (Sassoè-Pognetto and Fritschy, 2001;Panzanelli et al., 2011). The genetic ablation of gephyrin leads to a reduction in $GABA_A$ receptor populations and an overall decrease in GABAergic synapses (Yu and De Blas, 2008). Mutations in the gephyrin gene have been associated with neurological disorders (Reiss et al., 2001), autism, schizophrenia and seizures (Lionel et al., 2013).

In the mammalian brain, $GABA_A$ receptors are essential for fast and slow GABAergic synaptic inhibition. Structurally, they are pentameric, consisting of different subunits. For instance, in the mammalian cortex, the majority of $GABA_A$ receptors are composed of one of six subunits, which, in turn, have distinguished physiology and subcellular localization (Mody and Pearce, 2004). Understanding the mechanisms that mediate $GABA_A$ receptors' synaptic formation, clustering and maturation remains central to cognitive neuroscience (Sassoè-Pognetto and Fritschy, 2001;Patrizi et al., 2008;Hines et al., 2013). In schizophrenia, there is a selective reduction of the $GABA_A$ receptor alpha-1 subunit and GAD67 expression at PVBcs to excitatory cell synapses (Lewis et al., 2012). $GABA_A$ receptor alpha-2 is another $GABA_A$ receptor subunit that is highly relevant to cognitive capacity. The two subunits are expressed in the majority of GABAergic synapses (Loup et al., 1998). Furthermore, compared to other subunits, they exhibit great affinity for GABA (Levitan et al., 1988;Lavoie et al., 1997). In addition, they are expressed highly in the neuronal perisomatic and axo-axonic regions, which implicate them functionally as principal modulators of the GABAergic inhibition. Schizophrenic postmortem studies reported an elevation in alpha-2 immunoreactivity (Lewis et al., 2005;Hines et al., 2013). So both alpha-1 and alpha-2 $GABA_A$ receptor subunits are critical determinants of cognitive function.

Overall, reduced levels of GABAergic synaptic function constitute a hallmark of schizophrenia, depression, bipolar disorder, and autism (Shulman and Tibbo, 2005 ;Yu et al.,

2006;Chao et al., 2010;Brady et al., 2013). However, the molecular and cellular mechanisms underlying these dysfunctions are not yet clear.

4.2 Methods

Methods for *Fgf14*$^{-/-}$ colony maintenance, perfusion, tissue preparation and sectioning, Immunofluorescence, image acquiring and analysis, and cresyl violet were outlined previously in this work. A complete description of these techniques is detailed in **Chapter 2**.

4.3 Results

4.3.1 Genetic deletion of Fgf14 lacks any significant effects on GABAergic postsynaptic components

We started our postsynaptic studies with gephyrin **(Figure 4**:1**A, B)**. Gephyrin is a scaffold protein in the inhibitory synapses that stabilizes and clusters postsynaptic $GABA_A$ receptors (Yu and De Blas, 2008;Tyagarajan and Fritschy, 2014). The quantifications of the gephyrin puncta area revealed no significant difference between both genotypes **(Figure 4**:1**A-D)**. The analysis of the gephyrin puncta number was comparable in both *Fgf14*$^{+/+}$ and *Fgf14*$^{-/-}$ **(Figure 4**:1**F)**. The mean fluorescence intensity analysis of gephyrin was significantly increased in *Fgf14*$^{-/-}$ compared to *Fgf14*$^{+/+}$. **(**Figure 4:1**E**). This suggested a possible compensatory mechanism at the postsynaptic sites in *Fgf14*$^{-/-}$.

Since, gephyrin anchored GABA receptor subunits and regulated their structure and function, I went on to examine $GABA_A$ receptor alpha-1 and alpha-2 subunits, which were both implicated in brain disorders. In *Fgf14*$^{-/-}$ mice, both $GABA_A$ alpha-1 **(Figure 4**:1**G, I)** and alpha-2 **(Figure 4**:1**H, J)** subunits did not show any puncta size or protein expression alterations in comparison to those in *Fgf14*$^{+/+}$ mice. These phenotypes suggested that the effect of FGF14 genetic deletion was milder in the GABAergic postsynapses than in the presynapses.

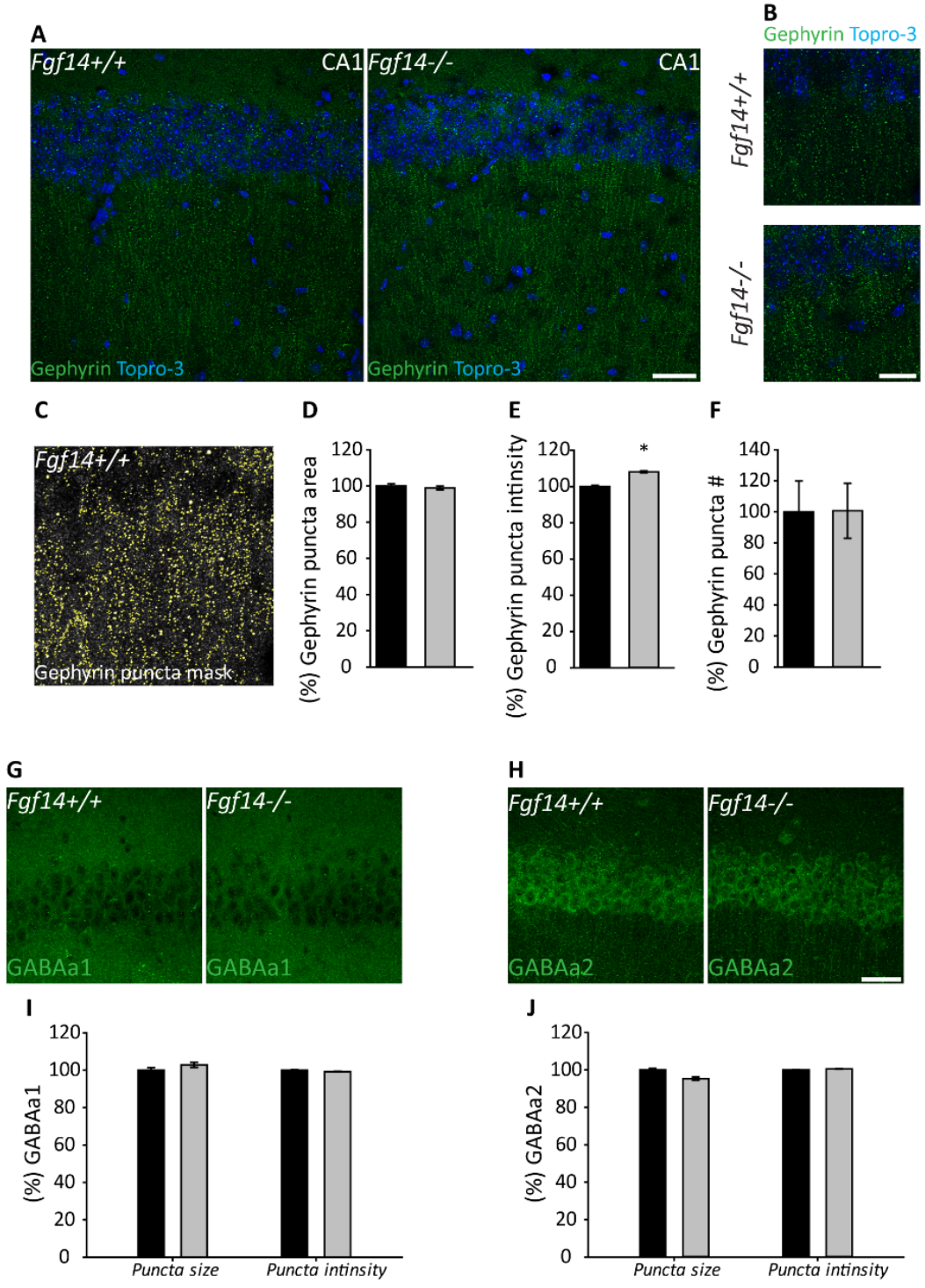

Figure 4:1 The effect of *Fgf14* genetic ablation on GABAergic postsynaptic elements in the hippocampal CA1 region.

A. Sagittal hippocampal sections show gephyrin expression (green) and Topro-3 (blue) at 63x magnification from *Fgf14*$^{-/-}$ mice and *Fgf14*$^{+/+}$ controls. **B.** Represent zooms of selected area from both genotype. **C.** The mask generated by ImageJ software and used to measure gephyrin puncta

area, intensity, and number in both genotypes. **D.** Quantification of gephyrin puncta, **E.** puncta intensity and **F.** puncta number. **G.** Representative confocal images of GABAa alpha-1 receptor subunit from *Fgf14*$^{-/-}$ mice and *Fgf14*$^{+/+}$ controls. **I.** Quantification of GABAa alpha-1 receptor subunit fluorescence intensity. **H.** The green channel represents of GABAa alpha-2 receptor subunit from both genotypes. **I.** Quantification of GABAa alpha-2 receptor subunit fluorescence intensity. Data represent mean ± SEM, ***p<0.05* statistical differences were assessed by non-parametric Mann-Whitney test. Scale bars: **A**=40 µm, **B**=20 µm, **G, H**=40 µm. (n=3 mice per group, 2-4 sections per mouse, Student's t test).

4.4 Discussion

Data from our experiments in chapter 3 indicate that the presynaptic components are reduced upon fgf14 genetic deletion. This suggests that FGF14 is involved in inhibitory presynaptic regulation. This potential role could involve protein degradation, trafficking, or loading. Previous studies have shown that the rearrangements of inhibitory synapses are highly dynamic and activity dependent. Both intrinsic neuronal connectivity and synaptic plasticity have influenced the formation of new GABAergic synapses (Flores et al., 2015).

The question raised is whether the lack of FGF14 would disrupt the inhibitory postsynapses. In this chapter, I expand our analyses to gephyrin and $GABA_A$ alpha-1 and alpha-2 receptor subunits, which are inhibitory postsynaptic components that are highly implicated in cognitive deficits. Our observations suggest that FGF14 has a marginal effect on GABAergic postsynaptic terminals compared to that on presynaptic terminals. This could be interpreted as a possible compensatory mechanism. There are two possibilities for the mechanism of compensation at the inhibitory postsynaptic terminals. The first involves making novel terminals, thus increasing the postsynaptic puncta number. The second involves increasing the size of the postsynaptic terminal, thus enhancing the strength of the inhibitory drive.

Studies involving schizophrenic postmortem tissue reported that the reduction in the inhibitory presynaptic terminals accompanied an increase in the inhibitory postsynaptic terminals. This indicated a possible coordinative interplay between GABAergic presynaptic and postsynaptic sites to compensate for the deficits in GABA synthesis and transport. Thus, impaired GABA signaling would be enhanced (Volk et al., 2002;Lewis et al., 2005;Lewis et al., 2012).

Previous study reported other FGFs to function as selective presynaptic target modulators. In Terauchi et al study other members of the FGF family (FGF7 and FGF22). They reported that specific FGFs functioned as a presynaptic regulator, called it a "target-derived organizer". They showed that FGF7 modulated the inhibitory presynaptic terminal differentiation. Upon FGF7 genetic deletion, VGAT fluorescence intensity reduced significantly. Moreover, the electron microscopy ultrastructural analysis indicated that the inhibitory (symmetric) synaptic vesicles were fewer and their size was reduced in the hippocampus of the *Fgf14*$^{-/-}$ mice. FGF7 overexpression rescued these defects in the postsynaptic terminals (Terauchi et al., 2010).

4.5 Conclusions

In summary, we coclude that *Fgf14*: 1) contributes to PV neurons cellular and functional diversity; 2) is not likely to be required for synaptogenesis since the number of the synapses is not altered; 3) modulates the inhibitory presynaptic terminals at a greater extent compared to the postsynaptic sites. 4) might be critical for proper synapse development and synaptic protein loading/degradation. The inclusion of an ultrastructural electron microscopic analysis might help pursing out these putative functions of *Fgf14* at the synapse.

Collectively, these observations indicate that FGF14 is a critical determinant for PVIs development and the homeostasis of the GABAergic inhibitory signaling. Posing questions related to the molecular mechanisms underlie these phenotypic alterations in the inhibitory circuitry

especially GABAergic presynaptic components associated with the deletion of *Fgf14* remain to be determined. Providing answers to these questions will fill our knowledge gap and provides more understanding of the complex nature of brain disorders. Also, it will provide a great opportunity for identifying biomarkers and/or drug target for psychiatric disorders.

Chapter 5: **Possible mechanisms underlying the loss of PVIs in *Fgf14*$^{-/-}$ the CA1 hippocampal region**

PVIs are the primary source of GABAergic synapses in the CA1 hippocampal region. The reduction in the inhibitory drive exerts a powerful effect on hippocampal synchronized activity since GABAergic inhibitory interneurons regulate a large population of principal neurons. Studies have reported that the reduction in PVIs is strongly involved in psychiatric disorders associated with cognitive deficits. Identifying molecules involved in the maintenance of PVIs that are highly implicated in learning and memory would elucidate the basics of cognitive capacity and halt cognitive impairment. To provide a link between *Fgf14* genetic ablation and the loss in PVIs, I formulated the following hypothesis: the lack of *Fgf14* might impair the maturation of PVIs; induce apoptosis; genetic deletion of *Fgf14* lead to global dysfunction in the hippocampal circuitry. These hypotheses are tested in this chapter.

5.1 Introduction

Our studies indicated that lacking of *Fgf14* causes a loss of PVIs, which are the main inhibitory interneurons in the CA1 region. Furthermore, we found that lacking of *Fgf14* is associated with a loss in GABA synthesis and transport machinary, also the inhibitroy transmission is disrupted. Both fast and slow gamma oscillations are reduced, and the spatial working memory is disrupted in *Fgf14*$^{-/-}$ mice. Some changes at the GABAergic postsynaptic terminals suggests a possible compensatory mechanism in *Fgf14*$^{-/-}$ mice. What could be the mechanisms underlying these phenotypic alterations.

The loss in PVIs could be due to three possible mechanisms. First, alteration in the developmental regulation lead to the loss/impairment of maturation of PVIs. Second, the loss in

PVIs could be driven by neuronal death. Third, the dysfunction in the circuitry and circuitry elements might be the cause behind PVIs loss, since PVIs development is highly dependent on the circuitry.

Regarding the first mechanism, alterations in the neuronal development and aging have been studied in the context of brain disorders. In healthy individuals, aging drives decline in cognitive capacities and susceptibility to neurodegenerative diseases by changing both the structure and the function of neuronal populations (Hedden and Gabrieli, 2004;Mattson and Magnus, 2006;Villeda et al., 2014). Cognitive capacity, especially spatial working memory, decline with aging. In humans and rodents, the hippocampal formation is preferentially vulnerable to age-related changes (Nicholson et al., 2004;Andrews-Hanna et al., 2007;Scheff et al., 2007).

Subtle alterations in PVIs have been linked to a variety of neurodevelopment disorders. For instance, in motor disorder investigations, it has been reported that dystonia and motor-related dysfunctions may be related to the decline in PVI cells or function (Gernert et al., 2000;Bennay et al., 2001;Reiner et al., 2013). Moreover, alteration in PVIs during aging has been suggested to be a crucial determinant of age-dependent cognitive deficits since they temper the principal cells' excitatory inputs and regulate the timing of brain development. In autism, a neurodevelopment disorder, genome-wide studies have revealed multiple genetic determinants. When studies involving the genetic manipulation of these different genes were conducted, PVIs were found to have been lost in nine animal models, which harbored autism-like behaviors (Gogolla et al., 2009). The dysfunction in the excitatory and inhibitory circuitry is the most held hypothesis for the vulnerability of PVIs (Kinney et al., 2006;Cheah et al., 2012;Verret et al., 2012).

In situ hybridization analysis indicated that FGF14 mRNA was detectable in multiple brain regions during the prenatal and postnatal stages (Wang et al., 2002;Xiao et al., 2007), suggesting

that it was essential for proper neuronal maintenance and development. In addition, previous studies using the water maze test (Wozniak et al., 2007) and eight arm maze test (Chapter 3) reported cognitive impairment in *Fgf14*$^{-/-}$. Moreover, electrophysiological studies of acute hippocampal slices suggested that *Fgf14*$^{-/-}$ mice exhibit impaired LTP, which are electrophysiological alterations highly implicated in learning and memory tasks (Wozniak et al., 2007;Xiao et al., 2007).

Fgf14$^{-/-}$ mice exhibited an endophenotype related to immature dentate gyrus, a condition characterized by impaired adult neuronal cells maturation (Hagihara et al., 2013). In this condition, most of the hippocampal stem cells are stuck in immature stages and express doublecortin and calretinin (immature markers), demonstrating that FGF14 is critical for proper neuronal maturation. Thus, we hypothesize that FGF14 is essential for PVIs specification and maturation that are important for hippocampal network, mature cognitive function, particularly, gamma oscillations that are refined at early adulthood stages, and seem to be changed in cognitive disorders, including schizophrenia.

The second possible mechanism is the neuronal death. Since the lack of *Fgf14* affects PVIs in region and cell-specific manner, I asked whether these phenotypic alterations could be driven by activated programmed cell-death. loss in PVIs could be a consequence of activate the cell programmed death that is triggered by the ablation of FGF14. FGF members are neurotrophic factors that are highly implicated in regulating the physiological events during development (Bikfalvi et al., 1997;Itoh and Ornitz, 2004). To further examine the role of *Fgf14* in the regulation of neuronal development and, specifically, in susceptibility to apoptosis I examined caspase-3 activity n *Fgf14*$^{+/+}$ and *Fgf14*$^{-/-}$ mice. Caspase family is proteases signaling proteins that mediate cellular apoptosis via endoplasmic reticulum stress, disruption of the mitochondria, and activation

of the death receptors. After activation the apoptotic signaling cascades, multiple events converge and eventually caspase-3 is triggered, the executioner (Scholz et al., 2005).

The third possible mechanism that I hypothesized is that lacking *Fgf14* leads to a global dysfunction of the hippocampal circuitry that alter expression, distribution, and function of molecules at the axon initial segment (AIS) by impairing intrinsic excitability. In the developing visual cortex, during the critical periods, AIS length is dynamically regulated. This suggests that experience-related critical periods highly influence the structure and plasticity of the AIS (Gutzmann et al., 2014). The AIS is the subcellular domain where action potential is generated and propagated. The master component is the scaffold protein ankyrin-G, which recruits/binds the cytoskeleton protein, spectrin, and, subsequently, recruits different isoforms of sodium channels and proteins to make the AIS macrocomplex (Jenkins and Bennett, 2001). The structure of this complex is dynamically regulated in multiple pathological and physiological statuses. During visual cortex postnatal development, dark rearing affects the AIS structure (Gutzmann et al., 2014). PVIs were found to be reduced in response to dark rearing events (Morales et al., 2002 2002).

In animal studies, AIS components are highly detectable young groups. Suggesting the physiological and developmental needs trigger recruitments of these elements. For instance, spectrin which is a crucial molecule of the AIS structure. It is essential to recruit and maintain the stability, and dynamics of AIS macrocomplex structure during the development and thickening of cortical regions. At young age, the formation of multiple components of the GABAergic system takes place (Hoftman and Lewis, 2011). However, shaping the connectivity between GABAergic interneurons particularly the PVChcs occur at adolescence, where axo-axonic synapses are developed, and the density of these cells buttons around the principal cells axons are increased (Fish et al., 2013). Indicating that the structural refinement of circuitry components occurs at later

developmental stages. These accumulated lines of evidence suggest that the AIS structure might influence PVIs development.

In schizophrenia research accumulated lines of evidence suggest that reduced GAD67 and PV expression are a consequence of the decline in the excitatory drive (Akbarian et al., 1995;Olney et al., 1999;Gonzalez-Burgos and Lewis, 2012;Gonzalez-Burgos et al., 2015). For example, a previous study in neuronal culture reported that the reduction in the glutamatergic input was linked to that decline in PVIs. It showed that NR2A (an NMDA receptor subunit) was critical for the maintenance of PVIs. While the acute treatment of neuronal cultures with selective subunit antagonists did not influence the mRNA level, it significantly reduced the PVI cell counts. suggesting that it affected the protein degradation.

Here I examined these three possible mechanisms. I conducted a time course study to examine the total PVIs cell count. Also, I examined the active caspase-3 immunoreactivity. Finally, I evaluated the effect of FGF14 genetic ablation on the AIS structure in the CA1 region in *Fgf14*$^{-/-}$ mice.

5.2 Methods

Methods for *Fgf14*$^{-/-}$ colony maintenance, perfusion, tissue preparation and sectioning, Immunofluorescence, image acquiring and analysis, and cresyl violet were outlined previously in this work. A complete description of these techniques is detailed in **Chapter 2**.

5.3 Results

Age-related changes in PV interneurons in Fgf14$^{-/-}$ *mice, the developmental hypothesis.*

PVIs have been studied extensively in the context of development and aging (Ouda et al., 2008;Ouda et al., 2012;Rubio et al., 2012;Ouda et al., 2015). To investigate the effect of FGF14

ablation on PVI development, I designed a study to examine PVIs in young (1 to 3 month old), adult (4 to 5 month old), and aged (9 to 11 month old) mice. The results suggest that there was no significant difference of the main effect of genotype or age on PVIs cell count. However, the age × genotype interaction was significant (F=3.592, P=0.030, df=2). Moreover, Fisher LSD *post hoc* analysis revealed a significant difference between the means of PVIs in the young $Fgf14^{-/-}$ mice versus the adult $Fgf14^{-/-}$ mice (P=0.028). Furthermore, the comparison of the PVIs means revealed a clear tendency to significance in $Fgf14^{+/+}$ adult mice versus the $Fgf14^{+/+}$ aged group (P= 0.056) **Figure 5:1**.

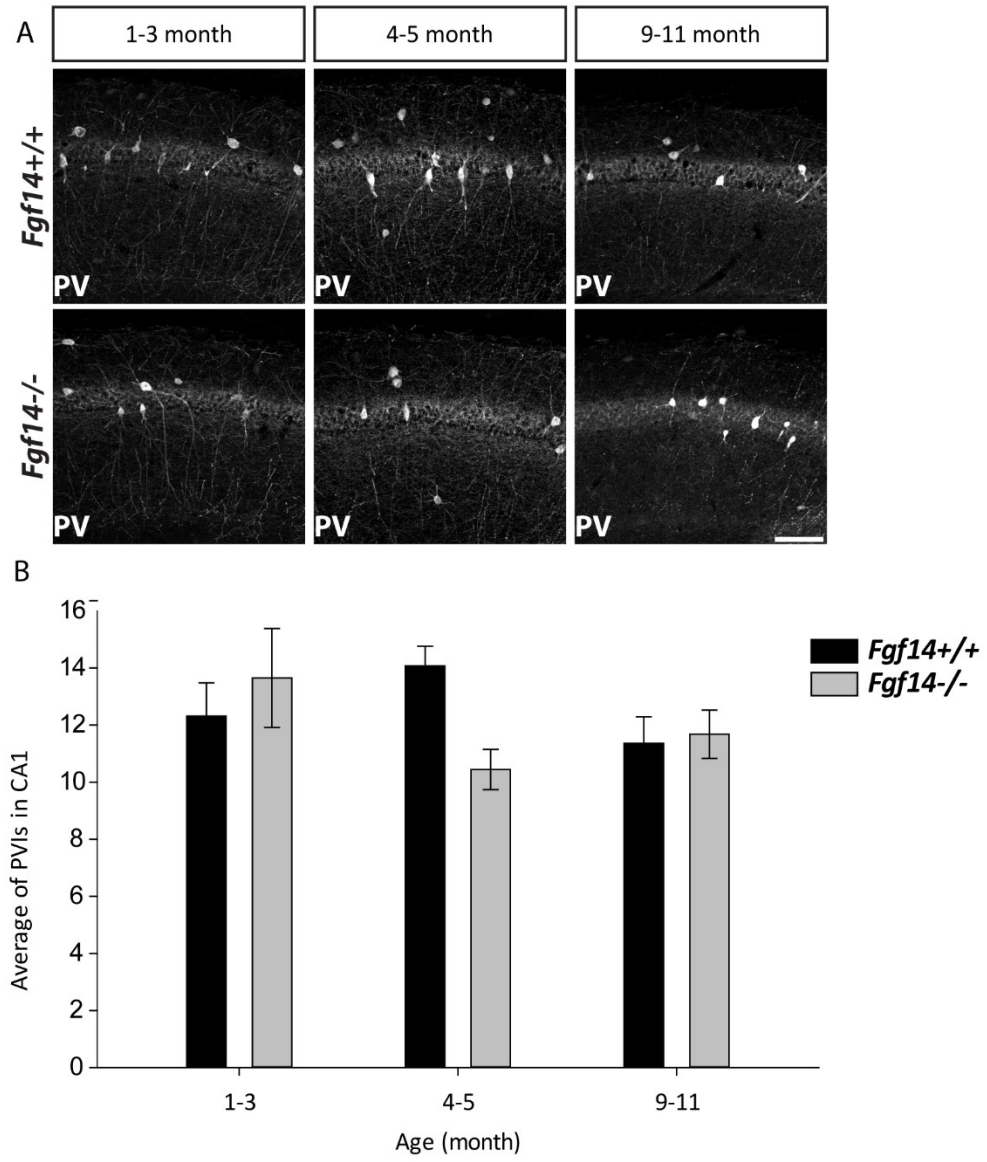

Figure 5:1 Age-related changes in PVIs in *Fgf14*$^{-/-}$.

A. Representative confocal images of PV expression in the hippocampal CA1 region in *Fgf14*$^{+/+}$ and *Fgf14*$^{-/-}$ mice in the three selected age groups young (1-3 months old, n=3 mice per group, 6-7 sections per mouse), adult (4-5 months old n=4 mice per group, 5-7 sections per mouse) and aged (9-11 months old, n= 3 mice per group, 7-8 sections per mouse) mice. **B.** PVIs quantifications in hippocampal CA1 region in *Fgf14*$^{+/+}$ and *Fgf14*$^{-/-}$ as a function of age was assessed using Two-way ANOVA and *post hoc* Fisher LSD test. Data represent mean ± SEM. Scale bars: **A**= 100 µm.

Next, I asked whether the genetic deletion of FGF14 affected the overall structure of CA1. Consistent with previous reports (Wang et al., 2002;Xiao et al., 2007) and **Figure 2:5 A** and **B**, the genetic deletion of *Fgf14* did not lead to alterations in the gross anatomy. Then I examined the brain weight at different developmental stages. The main effect genotype on brain weight was significant (F=12.44, P=0.001, df=1). *Fgf14*$^{-/-}$ mice have less overall brain weight compared to the *Fgf14*$^{+/+}$ mice. Along with the main effect of genotype, the age significantly affects the brain weight (F=4.962, P=0.012, df=2). Older mice have larger brain weight. The Two-way ANOVA analysis revealed a trend in the interaction effect between the genotype and the age (F=3.078, P=.057, df=2) this difference was not statistically significant likely due to variability issues **Figure 5:2** This suggested that the reduction in *Fgf14*$^{-/-}$ brain weight was more associated with synapses, synaptic connections, and neuronal connectivity than with direct neuronal loss.

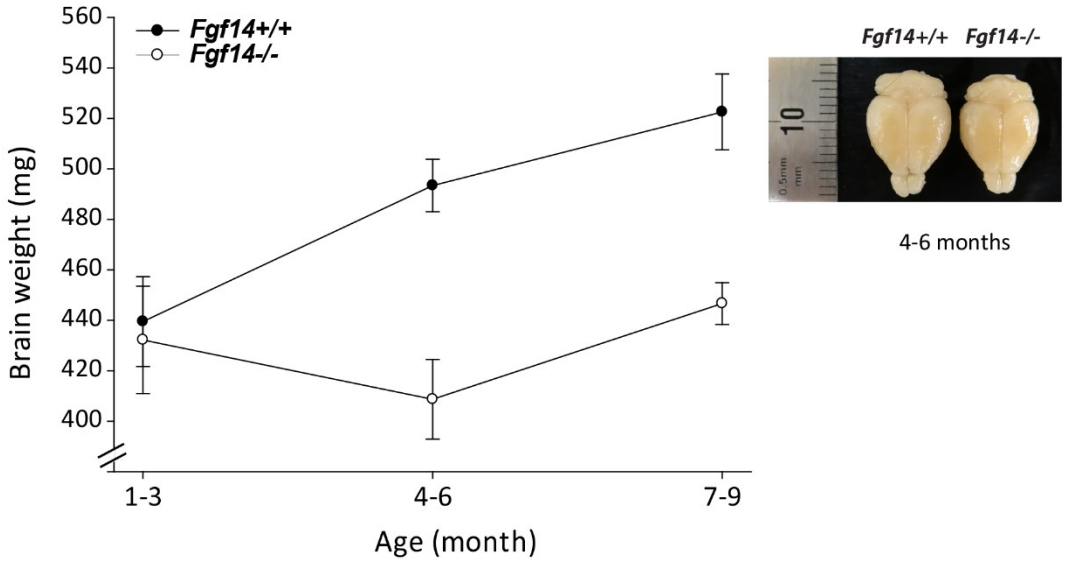

Figure 5:2 Age-related changes in *Fgf14*$^{-/-}$ brain weight.
A. Representative image of the brain size of 4-6 months *Fgf14*$^{+/+}$ and *Fgf14*$^{-/-}$ mice. **B.** *Fgf14*$^{+/+}$ and *Fgf14*$^{-/-}$ brain weights tracking at different age groups young (1-3 months old, n=11 *Fgf14*$^{+/+}$ and 10 *Fgf14*$^{-/-}$), adult (4-6 months old, n=5 *Fgf14*$^{+/+}$ and 3 *Fgf14*$^{-/-}$) and aged (7-9 months old, n=9 *Fgf14*$^{+/+}$ and 10 *Fgf14*$^{-/-}$). Data represent mean ± SEM, statistical differences were assessed by Two-way ANOVA.

Active Caspase3 (death cascade) activity in Fgf14$^{-/-}$ *mice, the Neuronal death hypothesis.*

To evaluate whether *Fgf14* would trigger the apoptotic machinery, I examine the active caspase-3 activity. I measured the immunofluorescence of caspase-3 by masking NEUN positive cells in the hippocampal CA1. The quantification of cappase-3 protein expression in *Fgf14*$^{-/-}$ mice, indicate that activated caspase-3 protein is slightly increased **Figure 5:3**. However, the pattern of expression was sparse puncta, rather than diffused pol in the soma. This suggested that the increase in caspase-3 might have been a trend rather than being causative of the overall alterations in the *Fgf14*$^{-/-}$ CA1 region.

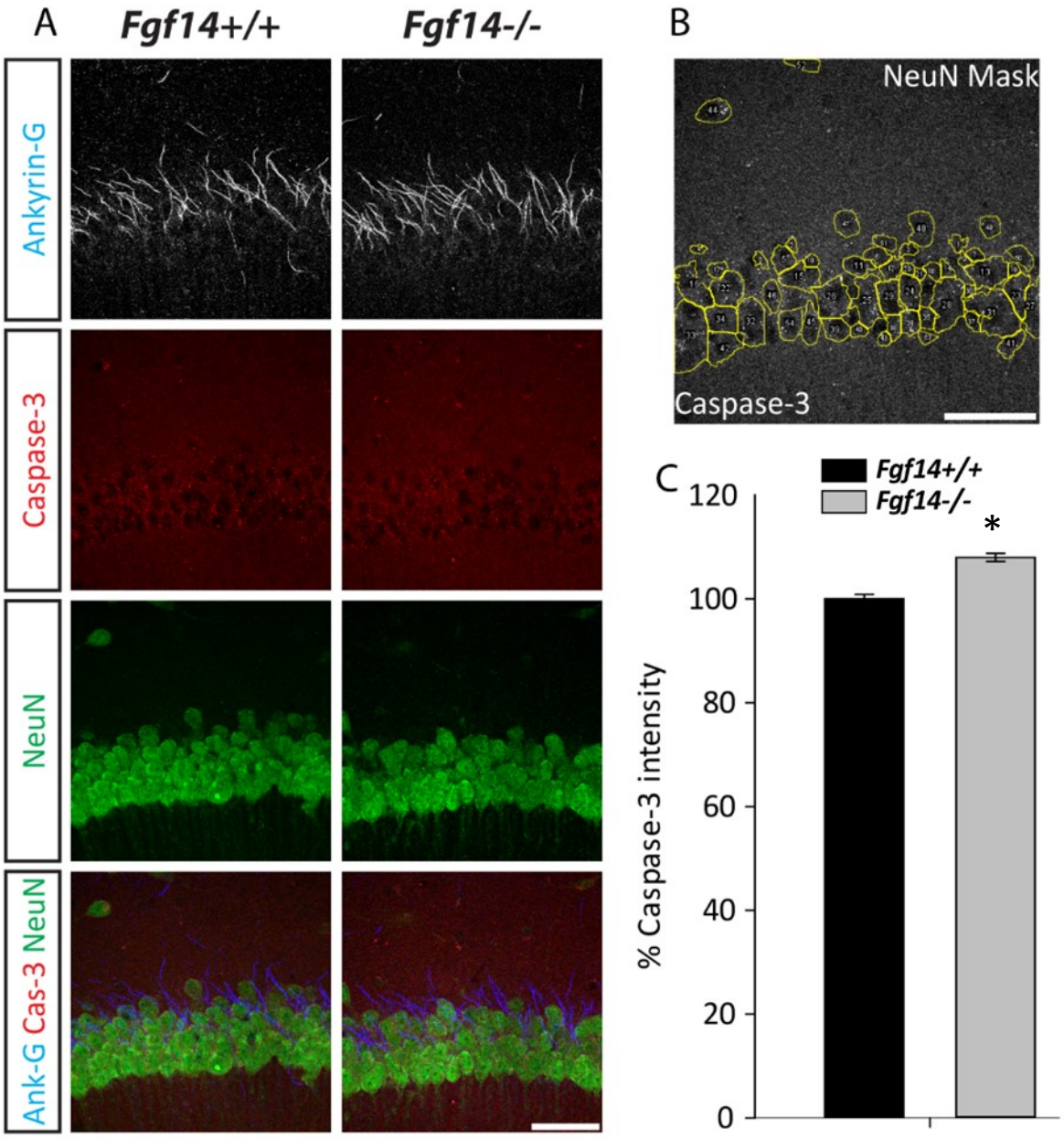

Figure 5:3 Active Caspase-3 (death cascade) activity in *Fgf14*$^{-/-}$.
A. Representative confocal images of triple immunofluorescence, the gray channel represent Ankyrin-G immunoreactivity, the red Caspase3, and the green NeuN in *Fgf14*$^{+/+}$ and *Fgf14*$^{-/-}$ hippocampal CA1 region. **B**. the NeuN mask generated by ImageJ software that has been used for active caspase3 fluorescence intensity quantifications in **C**. Data represent mean ± SEM, statistical differences were assessed by non-parametric Mann-Whitney test. Scale bars: **A**= 40 µm. (n=3 mice per group, 2 sections per mouse, *P < 0.05, Student's t test).

The effect of FGF14 on AIS structure, the activity-dependent hypothesis.

A previous report suggested that dysfunctions in AIS structure, including macrocomplex targeting, trafficking, and function might be the leading cause of developmental defects that arise earlier than pathological symptoms in an Alzheimer's disease transgenic mouse model (Sun et al., 2014). Moreover, neurodegenerative investigations, including postmortem studies and axonal structural alterations were reported (Greco et al., 2002). Age-dependent alterations in AIS structure, organization, and trafficking had been reported previously (Buffington and Rasband, 2011). The inhibitory circuitry, including feedback and feed-forward inhibition, were critical for synapsing with the AIS. The high-fidelity coordinated circuitry had a huge impact on PVI maturation (Sauer and Bartos, 2010;Pelkey et al., 2015). These facts raised the possibility that lacking *Fgf14* alter the axon structure in the hippocampal CA1 region. This, in turn, might have led to loss in PVIs as a consequence of overall dysfunction in the circuitry and would have been consistent with our previous report (Chapter-3).

Ankyrin-G plays a vital role in AIS formation. This scaffold cytoskeletal element modulates AIS component targeting and stabilization, mostly by linking them to spectrin βIV, another AIS scaffold protein (Bennett and Lambert, 1999). Initially, Ankyrin-G localizes to the AIS, then it recruits spectrin (Yang et al., 2007). Next, βIV spectrin masters AIS organization via a network complex (Buffington and Rasband, 2011), including multiple isoforms of Nav (Gollan et al., 2002).

In chapter 3, I showed that FGF14 is a component of the AIS. Here, I further validate this by conducting Ankyrin-G/ *Fgf14* double labelling experiment. Moreover, the spectrin/*Fg14*

immunolabelling experiment confirms the colocalization of FGf14 and AIS master regulators Figure 5.5.

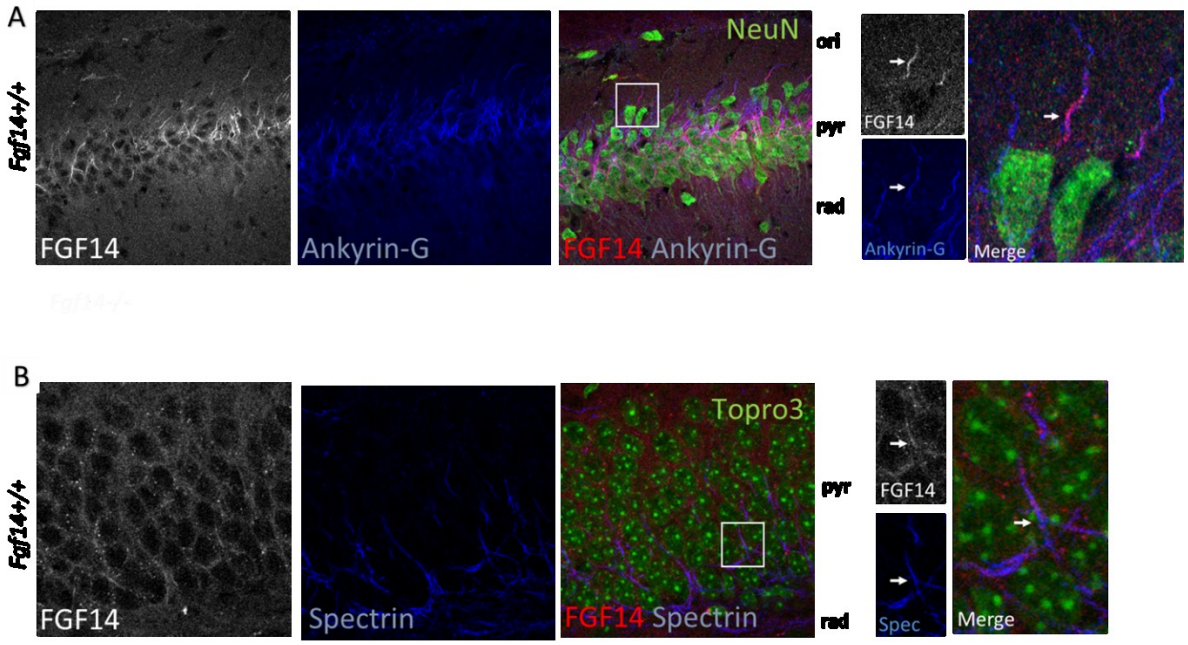

Figure 5:4 *Fgf14*, Ankyrin and spectrin.
A. The gray/red channels represent FGF14 immunosignals, the green channel represent NeuN immunoreactivity and the blue channel represents the Ankyrin-G in the hippocampal CA1 regions, the zoom image of the boxed area. **B.** The gray/red channels represent FGF14 immunoreactivity; the blue channel represents the Spectrin signals; and the green channel represents NeuN immunoreactivity. The zoom image of the boxed area.

To examine the AIS structure, I started with Ankyrin-G. The immunosignals that immunohistochemistry experiments detected indicated that the lack of FGF14 had no effect on Ankyrin-G protein expression **Figure 5:5**. Next, I analyzed spectrin immunosignals. Upon analyzing spectrin, I found that the spectrin fluorescence intensity was reduced in *Fgf14*$^{-/-}$ Figure 5:5This suggested that the AIS cytoskeletal structure might have been dysfunctional, supporting other reports that indicated that circuitry influenced proper neuronal maturation and development (Sauer and Bartos, 2010;Pelkey et al., 2015). Next, I examined Nav1.1 expression in *Fgf14*$^{-/-}$, and

I found that Nav1.1 signals were comparable in both genotypes Figure 5:6, indicating that FGF4 did not influence Nav1.1 expression and structure.

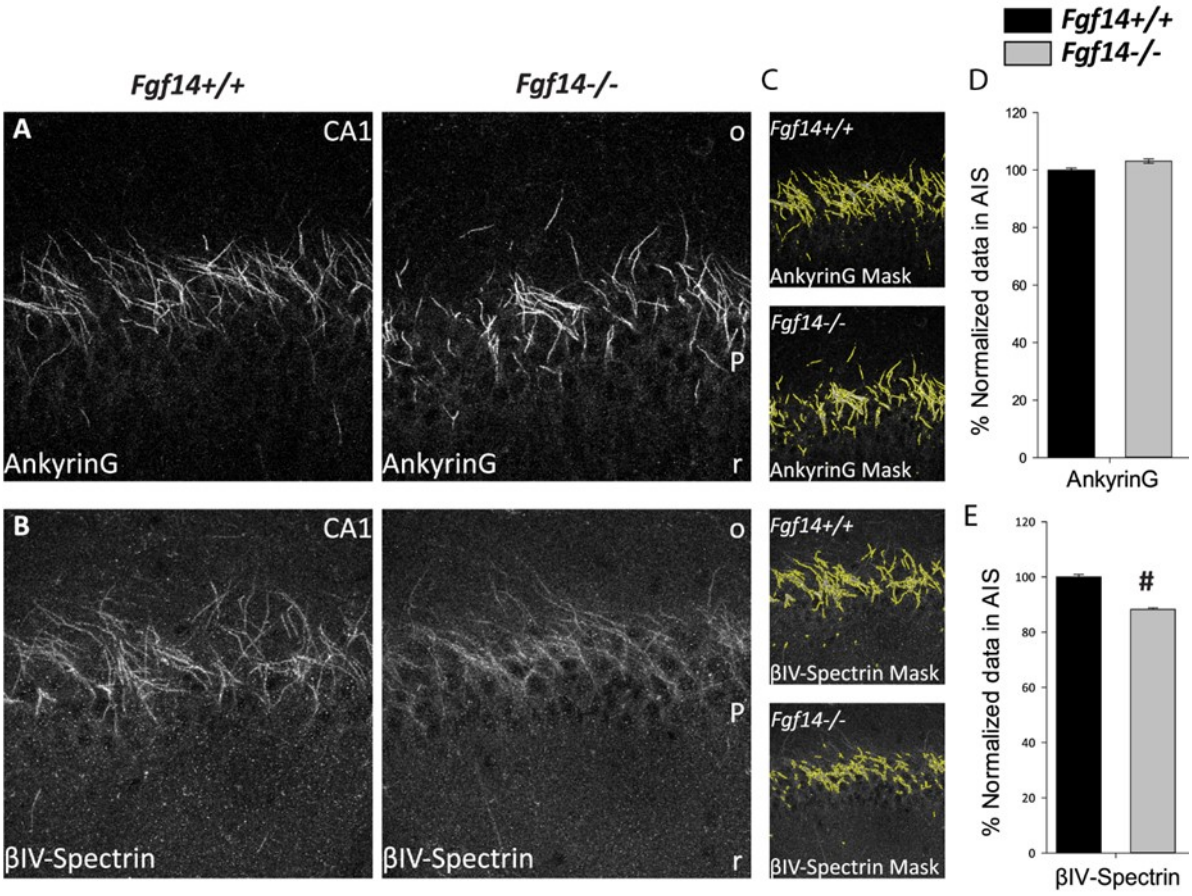

Figure 5:5 Genetic deletion of FGF14 disrupts the AIS structure.
A. The gray channel represents confocal images of Ankyrin-G immunofluorescence in *Fgf14*$^{+/+}$ and *Fgf14*$^{-/-}$. **B.** The gray channel represents βIV spectrin immunoreactivity at the AIS in *Fgf14*$^{+/+}$ and *Fgf14*$^{-/-}$. **C.** The AIS mask generated by adjusting the threshold on Ankyrin-G and βIV spectrin respectively, using ImageJ software in the hippocampal CA1 of in *Fgf14*$^{+/+}$ and *Fgf14*$^{-/-}$. **D.** Ankyrin-G fluorescence intensity quantifications. **E.** The quantifications of βIV spectrin signals at the AIS. Data represent mean ± SEM, statistical differences were assessed by non-parametric Mann-Whitney test. n=3 mice per group, 3-4 sections per mouse, # $P < 0.01$, Student's t test.

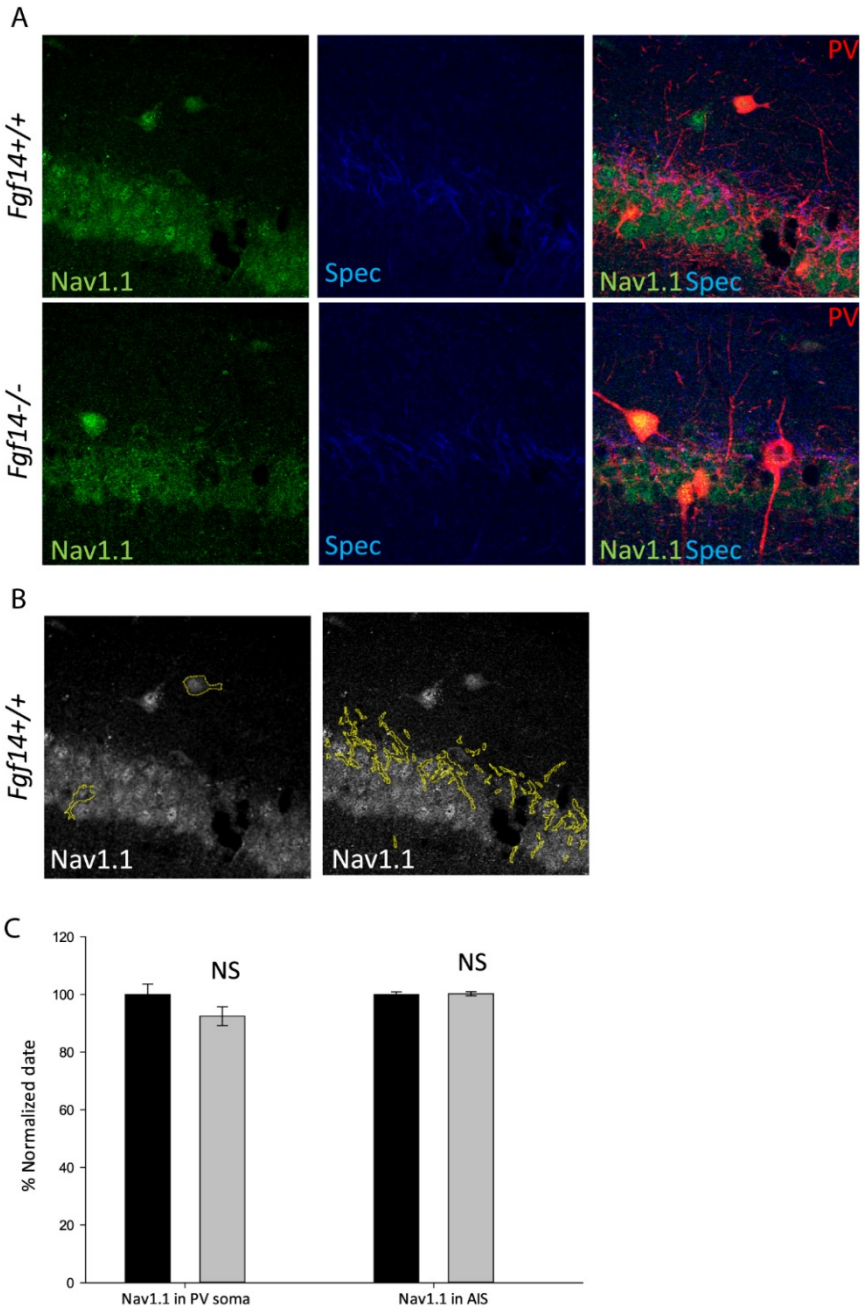

Figure 5:6 Genetic deletion of FGF14 does not influence Nav1.1 structure.

A. Confocal images of Nav1.1 visualized by the green channel, βIV spectrin immunofluorescence that are represented by the blue channel, and PV in red channel in *Fgf14*$^{+/+}$ and *Fgf14*$^{-/-}$. **B**. The masks generated by adjusting the threshold on PV soma and βIV spectrin AIS immunoreactivity using ImageJ software in the hippocampal CA1 of in *Fgf14*$^{+/+}$ and *Fgf14*$^{-/-}$. **C**. Nav1.1 fluorescence intensity quantifications. Data represent mean ± SEM, statistical differences were assessed non-parametric Mann-Whitney test. (n=3 mice per group, 3-4 sections per mouse, *P < 0.05, Student's t test. NS: not significant; Spec: spectrin.

5.4 Discussion

Here I examined three potential mechanisms underlie the loss of PVIs in *Fgf14*$^{-/-}$ mice. I report that the genetic deletion of *Fgf14* might result in impaired maturation of PVIs. Furthermore, examining neuronal loss due to apoptosis suggest that Caspase-3 activity was slightly increased in the hippocampal CA1 region in *Fgf14*$^{-/-}$ mice. The overall brain size was reduced in *Fgf14*$^{-/-}$ mice. However, this was not due to neuronal loss since cresyl violet quantifications were comparable in both genotypes. Moreover, I reported that the expression of the AIS cytoskeletal protein spectrin-G is reduced, suggesting that proper AIS assembly is disrupted (Komada and Soriano, 2002). These results indicated significant age-related alterations in PVI population counts in the hippocampal CA1 region of the *Fgf14*$^{-/-}$ mice, which comprised decreases in the inhibitory drive. Indicating that the excitatory-inhibitory circuitry balance had gone awry in *Fgf14*$^{-/-}$ mice.

Age-related changes in PV interneurons in Fgf14$^{-/-}$ *mice, the developmental hypothesis.*

Previous studies showed that during the critical period the maturation of GABAergic components occur, thus shaping the synaptic plasticity take place. Through this period dependent shaping, the PVIs and inhibitory GABAergic synthesis (both decarboxylase isoforms – GAD65 and GAD67), transport (VGAT), and release PVIs increased. (Huang et al., 1999;Chattopadhyaya et al., 2004;Lazarus and Huang, 2011). The role and the pattern of PVI expression in the visual cortex and the auditory cortex in critical periods have been extensively studied. In the early postnatal stages, PVIs are essential for shaping E/I balance. Experience and environment influence the need for GABAergic components and PV. For example, in visual cortex studies immediately following eye opening at P15, the immunohistochemistry analysis demonstrated an increase in PVIs and GABAergic proteins. Hippocampal studies showed that PVIs increased in mid-adulthood stages, suggesting that, in those stages, PVIs were required for shaping the circuitry and the

inhibitory drive, and were needed for adulthood's higher cognitive tasks (Fish et al., 2013). In schizophrenia, cognitive impairments precede other symptoms. They appear during early adulthood, suggesting that cognitive deficits arise from perturbed neuronal maturation (Huang et al., 2009;Marín, 2012;Barnes et al., 2015).

In a model of autism, the number of ethyl-CpG-binding protein 2 (MeCP2) mutant mice, PV, and the inhibitory system components were increased at critical periods of synaptic plasticity. Moreover, the functional activity and network recordings revealed that the mIPSCs amplitude was significantly increased. Suggesting that the mutation in the MeCP2 encoding gene, resulted in the acceleration of PVI maturation (Krishnan et al., 2015).

A recent study by our group showed that, in *Fgf14*$^{-/-}$, hippocampal adult stem cell maturation was disrupted. Under physiological conditions, adult stem cells were continuously produced in the hippocampal DG region, undergoing multiple phases until they reached maturity. The process lasted about one month and various markers, along with BrdU incorporation studies, verified it. During the early stages, the cells expressed SOX2 and nestin. Once they exited the cell cycle, the expression of these proteins reduced and the cells start to express doublecortin. The migratory neuroblasts exited the mitotic stage, doublecortin expression began to decrease, and immature stem cells became calretinin positive. One month after generating adult stem cells, they became fully mature and started to express calbindin. In *Fgf14*$^{-/-}$ mice, most of the one-month-old stem cells, traced by BrdU signals, were doublecortin and calretinin-positive. Indicating that the newborn neurons in the hippocampus were trapped in immature stages. These facts suggested that *Fgf14* modulate adult hippocampal stem cells maturation. Raising the possibility of the potential role of *Fgf14* in regulating PVIs maturation.

Active Caspase3 (death cascade) activity in Fgf14$^{-/-}$ mice, the Neuronal death hypothesis.

The second possible mechanism that might underlie the loss of PVIs in *Fgf14*$^{-/-}$ mice is induced apoptosis. To test this mechanism, I examined caspase-3 activity. The fluorescence intensity of the active caspase-3 levels in the hippocampal CA1 region of *Fgf14*$^{-/-}$ mice was slightly increased compared to that in wild-type mice. Our observations suggest that caspase-3 is expressed in punctate pattern within NeuN positive cells throughout the CA1 cells, the typical pattern of caspase-3 immunoreactivity is diffused pool within the apoptotic targeted soma (Pasinelli et al., 2000;Correia et al., 2007;Sabri et al., 2008;Vicario et al., 2015). The overall deprivation condition due to the lack of *Fgf14* could have explained this trend. The loss in neurotrophic and growth factors influenced the survival promoting and apoptotic pathways (Mattson, 2000). Another possibility is that lacking *Fgf14* would affect a particular type of PVIs such as PVBcs or PVChcs, and upon genetic ablation of *Fgf14*, caspase-3 would be activated to eliminate the most vulnerable type of PVIs, if any.

The effect of FGF14 on AIS structure, the activity-dependent hypothesis.

Next, I examined the AIS structure and found that spectrin fluorescence intensity was reduced, suggesting that less spectrin protein content was expressed in *Fgf14*$^{-/-}$ mice. On the other hand, *Fgf14* genetic deletion did not affect Ankyrin-G expression. The reduction in spectrin was expected to interrupt the appropriate targeting and assembly of AIS macrocomplex components. As a consequence of disrupted AIS elements recruitment, the inhibitory drive would have been compromised, leading to an E/I imbalance in the hippocampal circuitry. Since the circuitry influenced PVI maturation, the downregulation in spectrin could have resulted in alterations in both the structure and function of the AIS, leading to failure in PVI maturation and development and, eventually, reduction in PVIs.

Previous studies have shown that FGF14 binds and regulates Nav1.1 (Lou et al., 2005). Hence, the absence of a detectable effect of *Fgf14* genetic deletion on Nav1.1 protein expression could be interpreted as *Fgf14* ablation affecting the function of Nav1.1. Moreover, the structure of other Nav isoforms - such as Nav1.6 - could be affected.

A recent review suggested that there were two potential mechanisms for E/I imbalance in schizophrenia. The first one was due to a defect in the inhibitory drive. While the second favored impaired excitatory input, eventually both mechanisms were linked to impaired feedback and forward inhibition. As a consequence, an imbalance in the circuitry took place (Gonzalez-Burgos et al., 2015). Moreover, previous studies implicated neurotrophins and growth factors in the regulation of synaptic formation and axon maintenance in the maturation of GABAergic interneurons (Vicario-Abejon et al., 1998;Chattopadhyaya, 2011).

In developmental psychiatric disorders such as schizophrenia, Rett syndrome, and autism, alterations in neuronal connectivity and synaptic plasticity have been reported (Belmonte et al., 2004;Crabtree and Gogos, 2014). At specific time windows, "critical periods" during postnatal development, experience shapes the neuronal circuitry. These experience-dependent critical periods are important for shaping synaptic plasticity and wiring proper neuronal connectivity, which mediate cognitive, motor, and sensory functions (Hensch, 2005). The timing and proper shaping of these critical periods of development are extremely sensitive to any subtle alterations in PVIs. Deficits in PVI maturation have been reported to be modulators of critical period plasticity (Hensch et al., 1998;Huang et al., 1999;Krishnan et al., 2015).

5.5 Conclusions

In this chapter, I have identified two potential roles of FGF14. First, it has a conserved role in the regulation of AIS structure. Its second possible role includes the modulation of PVIs

maturation. The relationship between GABA synthesis, axon structure, and PVI maturation have been studied previously (Chattopadhyaya et al., 2007;Fish et al., 2013;Schubert et al., 2013;Hoon et al., 2015). Overall, this work suggests that FGF14 orchestrates the time course development of PVIs and hippocampal network refinement.

Chapter 6: **Conclusions and Future Directions**

This dissertation describes a new role of FGF14 in the GABAergic system within the hippocampal CA1 region. We studied the PV cell numbers of different age groups, GAD67 and Vgat expression, CA1 inhibitory transmission, gamma oscillations, spatial working memory, and bioinformatic analysis. This work showed that FGF14 modulated GABAergic synthesis, transport, and release (PVIs) in the hippocampal CA1 area. In this chapter, I examine the fundamental findings of this study and address its general limitations and future considerations along with a number of questions: I discuss the cellular and molecular alterations that *Fgf14* genetic deletions mediate; (2) the changes in cellular transmission in *Fgf14*$^{-/-}$ mice; the functional changes, including those at the network and behavioral levels; (4) bioinformatics and genetic transcriptomic reports; (5) examining three possible mechanisms underlying the loss of PVIs in the CA1 hippocampal region *Fgf14*$^{-/-}$ mice; and (5) future directions. **Figure 6**:1 demonstrates the working model of the alterations in *Fgf14*$^{-/-}$ mice.

6.1 Cellular and molecular alterations

This work began by investigating the role of FGF14 in the adult mouse (4-5 months) since previous studies reported cognitive impairment and disrupted hippocampal CA1 excitatory circuitry in *Fgf14*$^{-/-}$at this age (Wang et al., 2002;Wozniak et al., 2007). The analysis of PVI cell counts in *Fgf14*$^{-/-}$ hippocampi revealed a cell count reduction. This loss was more pronounced in the SO and SP, suggesting that the genetic ablation of *Fgf14* compromised both perisomatic and axo-axonic inhibition. The quantification of the intensity of PV fluorescence suggests that the remaining cells in *Fgf14*$^{-/-}$ express comparable PV content per cell soma. *Fgf14* genetic ablation did not affect the total hippocampal CA1 neuronal populations, which were measured by the

thickness of CA1 layers using cresyl violet and Topro-3 positive cell counting. Since the total inhibitory populations in CA1 is a minority population, the loss in PVIs may be very selective and specific to certain type of PVIs (for instance, the PVBcs or PVChcs). Furthermore, we addressed the question of whether these cellular alterations accompanied structural deficits in the neuronal connectivity of the remaining PV neurons. Thus, we analyzed the neuropil density and found that the lack of FGF14 did not affect the neuronal connections.

Next, we investigated GABA synthesis by analyzing GAD67 puncta size, number, and protein contents. FGF14 deletions did not affect the size or number of GAD67 presynaptic puncta, suggesting that FGF14 did not influence synaptogenesis. However, the protein content, measured by fluorescence intensity, was reduced in *Fgf14*$^{-/-}$, indicating that FGF14 modulated the maintenance of the GAD67 synapse by guaranteeing adequate protein loading or modulating the protein degradation per synapse. Similar findings were observed in the investigation of GABA transporting machinery (VGAT). The lack of FGF14 did not affect the number or size of the synapse, whereas the fluorescence intensity was reduced, indicating lower VGAT protein content in *Fgf14*$^{-/-}$ mice. I interpreted these observations as a defect in GABAergic presynaptic protein loading or degradation in *Fgf14*$^{-/-}$ mice.

After investigating the presynaptic GABAergic components, I went on to study the postsynaptic proteins that were relevant to cognitive deficit. I began with gephyrin, the scaffold protein that mastered the organization of GABAergic receptors and observed an increase in gephyrin fluorescence intensity in *Fgf14*$^{-/-}$ mice. The ablation of FGF14 did not affect $GABA_A$ alpha-1 or alpha-2 subunits. Postmortem schizophrenic studies reported that presynaptic proteins such as GAD67 and VGAT were fewer than those in the matched control. However, postsynaptic

proteins such as some $GABA_A$ subunits showed increases, suggesting a possible compensatory mechanism at the postsynaptic site (Volk et al., 2002).

6.2 Changes in cellular transmission

After performing whole-cell patch clamp recordings of pyramidal cells' sIPSCs and mIPSCs, we found that the amplitudes and frequencies of IPSCs' miniature and spontaneous recordings were comparable in both genotypes. However, the AP-driven presynaptic firing and the GABA-release functional readout by sIPSCs were indicative of aberrant transmission, which was measured by alterations in the number and amplitude of the inter-event intervals. mIPSC recordings allowed the examination of the mechanism of GABA release independently of the AP-driven inhibitory events. These studies required the blocking of sodium channels, and the recordings occurred in the presence of tetrodotoxin. In agreement with our cellular and molecular findings, the electrophysiology studies confirmed that FGF14 modulated inhibitory transmission, whereas FGF14 genetic ablation affected presynaptic and postsynaptic structures.

6.3 Functional changes (*in vivo* EEG alterations and behavioral changes)

Within the cortical regions, particularly the hippocampus, gamma oscillations can be classified as fast (65-100 Hz) and slow gamma (30-65 Hz) (Buzsaki and Wang, 2012). Each type plays a characteristic role in learning and memory. Fast gamma, which the entorhinal cortex network input drives, plays a role in LTP maintenance and generation. In this regard, fast gamma has a distinguished role in memory encoding. On the other hand, slow oscillations emerge from the hippocampal CA3 region. Thus, it has been proposed to be critical for memory retrieval (Colgin and Moser, 2010). Both types are synchronized gamma oscillations that are crucial for memory, attention, and executive functions (Lewis et al., 2004). Studies conducted on psychiatric disorders suggested that the reduction in PVIs in cortical regions was linked to the desynchronized network

function and the disruption in the E/I balance leading to a decrease in gamma oscillations (Lewis et al., 2012). The *in vivo* local field potential (LFP) recordings indicated that both slow and fast gamma oscillations were reduced in *Fgf14*$^{-/-}$, suggesting that gamma oscillations that Schaffer's collaterals and the entorhinal cortex generated were compromised (Csicsvari et al., 2003;Colgin et al., 2009;Papp, 2013;Yamamoto et al., 2014).

Next, we profiled *Fgf14*$^{-/-}$ mice by examining their spatial working memory using the 8-arm maze test. Our results showed that *Fgf14*$^{-/-}$ mice exhibited more latency and more errors during the test performance, suggesting impaired working memory. The behavioral studies provided further evidence that *Fgf14*$^{-/-}$ mice exhibited salient phenotypes that had been observed in psychiatric disorders.

6.4 Bioinformatics and genetic transcriptomic reports

To provide more insight into our examination, we conducted bioinformatics studies using existing transcriptomic datasets that had been deposited at NCBI's GEO public libraries. We studied FGF14 functional clustering with PVALB, GAD67, and VGAT from schizophrenic postmortem datasets. Using the SEEK search engine, the computational tool for evaluating gene co-expression, we found that FGF14 functionally clustered with the GABAergic signaling genes. We also found that FGF14, PVALB, GAD67, and VGAT genes were reduced in schizophrenic tissues. Moreover, we confirmed the strong functional correlations using two schizophrenic datasets, obtained from different brain regions, and two functional annotation analyses (GO and KEGG). Finally, the computational studies suggested the existence of potential regulations at the genetic level between FGF14 and the GABAergic signaling genes.

6.5 Possible mechanisms underlying the loss of PVIs in the CA1 hippocampal region *Fgf14*$^{-/-}$ mice

In chapter five, I designed a developmental study that covered PVIs in three age groups. In chapter three we examined PVIs in the adult stage (4-6 months), and, in this developmental studies, I expanded the investigation to include young (1-3 months old) and aged (9-11 months old) *Fgf14*$^{-/-}$ mice, comparing them to the wild type. I observed possible impaired maturation/acceleration in aging of PVI in *Fgf14*$^{-/-}$ mice; normal-aged PVI cell counts appeared at an earlier age in the wild type. Next, to understand the putative mechanisms behind the loss in PVIs, I examined caspase-3 activity. This studies showed that the lack of FGF14 slightly increase the apoptosis mechanism. I then asked whether the lack of FGF14 would impact the AIS structure, which would have impaired the network, desynchronized the circuitry, and, as a consequence, affected PVI maturation and development.

The third potential mechanism is related to activity-dependent development of AIS structure. Thus, I analyzed different components of AIS. The results suggested that FGF14 modulated spectrin expression. Spectrin is a cytoskeletal protein that recruits multiple elements to the AIS. The results of these investigations indicated that the lack of FGF14 induced defects in the hippocampal CA1 neuronal population's AIS structure, which in turn had a powerful effect on hippocampal synchronized activity and PVI development. These results incorporate Fgf14 into shaping hippocampal circuitry since it may influence PV neurons maturation and possible recruitment of AIS components. Such roles could converge to the circuitry tuning, amplification, and refinement.

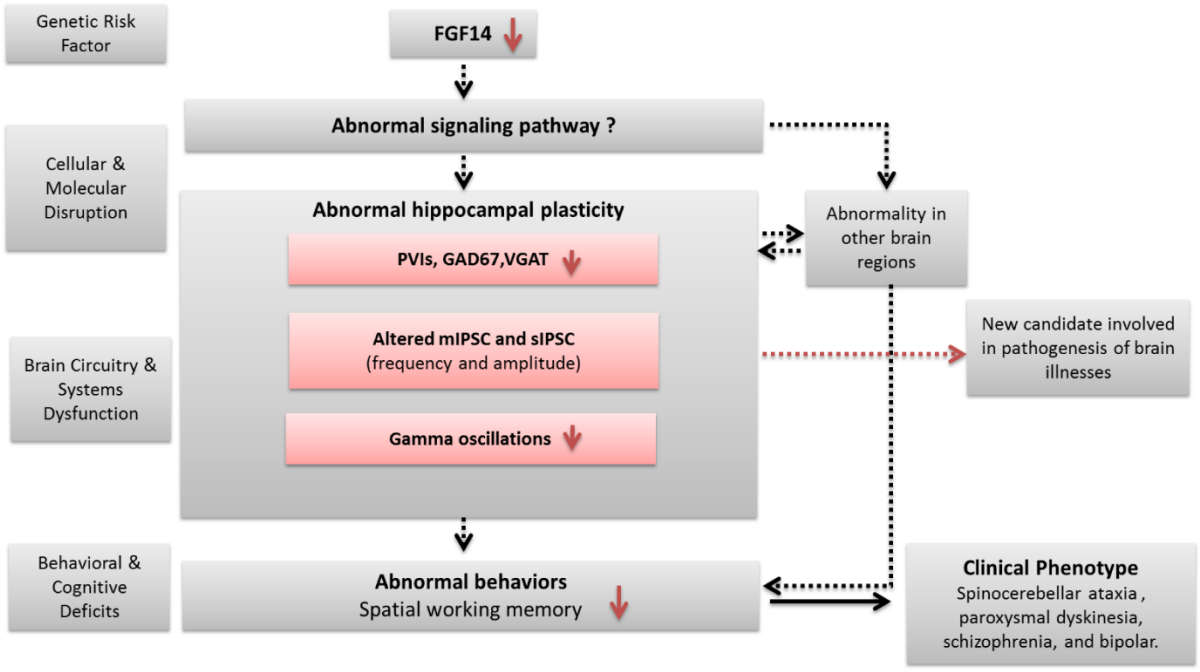

Figure 6:1 Working model scheme.
Lacking FGF14 leads to multiple alterations at the molecular, cellular, functional and behavioral levels.

6.6 Limitations

1. We used a global knocked out mouse model (*Fgf14*$^{-/-}$ mice) to conduct this work. Thus, to examine the role of FGF14 in influencing PVI structure, function, and development, we need a transgenic animal model in which FGF14 is selectively deleted in PVIs. One of the possibilities is a complex but more versatile approach, the CRE/Lox system, which basically involves crossbreeding *Fgf14*$^{-/-}$ mice with the commercially available PV-Cre animals from Jackson's laboratory (B6; 129P2-Pvalbtm1 (cre) Arbr/J). PV-Cre transgenic mice have been used widely to investigate PVI morphology and functionality (Fuchs et al., 2007;Sohal et al., 2009;Pozzi et al., 2014); the advantage of this system is that it allows the restricted expression of Cre recombinase in PV interneurons (Potter et al., 2009). Upon the generation of F2 double transgenic mice (*Fgf14*$^{-/-}$/PV-Cre$^{+/+}$), we could reintroduce FGF14-IRES-GFP (or GFP) conditionally upon Cre-mediated

recombination, using a loxP-STOP-loxP (Hughes et al.) AAV shuttle plasmid (Kuhlman and Huang, 2008). The introduction of the viral vector in the CA1 region could challenging, due to the structure and lamination. However, this approach would be more successful in other brain regions e.g. the cortex.

2. We conducted electrophysiological recordings in the hippocampal CA1 pyramidal layer. However, to examine the role of FGF14 in PVI function we need to patch directly from PVIs. Direct recordings can be achieved using a commercially available transgenic animal model B6; SJL-Tg (Pvalb-COP4*H134R/ EYFP)15Gfng/J from the Jackson Laboratory. In these mice, the yellow fluorescence labeling protein is fused to the parvalbumin promoter, allowing the optical labeling of PVIs. We have generated a double transgenic animal model that is PV-YFP/*Fgf14*$^{-/-}$ by cross-mating the commercially available PV-labelled mice with *Fgf14*$^{-/-}$.

3. PVIs are classified as PVBcs or PVChcs, depending on the shape and organization of their soma and dendrites. The hippocampal CA1 region is tightly laminated and heavily packed (Rho et al., 2010;Alshammari et al., 2016). Thus, it is quite hard to visually classify PVIs as PVBcs or chandelier PVChcs. Similar investigations were extensively conducted in the prefrontal cortex (Akil and Lewis;Cruz et al., 2003;Fish et al., 2013;Povysheva et al., 2013). Since the area is less laminated and the layers are easily distinguished, it is more feasible to visually characterize both types of PVIs.

6.7 Future directions

Before this work, the role of FGF14 in modulating an inhibitory system had not been established. Thus, our results have opened up a whole new avenue. In future studies, I would like to address the limitations of this one. Currently, we have generated PV-FGF14 double transgenic mice. Which of the following would be a valuable tool for various studies on PVIs: 1) direct

electrophysiological recordings; 2) dendritic arborization tracing, axonal connectivity and cytoarchitecture profiling to evaluate the maturation of PVIs; 3) optogenetic studies. Optogenetics consists of experimental studies based on manipulating the light-sensitive channel, Channelrhodopsin-2, which, in turn, modulates action potential. For instance, exposing the transgenic animal model that expresses Channelrhodopsin-2 to a blue light enables ionic channel activations to take place, allowing cation (primarily Na^+) influx. As a consequence, action potential is generated. In comparison, yellow-green light illumination causes hyperpolarization by releasing Cl^- inside the cell (Zhang et al., 2010;Bernstein and Boyden, 2011;Tye et al., 2011). This powerful tool has been used to answer research questions in different types of studies, including those regarding memory formation and induction (Han et al., 2009), learning (Schroll et al., 2006), sociability (Yizhar et al., 2011), anxiety (Tye et al., 2011), aggressive behavior (Lin et al., 2011), and epilepsy (Tonnesen et al., 2009). Another question I want to address is that regarding the quantification of PVIs in PFC and the investigation of the role of FGF14 in influencing other interneurons, for instance, somatostatin, calbindin, calretinin, and cholecystokinin.

6.7.1 FGF14 regulates GABAergic system in a sex-dependent manner

A growing line of evidence indicates that sexual dimorphisms influence the healthy, aged, and disordered brain (Simerly, 2002;Cahill, 2006;Cosgrove et al., 2007;Goldstein et al., 2010;Holsen et al., 2011). In last the five years, NIMH has encouraged neuroscientists to conduct more hypothesis-driven investigations focusing on cognition and sex difference-related factors/regulators (NIMH, 2011;NIH, 2014) based on the following notions: 1) A recent study conducted on postmortem tissue and rodents reported that sex chromosomes affected GABA-related genes (Seney et al., 2013); 2) FGF14 regulates multiple components of the GABAergic system and function; and 3) Sex influences cognitive capacity (Gurvich and Rossell, 2015). I

would like to address the question of whether *Fgf14* considered as a sex-dependent molecule that is essential to regulate the GABAergic system and PVIs structure, connectivity and function.

6.7.2 PVBcs VS. PVChcs in Fgf14$^{-/-}$

The question raised here is whether the loss of PVIs in *Fgf14*$^{-/-}$ may be attributed to a selective loss of PVBcs, PVChcs, or both? In other words, does FGF14 affect certain populations of PVIs or not? So far, PVIs can be classified into three types on the basis of their structure and synaptic connectivity with excitatory cells: 1) PVBcs innervate principal cells' proximal dendrites and soma, so their innervations are called perisomatic and dendrodendritic; 2) PVChcs synapse onto the principal neurons' axons; thus, their innervations are called axo-axonic; 3) bistratified PVIs innervate principal neurons' dendrites. The first two groups are the most intensively studied, particularly PVBcs (Benes and Berretta, 2001;Jinno and Kosaka, 2002;Baude et al., 2007). Functionally, it is believed that, compared to other PVI types, they have a greater impact on shaping and tuning the excitatory network. Moreover, PVBcs innervate other inhibitory neurons. They fire synchronized fast spikes, which equip them to entrain principal cells, and, as a consequence, generate gamma-band oscillations in the brain. In the hippocampus, they represent the majority of PVIs (Freund, 2003;Klausberger et al., 2003;Baude et al., 2007;Freund and Katona, 2007).

To address whether FGF14 regulates PVBcs, PVChcs, or both, the investigation will be based on three criteria. First will be visual classification by the application of previously described criteria (Freund and Buzsaki, 1996;Marín, 2012). Second, the studies will be conducted in the PFC, where it will be easier to distinguish between them morphologically (Marín, 2012). Third will be the use of other markers, such as the AIS proteins of ankyrin and spectrin, in combination with PV to distinguish PVChcs from PVBcs (Panzanelli et al., 2011), and GAD65, which marks

presynaptic PVBcs boutons and is not expressed in PVChcs. Confirming a selective deficit in PVBcs in comparison to PVChcs is very important as it has been speculated to be the reason behind aberrant gamma oscillations and cognitive deficits in schizophrenia (Glausier et al., 2014). Moreover, in schizophrenia, there is a selective reduction in the $GABA_A$ receptor alpha-1 subunit and GAD67 expression at PVBcs to excitatory cell synapses, whereas GABA transporter-1 (GAT-1) density is reduced in PVChcs but not in PVBcs (Lewis et al., 2012). In our studies, we focused on the hippocampal CA1 region. Thus, we were technically challenged to identify whether the loss of PVIs was more pronounced in PVBcs or in PVChcs.

6.7.3 The role of FGF14 in critical-period synaptic plasticity.

Wiesel and Hubel won the Nobel Prize in the early sixties after introducing the concept of critical periods at early postnatal stages. These are periods during which the brain is adaptable and extremely dependent on early-life experiences, which are the basis for cortical circuit shaping and development. Moreover, they underlie synaptic plasticity, which modulates various cognitive functions, including learning and memory (Wiesel and Hubel, 1963). Experience-dependent critical periods in the auditory cortex (Kim et al., 2013) and visual cortex (Spiegel et al., 2014) have been studied extensively. In the context of critical-period synaptic plasticity, PVIs have been studied extensively (Kuhlman et al., 2013). This work, along with the milestone studies conducted on *Fgf14*$^{-/-}$, leads us to ask whether FGF14 modulates critical-period synaptic plasticity.

BIBLIOGRAPHY

Akbarian, S., Kim, J., Potkin, S., Hagman, J., Tafazzoli, A., WE, J.B., and Jones, E. (1995). Gene expression for glutamic acid decarboxylase is reduced without loss of neurons in prefrontal cortex of schizophrenics. *Arch Gen Psychiatry*, 258-266.

Akil, M., and Lewis, D.A. (1992). Postnatal development of parvalbumin immunoreactivity in axon terminals of basket and chandelier neurons in monkey neocortex. *Prog Neuropsychopharmacol Biol Psychiatry* 16, 329-337.

Ali, S.R., Panova, N., Stoilova-McPhie, S., and Laezza, F. (2014). Protein-Protein Interactions Based Drug Discovery Against the Voltage-Gated Sodium Channel. *Biophysical Journal* 106, 326a-326a.

Alshammari, M.A., Alshammari, T.K., and Laezza, F. (2016). Improved methods for fluorescence microscopy detection of macromolecules at the axon initial segment. *Frontiers in Cellular Neuroscience* 10. doi: 10.3389/fncel.2016.00005.

Alshammari, M.A., Alshammari, T.K., Nenov, M.N., Scala, F., and Laezza, F. (2015). Fibroblast Growth Factor 14 Modulates the Neurogenesis of Granule Neurons in the Adult Dentate Gyrus. *Mol Neurobiol*. doi: 10.1007/s12035-015-9568-5.

Andersen, P., Bliss, T.V., and Skrede, K.K. (1971). Lamellar organization of hippocampal pathways. *Exp Brain Res* 13, 222-238.

Andrews-Hanna, J.R., Snyder, A.Z., Vincent, J.L., Lustig, C., Head, D., Raichle, M.E., and Buckner, R.L. (2007). Disruption of large-scale brain systems in advanced aging. *Neuron* 56, 924-935. doi: 10.1016/j.neuron.2007.10.038.

Arai, H., Emson, P.C., Mountjoy, C.Q., Carassco, L.H., and Heizmann, C.W. (1987). Loss of parvalbumin-immunoreactive neurones from cortex in Alzheimer-type dementia. *Brain Res* 418, 164-169.

Baraban, S.C., and Tallent, M.K. (2004). Interneuron Diversity series: Interneuronal neuropeptides--endogenous regulators of neuronal excitability. *Trends Neurosci* 27, 135-142. doi: 10.1016/j.tins.2004.01.008.

Barnes, S.A., Sawiak, S.J., Caprioli, D., Jupp, B., Buonincontri, G., Mar, A.C., Harte, M.K., Fletcher, P.C., Robbins, T.W., Neill, J.C., and Dalley, J.W. (2015). Impaired Limbic Cortico-Striatal Structure and Sustained Visual Attention in a Rodent Model of

Schizophrenia. *International Journal of Neuropsychopharmacology* 18**,** pyu010. doi: 10.1093/ijnp/pyu010.

Baude, A., Bleasdale, C., Dalezios, Y., Somogyi, P., and Klausberger, T. (2007). Immunoreactivity for the GABAA receptor alpha1 subunit, somatostatin and Connexin36 distinguishes axoaxonic, basket, and bistratified interneurons of the rat hippocampus. *Cereb Cortex* 17**,** 2094-2107. doi: 10.1093/cercor/bhl117.

Beasley, C.L., and Reynolds, G.P. (1997). Parvalbumin-immunoreactive neurons are reduced in the prefrontal cortex of schizophrenics. *Schizophr Res* 24**,** 349-355.

Beasley, C.L., Zhang, Z.J., Patten, I., and Reynolds, G.P. (2002). Selective deficits in prefrontal cortical GABAergic neurons in schizophrenia defined by the presence of calcium-binding proteins. *Biol Psychiatry* 52**,** 708-715.

Belmonte, M.K., Allen, G., Beckel-Mitchener, A., Boulanger, L.M., Carper, R.A., and Webb, S.J. (2004). Autism and abnormal development of brain connectivity. *J Neurosci* 24**,** 9228-9231. doi: 10.1523/JNEUROSCI.3340-04.2004.

Benes, F.M., and Berretta, S. (2001). GABAergic interneurons: implications for understanding schizophrenia and bipolar disorder. *Neuropsychopharmacology* 25**,** 1-27. doi: 10.1016/S0893-133X(01)00225-1.

Benham, R.S., Engin, E., and Rudolph, U. (2014). Diversity of neuronal inhibition: a path to novel treatments for neuropsychiatric disorders. *JAMA Psychiatry* 71**,** 91-93. doi: 10.1001/jamapsychiatry.2013.3059.

Bennay, M., Gernert, M., and Richter, A. (2001). Spontaneous remission of paroxysmal dystonia coincides with normalization of entopeduncular activity in dt(SZ) mutants. *J Neurosci* 21**,** RC153.

Bennett, V., and Lambert, S. (1999). Physiological roles of axonal ankyrins in survival of premyelinated axons and localization of voltage-gated sodium channels. *J Neurocytol* 28**,** 303-318.

Bernard, C., Esclapez, M., Hirsch, J.C., and Ben-Ari, Y. (1998). Interneurones are not so dormant in temporal lobe epilepsy: a critical reappraisal of the dormant basket cell hypothesis. *Epilepsy Research* 32**,** 93-103.

Bernstein, J.G., and Boyden, E.S. (2011). Optogenetic tools for analyzing the neural circuits of behavior. *Trends Cogn Sci* 15**,** 592-600. doi: 10.1016/j.tics.2011.10.003.

Bikfalvi, A., Klein, S., Pintucci, G., and Rifkin, D.B. (1997). Biological roles of fibroblast growth factor-2. *Endocr Rev* 18**,** 26-45. doi: 10.1210/edrv.18.1.0292.

Boley, A.M., Perez, S.M., and Lodge, D.J. (2014). A fundamental role for hippocampal parvalbumin in the dopamine hyperfunction associated with schizophrenia. *Schizophr Res* 157**,** 238-243. doi: 10.1016/j.schres.2014.05.005.

Bosch, M.K., Carrasquillo, Y., Ransdell, J.L., Kanakamedala, A., Ornitz, D.M., and Nerbonne, J.M. (2015). Intracellular FGF14 (iFGF14) Is Required for Spontaneous and Evoked Firing in Cerebellar Purkinje Neurons and for Motor Coordination and Balance. *J Neurosci* 35**,** 6752-6769. doi: 10.1523/JNEUROSCI.2663-14.2015.

Brady, J.R.O., McCarthy, J.M., Prescot, A.P., Jensen, J.E., Cooper, A.J., Cohen, B.M., Renshaw, P.F., and Öngür, D. (2013). Brain gamma-aminobutyric acid (GABA) abnormalities in bipolar disorde. *Bipolar Disorders* 15**,** 434–439.

Brambilla, P., Perez, J., Barale, F., Schettini, G., and Soares, J. (2003). GABAergic dysfunction in mood disorders. *Molecular Psychiatry* 8**,** 721–737.

Brennand, K.J., Simone, A., Jou, J., Gelboin-Burkhart, C., Tran, N., Sangar, S., Li, Y., Mu, Y., Chen, G., Yu, D., McCarthy, S., Sebat, J., and Gage, F.H. (2011). Modelling schizophrenia using human induced pluripotent stem cells. *Nature* 473**,** 221-225. doi: 10.1038/nature09915.

Brusse, E., de Koning, I., Maat-Kievit, A., Oostra, B.A., Heutink, P., and van Swieten, J.C. (2006). Spinocerebellar ataxia associated with a mutation in the fibroblast growth factor 14 gene (SCA27): A new phenotype. *Mov Disord* 21**,** 396-401.

Buffington, S.A., and Rasband, M.N. (2011). The axon initial segment in nervous system disease and injury. *Eur J Neurosci* 34**,** 1609-1619. doi: 10.1111/j.1460-9568.2011.07875.x.

Buzsaki, G., and Wang, X.J. (2012). Mechanisms of gamma oscillations. *Annu Rev Neurosci* 35**,** 203-225. doi: 10.1146/annurev-neuro-062111-150444.

Buzzi, A., Chikhladze, M., Falcicchia, C., Paradiso, B., Lanza, G., Soukupova, M., Marti, M., Morari, M., Franceschetti, S., and Simonato, M. (2012). Loss of cortical GABA terminals

in Unverricht-Lundborg disease. *Neurobiol Dis* 47**,** 216-224. doi: 10.1016/j.nbd.2012.04.005.

Cahill, L. (2006). Why sex matters for neuroscience. *Nat Rev Neurosci* 7**,** 477-484. doi: 10.1038/nrn1909.

Caillard, O., Moreno, H., Schwaller, B., Llano, I., Celio, M.R., and Marty, A. (2000). Role of the calcium-binding protein parvalbumin in short-term synaptic plasticity. *Proc Natl Acad Sci U S A* 97**,** 13372-13377. doi: 10.1073/pnas.230362997.

Campbell, D.B., Li, C., Sutcliffe, J.S., Persico, A.M., and Levitt, P. (2008). Genetic evidence implicating multiple genes in the MET receptor tyrosine kinase pathway in autism spectrum disorder. *Autism Res* 1**,** 159-168. doi: 10.1002/aur.27.

Cardin, J.A., Carlen, M., Meletis, K., Knoblich, U., Zhang, F., Deisseroth, K., Tsai, L.H., and Moore, C.I. (2009). Driving fast-spiking cells induces gamma rhythm and controls sensory responses. *Nature* 459**,** 663-667. doi: 10.1038/nature08002.

Castillo, P.E. (2012). Presynaptic LTP and LTD of Excitatory and Inhibitory Synapses. *Cold Spring Harbor Perspectives in Biology* 4**,** a005728. doi: 10.1101/cshperspect.a005728.

Chand, A.N., Galliano, E., Chesters, R.A., and Grubb, M.S. (2015). A Distinct Subtype of Dopaminergic Interneuron Displays Inverted Structural Plasticity at the Axon Initial Segment. *The Journal of Neuroscience* 35**,** 1573-1590. doi: 10.1523/jneurosci.3515-14.2015.

Chao, H.-T., Chen, H., Samaco, R.C., Xue, M., Chahrour, M., Yoo, J., Neul, J.L., Gong, S., Lu, H.-C., Heintz, N., Ekker, M., Rubenstein, J.L.R., Noebels, J.L., Rosenmund, C., and Zoghbi, H.Y. (2010). GABAergic dysfunction mediates autism-like stereotypies and Rett syndrome phenotypes. *Nature* 468**,** 263-269. doi: 10.1038/nature09582.

Chard, P.S., Bleakman, D., Christakos, S., Fullmer, C.S., and Miller, R.J. (1993). Calcium buffering properties of calbindin D28k and parvalbumin in rat sensory neurones. *J Physiol* 472**,** 341-357.

Chattopadhyaya, B. (2011). Molecular mechanisms underlying activity-dependent GABAergic synapse development and plasticity and its implications for neurodevelopmental disorders. *Neural Plast* 2011**,** 734231. doi: 10.1155/2011/734231.

Chattopadhyaya, B., Di Cristo, G., Higashiyama, H., Knott, G.W., Kuhlman, S.J., Welker, E., and Huang, Z.J. (2004). Experience and activity-dependent maturation of perisomatic GABAergic innervation in primary visual cortex during a postnatal critical period. *J Neurosci* 24**,** 9598-9611. doi: 10.1523/JNEUROSCI.1851-04.2004.

Chattopadhyaya, B., Di Cristo, G., Wu, C.Z., Knott, G., Kuhlman, S., Fu, Y., Palmiter, R.D., and Huang, Z.J. (2007). GAD67-mediated GABA synthesis and signaling regulate inhibitory synaptic innervation in the visual cortex. *Neuron* 54**,** 889-903. doi: 10.1016/j.neuron.2007.05.015.

Cheah, C.S., Yu, F.H., Westenbroek, R.E., Kalume, F.K., Oakley, J.C., Potter, G.B., Rubenstein, J.L., and Catterall, W.A. (2012). Specific deletion of NaV1.1 sodium channels in inhibitory interneurons causes seizures and premature death in a mouse model of Dravet syndrome. *Proc Natl Acad Sci U S A* 109**,** 14646-14651. doi: 10.1073/pnas.1211591109.

Chen, H.M., DeLong, C.J., Bame, M., Rajapakse, I., Herron, T.J., McInnis, M.G., and O'Shea, K.S. (2014). Transcripts involved in calcium signaling and telencephalic neuronal fate are altered in induced pluripotent stem cells from bipolar disorder patients. *Transl Psychiatry* 4**,** e375. doi: 10.1038/tp.2014.12.

Chevaleyre, V., and Siegelbaum, S.A. (2010). Strong CA2 pyramidal neuron synapses define a powerful disynaptic cortico-hippocampal loop. *Neuron* 66**,** 560-572. doi: 10.1016/j.neuron.2010.04.013.

Colciaghi, F., Finardi, A., Nobili, P., Locatelli, D., Spigolon, G., and Battaglia, G.S. (2014). Progressive brain damage, synaptic reorganization and NMDA activation in a model of epileptogenic cortical dysplasia. *PLoS One* 9**,** e89898. doi: 10.1371/journal.pone.0089898.

Colgin, L.L., Denninger, T., Fyhn, M., Hafting, T., Bonnevie, T., Jensen, O., Moser, M.B., and Moser, E.I. (2009). Frequency of gamma oscillations routes flow of information in the hippocampus. *Nature* 462**,** 353-357. doi: 10.1038/nature08573.

Colgin, L.L., and Moser, E.I. (2010). Gamma oscillations in the hippocampus. *Physiology (Bethesda)* 25**,** 319-329. doi: 10.1152/physiol.00021.2010.

Conde, F., Lund, J.S., Jacobowitz, D.M., Baimbridge, K.G., and Lewis, D.A. (1994). Local circuit neurons immunoreactive for calretinin, calbindin D-28k or parvalbumin in monkey prefrontal cortex: distribution and morphology. *J Comp Neurol* 341**,** 95-116. doi: 10.1002/cne.903410109.

Connors, B.W., and Gutnick, M.J. (1990). Intrinsic firing patterns of diverse neocortical neurons. *Trends Neurosci* 13**,** 99-104.

Correia, A.S., Anisimov, S.V., Roybon, L., Li, J.Y., and Brundin, P. (2007). Fibroblast growth factor-20 increases the yield of midbrain dopaminergic neurons derived from human embryonic stem cells. *Front Neuroanat* 1**,** 4. doi: 10.3389/neuro.05.004.2007.

Cosgrove, K.P., Mazure, C.M., and Staley, J.K. (2007). Evolving knowledge of sex differences in brain structure, function, and chemistry. *Biol Psychiatry* 62**,** 847-855. doi: 10.1016/j.biopsych.2007.03.001.

Cossart, R., Bernard, C., and Ben-Ari, Y. (2005). Multiple facets of GABAergic neurons and synapses: multiple fates of GABA signalling in epilepsies. *Trends in Neurosciences* 28**,** 108-115. doi: http://dx.doi.org/10.1016/j.tins.2004.11.011.

Crabtree, G.W., and Gogos, J.A. (2014). Synaptic plasticity, neural circuits, and the emerging role of altered short-term information processing in schizophrenia. *Front Synaptic Neurosci* 6**,** 28. doi: 10.3389/fnsyn.2014.00028.

Craig, M.T., and McBain, C.J. (2015). Fast Gamma Oscillations Are Generated Intrinsically in CA1 without the Involvement of Fast-Spiking Basket Cells. *J Neurosci* 35**,** 3616-3624. doi: 10.1523/JNEUROSCI.4166-14.2015.

Cruz, D.A., Eggan, S.M., and Lewis, D.A. (2003). Postnatal development of pre- and postsynaptic GABA markers at chandelier cell connections with pyramidal neurons in monkey prefrontal cortex. *J Comp Neurol* 465**,** 385-400. doi: 10.1002/cne.10833.

Csicsvari, J., Jamieson, B., Wise, K.D., and Buzsaki, G. (2003). Mechanisms of gamma oscillations in the hippocampus of the behaving rat. *Neuron* 37**,** 311-322.

Curley, A.A., Eggan, S.M., Lazarus, M.S., Huang, Z.J., Volk, D.W., and Lewis, D.A. (2013). Role of glutamic acid decarboxylase 67 in regulating cortical parvalbumin and GABA membrane transporter 1 expression: implications for schizophrenia. *Neurobiol Dis* 50**,** 179-186. doi: 10.1016/j.nbd.2012.10.018.

Dalski, A., Atici, J., Kreuz, F.R., Hellenbroich, Y., Schwinger, E., and Zuhlke, C. (2005). Mutation analysis in the fibroblast growth factor 14 gene: frameshift mutation and polymorphisms in patients with inherited ataxias. *Eur J Hum Genet* 13**,** 118-120. doi: 10.1038/sj.ejhg.5201286.

Dani, V.S., Chang, Q., Maffei, A., Turrigiano, G.G., Jaenisch, R., and Nelson, S.B. (2005). Reduced cortical activity due to a shift in the balance between excitation and inhibition in a mouse model of Rett syndrome. *Proc Natl Acad Sci U S A* 102**,** 12560-12565. doi: 10.1073/pnas.0506071102.

Deng, W., Aimone, J.B., and Gage, F.H. (2010). New neurons and new memories: how does adult hippocampal neurogenesis affect learning and memory? *Nat Rev Neurosci* 11**,** 339-350. doi: 10.1038/nrn2822.

Donato, F., Rompani, S.B., and Caroni, P. (2013). Parvalbumin-expressing basket-cell network plasticity induced by experience regulates adult learning. *Nature* 504**,** 272-276. doi: 10.1038/nature12866.

Drgon, T., Zhang, P.W., Johnson, C., Walther, D., Hess, J., Nino, M., and Uhl, G.R. (2010). Genome wide association for addiction: replicated results and comparisons of two analytic approaches. *PLoS One* 5**,** e8832. doi: 10.1371/journal.pone.0008832.

Dudchenko, P.A., Talpos, J., Young, J., and Baxter, M.G. (2013). Animal models of working memory: A review of tasks that might be used in screening drug treatments for the memory impairments found in schizophrenia. *Neuroscience and Biobehavioral Reviews* 37**,** 2111-2124. doi: DOI 10.1016/j.neubiorev.2012.03.003.

Duinen, M.V., Reneerkens, O.A., Lambrecht, L., Sambeth, A., Rutten, B.P., Os, J.V., Blokland, A., and Prickaerts, J. (2015). Treatment of Cognitive Impairment in Schizophrenia: Potential Value of Phosphodiesterase Inhibitors in Prefrontal Dysfunction. *Curr Pharm Des* 21**,** 3813-3828.

Dupret, D., Pleydell-Bouverie, B., and Csicsvari, J. (2008). Inhibitory interneurons and network oscillations. *Proceedings of the National Academy of Sciences* 105**,** 18079-18080. doi: 10.1073/pnas.0810064105.

Eggan, S.M., Lazarus, M.S., Stoyak, S.R., Volk, D.W., Glausier, J.R., Huang, Z.J., and Lewis, D.A. (2012). Cortical glutamic acid decarboxylase 67 deficiency results in lower cannabinoid 1 receptor messenger RNA expression: implications for schizophrenia. *Biol Psychiatry* 71**,** 114-119. doi: 10.1016/j.biopsych.2011.09.014.

Enoch, M.A., Zhou, Z., Kimura, M., Mash, D.C., Yuan, Q., and Goldman, D. (2012). GABAergic gene expression in postmortem hippocampus from alcoholics and cocaine addicts; corresponding findings in alcohol-naive P and NP rats. *PLoS One* 7**,** e29369. doi: 10.1371/journal.pone.0029369.

Erisir, A., Lau, D., Rudy, B., and Leonard, C.S. (1999). Function of specific K(+) channels in sustained high-frequency firing of fast-spiking neocortical interneurons. *J Neurophysiol* 82**,** 2476-2489.

Falco, A., Pennucci, R., Brambilla, E., and de Curtis, I. (2014). Reduction in parvalbumin-positive interneurons and inhibitory input in the cortex of mice with experimental autoimmune encephalomyelitis. *Exp Brain Res* 232**,** 2439-2449. doi: 10.1007/s00221-014-3944-7.

Fatemi, S.H., Stary, J.M., Earle, J.A., Araghi-Niknam, M., and Eagan, E. (2005). GABAergic dysfunction in schizophrenia and mood disorders as reflected by decreased levels of glutamic acid decarboxylase 65 and 67 kDa and Reelin proteins in cerebellum. *Schizophr Res* 72**,** 109-122. doi: 10.1016/j.schres.2004.02.017.

Fish, K.N., Hoftman, G.D., Sheikh, W., Kitchens, M., and Lewis, D.A. (2013). Parvalbumin-containing chandelier and basket cell boutons have distinctive modes of maturation in monkey prefrontal cortex. *J Neurosci* 33**,** 8352-8358. doi: 10.1523/JNEUROSCI.0306-13.2013.

Flores, C.E., Nikonenko, I., Mendez, P., Fritschy, J.-M., Tyagarajan, S.K., and Muller, D. (2015). Activity-dependent inhibitory synapse remodeling through gephyrin phosphorylation. *Proceedings of the National Academy of Sciences* 112**,** E65-E72. doi: 10.1073/pnas.1411170112.

Floresco, S.B., Todd, C.L., and Grace, A.A. (2001). Glutamatergic afferents from the hippocampus to the nucleus accumbens regulate activity of ventral tegmental area dopamine neurons. *J Neurosci* 21**,** 4915-4922.

Floresco, S.B., West, A.R., Ash, B., Moore, H., and Grace, A.A. (2003). Afferent modulation of dopamine neuron firing differentially regulates tonic and phasic dopamine transmission. *Nat Neurosci* 6**,** 968-973. doi: 10.1038/nn1103.

Forster, E., Zhao, S., and Frotscher, M. (2006). Laminating the hippocampus. *Nat Rev Neurosci* 7**,** 259-268.

Freund, T.F. (2003). Interneuron Diversity series: Rhythm and mood in perisomatic inhibition. *Trends Neurosci* 26**,** 489-495. doi: 10.1016/S0166-2236(03)00227-3.

Freund, T.F., and Buzsaki, G. (1996). Interneurons of the hippocampus. *Hippocampus* 6**,** 347-470. doi: 10.1002/(SICI)1098-1063(1996)6:4<347::AID-HIPO1>3.0.CO;2-I.

Freund, T.F., and Katona, I. (2007). Perisomatic inhibition. *Neuron* 56**,** 33-42. doi: 10.1016/j.neuron.2007.09.012.

Fuchs, E., Zivkovic, A., Cunningham, M., Middleton, S., Lebeau, F., Bannerman, D., Rozov, A., Whittington, M., Traub, R., Rawlins, J., and Monyer, H. (2007). Recruitment of parvalbumin-positive interneurons determines hippocampal function and associated behavior. *Neuron* 53**,** 591-604.

Galanopoulou, A.S. (2010). Mutations affecting GABAergic signaling in seizures and epilepsy. *Pflugers Arch* 460**,** 505-523. doi: 10.1007/s00424-010-0816-2.

Gernert, M., Hamann, M., Bennay, M., Loscher, W., and Richter, A. (2000). Deficit of striatal parvalbumin-reactive GABAergic interneurons and decreased basal ganglia output in a genetic rodent model of idiopathic paroxysmal dystonia. *J Neurosci* 20**,** 7052-7058.

Glausier, J., Fish, K., and Lewis, D. (2014). Altered parvalbumin basket cell inputs in the dorsolateral prefrontal cortex of schizophrenia subjects. *Molecular Psychiatry* 19**,** 30–36.

Glickfeld, L.L., Roberts, J.D., Somogyi, P., and Scanziani, M. (2009). Interneurons hyperpolarize pyramidal cells along their entire somatodendritic axis. *Nat Neurosci* 12**,** 21-23. doi: 10.1038/nn.2230.

Godsil, B.P., Kiss, J.P., Spedding, M., and Jay, T.M. (2013). The hippocampal-prefrontal pathway: the weak link in psychiatric disorders? *Eur Neuropsychopharmacol* 23**,** 1165-1181. doi: 10.1016/j.euroneuro.2012.10.018.

Goetz, R., Dover, K., Laezza, F., Shtraizent, N., Huang, X., Tchetchik, D., Eliseenkova, A.V., Xu, C.F., Neubert, T.A., Ornitz, D.M., Goldfarb, M., and Mohammadi, M. (2009). Crystal structure of a fibroblast growth factor homologous factor (FHF) defines a conserved surface on FHFs for binding and modulation of voltage-gated sodium channels. *J Biol Chem* 284**,** 17883-17896.

Gogolla, N., LeBlanc, J.J., Quast, K.B., Südhof, T.C., Fagiolini, M., and Hensch, T.K. (2009). Common circuit defect of excitatory-inhibitory balance in mouse models of autism. *J Neurodevelop Disord* 1**,** 172–181.

Goldfarb, M. (2005). Fibroblast growth factor homologous factors: evolution, structure, and function. *Cytokine Growth Factor Rev* 16**,** 215-220. doi: 10.1016/j.cytogfr.2005.02.002.

Goldfarb, M., Schoorlemmer, J., Williams, A., Diwakar, S., Wang, Q., Huang, X., Giza, J., Tchetchik, D., Kelley, K., Vega, A., Matthews, G., Rossi, P., Ornitz, D.M., and D'Angelo, E. (2007). Fibroblast growth factor homologous factors control neuronal excitability through modulation of voltage-gated sodium channels. *Neuron* 55**,** 449-463.

Goldstein, J.M., Jerram, M., Abbs, B., Whitfield-Gabrieli, S., and Makris, N. (2010). Sex differences in stress response circuitry activation dependent on female hormonal cycle. *J Neurosci* 30**,** 431-438. doi: 10.1523/JNEUROSCI.3021-09.2010.

Gollan, L., Sabanay, H., Poliak, S., Berglund, E.O., Ranscht, B., and Peles, E. (2002). Retention of a cell adhesion complex at the paranodal junction requires the cytoplasmic region of Caspr. *The Journal of Cell Biology* 157**,** 1247-1256. doi: 10.1083/jcb.200203050.

Gonzalez-Burgos, G., Cho, R.Y., and Lewis, D.A. (2015). Alterations in cortical network oscillations and parvalbumin neurons in schizophrenia. *Biol Psychiatry* 77**,** 1031-1040. doi: 10.1016/j.biopsych.2015.03.010.

Gonzalez-Burgos, G., and Lewis, D.A. (2012). NMDA receptor hypofunction, parvalbumin-positive neurons, and cortical gamma oscillations in schizophrenia. *Schizophr Bull* 38**,** 950-957. doi: 10.1093/schbul/sbs010.

Greco, C.M., Hagerman, R.J., Tassone, F., Chudley, A.E., Del Bigio, M.R., Jacquemont, S., Leehey, M., and Hagerman, P.J. (2002). Neuronal intranuclear inclusions in a new cerebellar tremor/ataxia syndrome among fragile X carriers. *Brain* 125**,** 1760-1771.

Green, M.F. (2007). Stimulating the development of drug treatments to improve cognition in schizophrenia. *Annu Rev Clin Psychol* 3**,** 159-180. doi: 10.1146/annurev.clinpsy.3.022806.091529.

Guidotti, A., Auta, J., Chen, Y., Davis, J.M., Dong, E., Gavin, D.P., Grayson, D.R., Matrisciano, F., Pinna, G., Satta, R., Sharma, R.P., Tremolizzo, L., and Tueting, P. (2011). Epigenetic GABAergic targets in schizophrenia and bipolar disorder. *Neuropharmacology* 60**,** 1007-1016. doi: 10.1016/j.neuropharm.2010.10.021.

Guidotti, A., Auta, J., Davis, J.M., Di-Giorgi-Gerevini, V., Dwivedi, Y., Grayson, D.R., Impagnatiello, F., Pandey, G., Pesold, C., Sharma, R., Uzunov, D., and Costa, E. (2000). Decrease in reelin and glutamic acid decarboxylase67 (GAD67) expression in schizophrenia and bipolar disorder: a postmortem brain study. *Arch Gen Psychiatry* 57**,** 1061-1069.

Gurvich, C., and Rossell, S.L. (2015). Dopamine and cognitive control: sex-by-genotype interactions influence the capacity to switch attention. *Behav Brain Res* 281**,** 96-101. doi: 10.1016/j.bbr.2014.11.045.

Gutzmann, A., Ergul, N., Grossmann, R., Schultz, C., Wahle, P., and Engelhardt, M. (2014). A period of structural plasticity at the axon initial segment in developing visual cortex. *Front Neuroanat* 8**,** 11. doi: 10.3389/fnana.2014.00011.

Hagihara, H., Takao, K., Walton, N.M., Matsumoto, M., and Miyakawa, T. (2013). Immature dentate gyrus: an endophenotype of neuropsychiatric disorders. *Neural Plast* 2013**,** 318596. doi: 10.1155/2013/318596.

Han, J.H., Kushner, S.A., Yiu, A.P., Hsiang, H.L., Buch, T., Waisman, A., Bontempi, B., Neve, R.L., Frankland, P.W., and Josselyn, S.A. (2009). Selective erasure of a fear memory. *Science* 323**,** 1492-1496. doi: 10.1126/science.1164139.

Han, S., ChaoTai, Westenbroek, R.E., FrankH.Yu, Cheah, C.S., Potter, G.B., Rubenstein, J.L., Scheuer, T., Iglesia, H.O.d.l., and Catterall, W.A. (2012). Autistic-like behaviour in Scn1a -/+ mice and rescue by enhanced GABA-mediated neurotransmission. *nature* 489**,** 385-389.

Hashimoto, T., Arion, D., Unger, T., Maldonado-Aviles, J.G., Morris, H.M., Volk, D.W., Mirnics, K., and Lewis, D.A. (2008). Alterations in GABA-related transcriptome in the dorsolateral prefrontal cortex of subjects with schizophrenia. *Mol Psychiatry* 13**,** 147-161.

Hashimoto, T., Bergen, S.E., Nguyen, Q.L., Xu, B., Monteggia, L.M., Pierri, J.N., Sun, Z., Sampson, A.R., and Lewis, D.A. (2005). Relationship of brain-derived neurotrophic factor and its receptor TrkB to altered inhibitory prefrontal circuitry in schizophrenia. *J Neurosci* 25**,** 372-383. doi: 10.1523/JNEUROSCI.4035-04.2005.

Hashimoto, T., Volk, D.W., Eggan, S.M., Mirnics, K., Pierri, J.N., Sun, Z., Sampson, A.R., and Lewis, D.A. (2003). Gene expression deficits in a subclass of GABA neurons in the prefrontal cortex of subjects with schizophrenia. *J Neurosci* 23**,** 6315-6326.

Hedden, T., and Gabrieli, J.D. (2004). Insights into the ageing mind: a view from cognitive neuroscience. *Nat Rev Neurosci* 5**,** 87-96. doi: 10.1038/nrn1323.

Hensch, T.K. (2005). Critical period plasticity in local cortical circuits. *Nat Rev Neurosci* 6**,** 877-888. doi: 10.1038/nrn1787.

Hensch, T.K., Gordon, J.A., Brandon, E.P., McKnight, G.S., Idzerda, R.L., and Stryker, M.P. (1998). Comparison of plasticity in vivo and in vitro in the developing visual cortex of normal and protein kinase A RIbeta-deficient mice. *J Neurosci* 18**,** 2108-2117.

Hill, E.L. (2004). Executive dysfunction in autism. *Trends Cogn Sci* 8**,** 26-32.

Hines, R.M., Hines, D.J., Houston, C.M., Mukherjee, J., Haydon, P.G., Tretter, V., Smart, T.G., and Moss, S.J. (2013). Disrupting the clustering of GABAA receptor alpha2 subunits in the frontal cortex leads to reduced gamma-power and cognitive deficits. *Proc Natl Acad Sci U S A* 110**,** 16628-16633. doi: 10.1073/pnas.1308706110.

Hodgkinson, C.A., Enoch, M.A., Srivastava, V., Cummins-Oman, J.S., Ferrier, C., Iarikova, P., Sankararaman, S., Yamini, G., Yuan, Q., Zhou, Z., Albaugh, B., White, K.V., Shen, P.H., and Goldman, D. (2010). Genome-wide association identifies candidate genes that influence the human electroencephalogram. *Proc Natl Acad Sci U S A* 107**,** 8695-8700. doi: 10.1073/pnas.0908134107.

Hoftman, G.D., Volk, D.W., Bazmi, H.H., Li, S., Sampson, A.R., and Lewis, D.A. (2015). Altered cortical expression of GABA-related genes in schizophrenia: illness progression vs developmental disturbance. *Schizophr Bull* 41**,** 180-191. doi: 10.1093/schbul/sbt178.

Holsen, L.M., Spaeth, S.B., Lee, J.H., Ogden, L.A., Klibanski, A., Whitfield-Gabrieli, S., and Goldstein, J.M. (2011). Stress response circuitry hypoactivation related to hormonal dysfunction in women with major depression. *J Affect Disord* 131**,** 379-387. doi: 10.1016/j.jad.2010.11.024.

Hoon, M., Sinha, R., Okawa, H., Suzuki, S.C., Hirano, A.A., Brecha, N., Rieke, F., and Wong, R.O. (2015). Neurotransmission plays contrasting roles in the maturation of inhibitory synapses on axons and dendrites of retinal bipolar cells. *Proc Natl Acad Sci U S A* 112**,** 12840-12845. doi: 10.1073/pnas.1510483112.

Hsu, W.C., Nenov, M.N., Shavkunov, A., Panova, N., Zhan, M., and Laezza, F. (2015). Identifying a kinase network regulating FGF14:Nav1.6 complex assembly using split-luciferase complementation. *PLoS One* 10**,** e0117246. doi: 10.1371/journal.pone.0117246.

Hsu, W.C., Nilsson, C.L., and Laezza, F. (2014). Role of the axonal initial segment in psychiatric disorders: function, dysfunction, and intervention. *Front Psychiatry* 5**,** 109. doi: 10.3389/fpsyt.2014.00109.

Hu, X.-L., Cheng, X., Cai, L., Tan, G.-H., Xu, L., Feng, X.-Y., Lu, T.-J., Xiong, H., Fei, J., and Xiong, Z.-Q. (2011). Conditional deletion of NRSF in forebrain neurons accelerates epileptogenesis in the kindling model. *Cerebral cortex (New York, N Y : 1991)* 21**,** 2158-2165.

Huang, d.W., Sherman, B.T., and Lempicki, R.A. (2009). Bioinformatics enrichment tools: paths toward the comprehensive functional analysis of large gene lists. *Nucleic Acids Res* 37**,** 1-13. doi: 10.1093/nar/gkn923.

Huang, Y., and Mucke, L. (2012). Alzheimer mechanisms and therapeutic strategies. *Cell* 148**,** 1204-1222. doi: 10.1016/j.cell.2012.02.040.

Huang, Z.J., Kirkwood, A., Pizzorusso, T., Porciatti, V., Morales, B., Bear, M.F., Maffei, L., and Tonegawa, S. (1999). BDNF regulates the maturation of inhibition and the critical period of plasticity in mouse visual cortex. *Cell* 98**,** 739-755.

Hughes, D.I., Boyle, K.A., Kinnon, C.M., Bilsland, C., Quayle, J.A., Callister, R.J., and Graham, B.A. (2013). HCN4 subunit expression in fast-spiking interneurons of the rat spinal cord and hippocampus. *Neuroscience* 237**,** 7-18. doi: 10.1016/j.neuroscience.2013.01.028.

Hunter, A.M., Leuchter, A.F., Power, R.A., Muthen, B., McGrath, P.J., Lewis, C.M., Cook, I.A., Garriock, H.A., McGuffin, P., Uher, R., and Hamilton, S.P. (2013). A genome-wide association study of a sustained pattern of antidepressant response. *J Psychiatr Res* 47**,** 1157-1165. doi: 10.1016/j.jpsychires.2013.05.002.

Insausti, R., and Munoz, M. (2001). Cortical projections of the non-entorhinal hippocampal formation in the cynomolgus monkey (Macaca fascicularis). *Eur J Neurosci* 14**,** 435-451.

Insel, T.R., and Sahakian, B.J. (2012). Drug research: a plan for mental illness. *Nature* 483**,** 269. doi: 10.1038/483269a.

Itoh, N., and Ornitz, D.M. (2004). Evolution of the Fgf and Fgfr gene families. *Trends Genet* 20**,** 563-569. doi: 10.1016/j.tig.2004.08.007.

Iwamoto, K., Bundo, M., and Kato, T. (2005). Altered expression of mitochondria-related genes in postmortem brains of patients with bipolar disorder or schizophrenia, as revealed by large-scale DNA microarray analysis. *Hum Mol Genet* 14**,** 241-253. doi: 10.1093/hmg/ddi022.

James, T.F., Nenov, M.N., Wildburger, N.C., Lichti, C.F., Luisi, J., Vergara, F., Panova-Electronova, N.I., Nilsson, C.L., Rudra, J.S., Green, T.A., Labate, D., and Laezza, F. (2015). The Na1.2 channel is regulated by GSK3. *Biochim Biophys Acta* 1850**,** 832-844. doi: 10.1016/j.bbagen.2015.01.011.

Jenkins, S.M., and Bennett, V. (2001). Ankyrin-G coordinates assembly of the spectrin-based membrane skeleton, voltage-gated sodium channels, and L1 CAMs at Purkinje neuron initial segments. *J Cell Biol* 155**,** 739-746. doi: 10.1083/jcb.200109026.

Jiang, Z., Cowell, R., and Nakazawa, K. (2013). Convergence of genetic and environmental factors on parvalbumin-positive interneurons in schizophrenia. *Front Behav Neurosci* 7.

Jimenez, D., Labate, D., Kakadiaris, I.A., and Papadakis, M. (2014). Improved Automatic Centerline Tracing for Dendritic and Axonal Structures. *Neuroinformatics*. doi: 10.1007/s12021-014-9256-z.

Jinno, S., and Kosaka, T. (2002). Patterns of expression of calcium binding proteins and neuronal nitric oxide synthase in different populations of hippocampal GABAergic neurons in mice. *J Comp Neurol* 449**,** 1-25. doi: 10.1002/cne.10251.

Johnson, M.A., Ables, J.L., and Eisch, A.J. (2009). Cell-intrinsic signals that regulate adult neurogenesis in vivo: insights from inducible approaches. *BMB Rep* 42**,** 245-259.

Jun, H., Mohammed Qasim Hussaini, S., Rigby, M.J., and Jang, M.H. (2012). Functional role of adult hippocampal neurogenesis as a therapeutic strategy for mental disorders. *Neural Plast* 2012**,** 854285. doi: 10.1155/2012/854285.

Jungerius, B.J., Hoogendoorn, M.L., Bakker, S.C., Van't Slot, R., Bardoel, A.F., Ophoff, R.A., Wijmenga, C., Kahn, R.S., and Sinke, R.J. (2008). An association screen of myelin-related genes implicates the chromosome 22q11 PIK4CA gene in schizophrenia. *Mol Psychiatry* 13**,** 1060-1068.

Kalanithi, P.S., Zheng, W., Kataoka, Y., DiFiglia, M., Grantz, H., Saper, C.B., Schwartz, M.L., Leckman, J.F., and Vaccarino, F.M. (2005). Altered parvalbumin-positive neuron distribution in basal ganglia of individuals with Tourette syndrome. *Proc Natl Acad Sci U S A* 102**,** 13307-13312. doi: 10.1073/pnas.0502624102.

Kalume, F., Yu, F.H., Westenbroek, R.E., Scheuer, T., and Catterall, W.A. (2007). Reduced sodium current in Purkinje neurons from Nav1.1 mutant mice: implications for ataxia in

severe myoclonic epilepsy in infancy. *J Neurosci* 27**,** 11065-11074. doi: 10.1523/JNEUROSCI.2162-07.2007.

Kann, O. (2015). The interneuron energy hypothesis: Implications for brain disease. *Neurobiol Dis*. doi: 10.1016/j.nbd.2015.08.005.

Kayakabe, M., Kakizaki, T., Kaneko, R., Sasaki, A., Nakazato, Y., Shibasaki, K., Ishizaki, Y., Saito, H., Suzuki, N., Furuya, N., and Yanagawa, Y. (2014). Motor dysfunction in cerebellar Purkinje cell-specific vesicular GABA transporter knockout mice. *Front Cell Neurosci* 7.

Kim, H., Gibboni, R., Kirkhart, C., and Bao, S. (2013). Impaired critical period plasticity in primary auditory cortex of fragile X model mice. *J Neurosci* 33**,** 15686-15692. doi: 10.1523/JNEUROSCI.3246-12.2013.

Kinney, J., Davis, C., Tabarean, I., Conti, B., Bartfai, T., and Behrens, M. (2006). A specific role for NR2A-containing NMDA receptors in the maintenance of parvalbumin and GAD67 immunoreactivity in cultured interneurons. *J Neurosci* 1**,** 1604-1615.

Klausberger, T., Magill, P.J., Marton, L.F., Roberts, J.D., Cobden, P.M., Buzsaki, G., and Somogyi, P. (2003). Brain-state- and cell-type-specific firing of hippocampal interneurons in vivo. *Nature* 421**,** 844-848. doi: 10.1038/nature01374.

Klausberger, T., and Somogyi, P. (2008). Neuronal diversity and temporal dynamics: the unity of hippocampal circuit operations. *Science* 321**,** 53-57.

Knable, M.B., Barci, B.M., Webster, M.J., Meador-Woodruff, J., Torrey, E.F., and Stanley Neuropathology, C. (2004). Molecular abnormalities of the hippocampus in severe psychiatric illness: postmortem findings from the Stanley Neuropathology Consortium. *Mol Psychiatry* 9**,** 609-620, 544. doi: 10.1038/sj.mp.4001471.

Komada, M., and Soriano, P. (2002). [Beta]IV-spectrin regulates sodium channel clustering through ankyrin-G at axon initial segments and nodes of Ranvier. *J Cell Biol* 156**,** 337-348. doi: 10.1083/jcb.200110003.

Konradi, C., Zimmerman, E.I., Yang, C.K., Lohmann, K.M., Gresch, P., Pantazopoulos, H., Berretta, S., and Heckers, S. (2011). Hippocampal interneurons in bipolar disorder. *Arch Gen Psychiatry* 68**,** 340-350. doi: 10.1001/archgenpsychiatry.2010.175.

Kosaka, T., Katsumaru, H., Hama, K., Wu, J.Y., and Heizmann, C.W. (1987). GABAergic neurons containing the Ca2+-binding protein parvalbumin in the rat hippocampus and dentate gyrus. *Brain Res* 419**,** 119-130.

Krishnan, K., Wang, B.S., Lu, J., Wang, L., Maffei, A., Cang, J., and Huang, Z.J. (2015). MeCP2 regulates the timing of critical period plasticity that shapes functional connectivity in primary visual cortex. *Proc Natl Acad Sci U S A* 112**,** E4782-4791. doi: 10.1073/pnas.1506499112.

Krook-Magnuson, E., Varga, C., Lee, S., and Soltesz, I. (2012). New dimensions of interneuronal specialization unmasked by principal cell heterogeneity. *Trends Neurosci* 35**,** 175-184.

Kuhlman, S.J., and Huang, Z.J. (2008). High-resolution labeling and functional manipulation of specific neuron types in mouse brain by Cre-activated viral gene expression. *PLoS One* 3**,** e2005. doi: 10.1371/journal.pone.0002005.

Kuhlman, S.J., Olivas, N.D., Tring, E., Ikrar, T., Xu, X., and Trachtenberg, J.T. (2013). A disinhibitory microcircuit initiates critical-period plasticity in the visual cortex. *Nature* 501**,** 543-546. doi: 10.1038/nature12485.

Laezza, F., Gerber, B.R., Lou, J.Y., Kozel, M.A., Hartman, H., Craig, A.M., Ornitz, D.M., and Nerbonne, J.M. (2007). The FGF14(F145S) mutation disrupts the interaction of FGF14 with voltage-gated Na+ channels and impairs neuronal excitability. *J Neurosci* 27**,** 12033-12044. doi: 10.1523/JNEUROSCI.2282-07.2007.

Laezza, F., Lampert, A., Kozel, M.A., Gerber, B.R., Rush, A.M., Nerbonne, J.M., Waxman, S.G., Dib-Hajj, S.D., and Ornitz, D.M. (2009). FGF14 N-terminal splice variants differentially modulate Nav1.2 and Nav1.6-encoded sodium channels. *Mol Cell Neurosci* 42**,** 90-101. doi: 10.1016/j.mcn.2009.05.007.

Lavoie, A.M., Tingey, J.J., Harrison, N.L., Pritchett, D.B., and Twyman, R.E. (1997). Activation and deactivation rates of recombinant GABA(A) receptor channels are dependent on alpha-subunit isoform. *Biophys J* 73**,** 2518-2526. doi: 10.1016/S0006-3495(97)78280-8.

Lawrence, J.J., and McBain, C.J. (2003). Interneuron diversity series: containing the detonation--feedforward inhibition in the CA3 hippocampus. *Trends Neurosci* 26**,** 631-640. doi: 10.1016/j.tins.2003.09.007.

Lazarus, M.S., and Huang, Z.J. (2011). Distinct maturation profiles of perisomatic and dendritic targeting GABAergic interneurons in the mouse primary visual cortex during the critical

period of ocular dominance plasticity. *J Neurophysiol* 106**,** 775-787. doi: 10.1152/jn.00729.2010.

Leterrier, C., and Dargent, B. (2014). No Pasaran! Role of the axon initial segment in the regulation of protein transport and the maintenance of axonal identity. *Semin Cell Dev Biol* 27**,** 44-51. doi: 10.1016/j.semcdb.2013.11.001.

Levitan, E.S., Schofield, P.R., Burt, D.R., Rhee, L.M., Wisden, W., Kohler, M., Fujita, N., Rodriguez, H.F., Stephenson, A., Darlison, M.G., and et al. (1988). Structural and functional basis for GABAA receptor heterogeneity. *Nature* 335**,** 76-79. doi: 10.1038/335076a0.

Lewis, D., and Moghaddam, B. (2006). Cognitive dysfunction in schizophrenia: convergence of gamma-aminobutyric acid and glutamate alterations. *Arch Neurol* 63**,** 1372-1376.

Lewis, D., Volk, D., and Hashimoto, T. (2004). Selective alterations in prefrontal cortical GABA neurotransmission in schizophrenia: a novel target for the treatment of working memory dysfunction. *Psychopharmacology* 174**,** 143-150.

Lewis, D.A., Curley, A.A., Glausier, J.R., and Volk, D.W. (2012). Cortical parvalbumin interneurons and cognitive dysfunction in schizophrenia. *Trends Neurosci* 35**,** 57-67.

Lewis, D.A., Hashimoto, T., and Morris, H.M. (2008). Cell and receptor type-specific alterations in markers of GABA neurotransmission in the prefrontal cortex of subjects with schizophrenia. *Neurotox Res* 14**,** 237-248. doi: 10.1007/BF03033813.

Lewis, D.A., Hashimoto, T., and Volk, D.W. (2005). Cortical inhibitory neurons and schizophrenia. *Nat Rev Neurosci* 6**,** 312-324. doi: 10.1038/nrn1648.

Light, G.A., Hsu, J.L., Hsieh, M.H., Meyer-Gomes, K., Sprock, J., Swerdlow, N.R., and Braff, D.L. (2006). Gamma band oscillations reveal neural network cortical coherence dysfunction in schizophrenia patients. *Biol Psychiatry* 60**,** 1231-1240. doi: 10.1016/j.biopsych.2006.03.055.

Lin, D., Boyle, M.P., Dollar, P., Lee, H., Lein, E.S., Perona, P., and Anderson, D.J. (2011). Functional identification of an aggression locus in the mouse hypothalamus. *Nature* 470**,** 221-226. doi: 10.1038/nature09736.

Lionel, A.C., Vaags, A.K., Sato, D., Gazzellone, M.J., Mitchell, E.B., Chen, H.Y., Costain, G., Walker, S., Egger, G., Thiruvahindrapuram, B., Merico, D., Prasad, A., Anagnostou, E.,

Fombonne, E., and Zwaig, L. (2013). Rare exonic deletions implicate the synaptic organizer Gephyrin GPHN in risk for autism schizophrenia and seizures. *Human Molecular Genetics* 22**,** 2055–2066.

Lisman, J.E., Pi, H.J., Zhang, Y., and Otmakhova, N.A. (2010). A thalamo-hippocampal-ventral tegmental area loop may produce the positive feedback that underlies the psychotic break in schizophrenia. *Biol Psychiatry* 68**,** 17-24. doi: 10.1016/j.biopsych.2010.04.007.

Liu, Q.-R., Drgon, T., Johnson, C., Walther, D., Hess, J., and Uhl, G.R. (2006). Addiction molecular genetics: 639,401 SNP whole genome association identifies many "cell adhesion" genes. *American journal of medical genetics Part B, Neuropsychiatric genetics : the official publication of the International Society of Psychiatric Genetics* 141B**,** 918-925.

Liu, Y., and Edwards, R.H. (1997). The role of vesicular transport proteins in synaptic transmission and neural degeneration. *Annu Rev Neurosci* 20**,** 125-156. doi: 10.1146/annurev.neuro.20.1.125.

Lou, J.Y., Laezza, F., Gerber, B.R., Xiao, M., Yamada, K.A., Hartmann, H., Craig, A.M., Nerbonne, J.M., and Ornitz, D.M. (2005). Fibroblast growth factor 14 is an intracellular modulator of voltage-gated sodium channels. *J Physiol* 569**,** 179-193. doi: 10.1113/jphysiol.2005.097220.

Loup, F., Weinmann, O., Yonekawa, Y., Aguzzi, A., Wieser, H.G., and Fritschy, J.M. (1998). A highly sensitive immunofluorescence procedure for analyzing the subcellular distribution of GABAA receptor subunits in the human brain. *J Histochem Cytochem* 46**,** 1129-1139.

Marder, S.R. (2006). The NIMH-MATRICS project for developing cognition-enhancing agents for schizophrenia. *Dialogues Clin Neurosci* 8**,** 109-113.

Marín, O. (2012). Interneuron dysfunction in psychiatric disorders *Nature Reviews Neuroscience* 10**,** 107-120.

Markou, A., Chiamulera, C., Geyer, M.A., Tricklebank, M., and Steckler, T. (2009). Removing obstacles in neuroscience drug discovery: the future path for animal models. *Neuropsychopharmacology* 34**,** 74-89. doi: 10.1038/npp.2008.173.

Mattson, M.P. (2000). Apoptosis in neurodegenerative disorders. *Nat Rev Mol Cell Biol* 1**,** 120-129. doi: 10.1038/35040009.

Mattson, M.P., and Magnus, T. (2006). Ageing and neuronal vulnerability. *Nat Rev Neurosci* 7**,** 278-294. doi: 10.1038/nrn1886.

McGovern-Institute *Brain Disorders: By the Numbers* [Online]. Available: http://mcgovern.mit.edu/brain-disorders/by-the-numbers [Accessed 2-19-2016 2016].

Megan E Tucker, F.M.K.a.L.F.E. (2013). Infant Spinocerebellar Ataxia Type 27: Early Presentation Due To a 13q33.1 Microdeletion Involving the FGF14 Gene. *Journal of Genetic Syndromes & Gene Therapy* 4. doi: 10.4172/2157-7412.10002.

Meisler, M.H., and Kearney, J.A. (2005). Sodium channel mutations in epilepsy and other neurological disorders. *J Clin Invest* 115**,** 2010-2017. doi: 10.1172/JCI25466.

Ming, G.L., and Song, H. (2005). Adult neurogenesis in the mammalian central nervous system. *Annu Rev Neurosci* 28**,** 223-250. doi: 10.1146/annurev.neuro.28.051804.101459.

Misceo, D., Fannemel, M., Baroy, T., Roberto, R., Tvedt, B., Jaeger, T., Bryn, V., Stromme, P., and Frengen, E. (2009). SCA27 caused by a chromosome translocation: further delineation of the phenotype. *Neurogenetics* 10**,** 371-374. doi: 10.1007/s10048-009-0197-x.

Mody, I., and Pearce, R.A. (2004). Diversity of inhibitory neurotransmission through GABA(A) receptors. *Trends Neurosci* 27**,** 569-575. doi: 10.1016/j.tins.2004.07.002.

Morales, B., Choi, S.Y., and Kirkwood, A. (2002). Dark rearing alters the development of GABAergic transmission in visual cortex. *J Neurosci* 22**,** 8084-8090.

Narayan, S., Tang, B., Head, S.R., Gilmartin, T.J., Sutcliffe, J.G., Dean, B., and Thomas, E.A. (2008). Molecular profiles of schizophrenia in the CNS at different stages of illness. *Brain Res* 1239**,** 235-248. doi: 10.1016/j.brainres.2008.08.023.

Need, A.C., Ge, D., Weale, M.E., Maia, J., Feng, S., Heinzen, E.L., Shianna, K.V., Yoon, W., Kasperaviciute, D., Gennarelli, M., Strittmatter, W.J., Bonvicini, C., Rossi, G., Jayathilake, K., Cola, P.A., McEvoy, J.P., Keefe, R.S., Fisher, E.M., St Jean, P.L., Giegling, I., Hartmann, A.M., Moller, H.J., Ruppert, A., Fraser, G., Crombie, C., Middleton, L.T., St Clair, D., Roses, A.D., Muglia, P., Francks, C., Rujescu, D., Meltzer, H.Y., and Goldstein, D.B. (2009). A genome-wide investigation of SNPs and CNVs in schizophrenia. *PLoS Genet* 5**,** e1000373. doi: 10.1371/journal.pgen.1000373.

Nestler, E.J., and Hyman, S.E. (2010). Animal models of neuropsychiatric disorders. *Nat Neurosci* 13**,** 1161-1169. doi: 10.1038/nn.2647.

Neves, G., Cooke, S.F., and Bliss, T.V. (2008). Synaptic plasticity, memory and the hippocampus: a neural network approach to causality. *Nat Rev Neurosci* 9**,** 65-75. doi: 10.1038/nrn2303.

Nicholson, D.A., Yoshida, R., Berry, R.W., Gallagher, M., and Geinisman, Y. (2004). Reduction in size of perforated postsynaptic densities in hippocampal axospinous synapses and age-related spatial learning impairments. *J Neurosci* 24**,** 7648-7653. doi: 10.1523/JNEUROSCI.1725-04.2004.

NIH (2014). "NIMH STRATEGIC PLAN FOR RESEARCH".).

NIMH (2011). *Sex Differences in Brain, Behavior, Mental Health and Mental Disorders* [Online]. National Institute of Mental Health. Available: www.nimh.nih.gov/research-priorities/scientific-meetings/2011/sex-differences-in-brain-behavior-mental-health-and-mental-disorders/index.shtml [Accessed February 28- March 1 2011].

Nissen, S., Liang, S., Shehktman, T., Kelsoe, J.R., Bipolar Genome, S., Greenwood, T.A., Nievergelt, C.M., McKinney, R., Shilling, P.D., Smith, E.N., Schork, N.J., Bloss, C.S., Nurnberger, J.I., Jr., Edenberg, H.J., Foroud, T., Koller, D.L., Gershon, E.S., Liu, C., Badner, J.A., Scheftner, W.A., Lawson, W.B., Nwulia, E.A., Hipolito, M., Coryell, W., Rice, J., Byerley, W., McMahon, F.J., Berrettini, W.H., Potash, J.B., Zandi, P.P., Mahon, P.B., McInnis, M.G., Zollner, S., Zhang, P., Craig, D.W., Szelinger, S., Barrett, T.B., and Schulze, T.G. (2012). Evidence for association of bipolar disorder to haplotypes in the 22q12.3 region near the genes stargazin, IFT27 and parvalbumin. *Am J Med Genet B Neuropsychiatr Genet* 159B**,** 941-950. doi: 10.1002/ajmg.b.32099.

Ogiwara, I., Miyamoto, H., Morita, N., Atapour, N., Mazaki, E., Inoue, I., Takeuchi, T., Itohara, S., Yanagawa, Y., Obata, K., Furuichi, T., Hensch, T.K., and Yamakawa, K. (2007). Nav1.1 localizes to axons of parvalbumin-positive inhibitory interneurons: a circuit basis for epileptic seizures in mice carrying an Scn1a gene mutation. *J Neurosci* 27**,** 5903-5914. doi: 10.1523/JNEUROSCI.5270-06.2007.

Okura, T., and Langa, K.M. (2011). Caregiver burden and neuropsychiatric symptoms in older adults with cognitive impairment: the Aging, Demographics, and Memory Study (ADAMS). *Alzheimer Dis Assoc Disord* 25**,** 116-121. doi: 10.1097/WAD.0b013e318203f208.

Olney, J.W., Newcomer, J.W., and Farber, N.B. (1999). NMDA receptor hypofunction model of schizophrenia. *J Psychiatr Res* 33**,** 523-533.

Olson, H., Shen, Y., Avallone, J., Sheidley, B.R., Pinsky, R., Bergin, A.M., Berry, G.T., Duffy, F.H., Eksioglu, Y., Harris, D.J., Hisama, F.M., Ho, E., Irons, M., Jacobsen, C.M., James,

P., Kothare, S., Khwaja, O., Lipton, J., Loddenkemper, T., Markowitz, J., Maski, K., Megerian, J.T., Neilan, E., Raffalli, P.C., Robbins, M., Roberts, A., Roe, E., Rollins, C., Sahin, M., Sarco, D., Schonwald, A., Smith, S.E., Soul, J., Stoler, J.M., Takeoka, M., Tan, W.-H., Torres, A.R., Tsai, P., Urion, D.K., Weissman, L., Wolff, R., Wu, B.-L., Miller, D.T., and Poduri, A. (2014). Copy number variation plays an important role in clinical epilepsy. *Annals of neurology* 75**,** 943-958.

Ornitz, D.M., and Itoh, N. (2015). The Fibroblast Growth Factor signaling pathway. *Wiley Interdiscip Rev Dev Biol* 4**,** 215-266. doi: 10.1002/wdev.176.

Ouda, L., Burianova, J., and Syka, J. (2012). Age-related changes in calbindin and calretinin immunoreactivity in the central auditory system of the rat. *Exp Gerontol* 47**,** 497-506. doi: 10.1016/j.exger.2012.04.003.

Ouda, L., Druga, R., and Syka, J. (2008). Changes in parvalbumin immunoreactivity with aging in the central auditory system of the rat. *Exp Gerontol* 43**,** 782-789. doi: 10.1016/j.exger.2008.04.001.

Ouda, L., Profant, O., and Syka, J. (2015). Age-related changes in the central auditory system. *Cell Tissue Res* 361**,** 337-358. doi: 10.1007/s00441-014-2107-2.

Panzanelli, P., Gunn, B.G., Schlatter, M.C., Benke, D., Tyagarajan, S.K., Scheiffele, P., Belelli, D., Lambert, J.J., Rudolph, U., and Fritschy, J.-M. (2011). Distinct mechanisms regulate GABAA receptor and gephyrin clustering at perisomatic and axo-axonic synapses on CA1 pyramidal cells *J Physiol* 4959–4980.

Papp, O. (2013). *Excitatory synaptic inputs onto parvalbuminpositive perisomatic region-targeting interneurons in the hippocampus* PhD Thesis János Szenthágotai Doctoral School of Neurosciences Semmelweis University

Pasinelli, P., Houseweart, M.K., Brown, R.H., Jr., and Cleveland, D.W. (2000). Caspase-1 and -3 are sequentially activated in motor neuron death in Cu,Zn superoxide dismutase-mediated familial amyotrophic lateral sclerosis. *Proc Natl Acad Sci U S A* 97**,** 13901-13906. doi: 10.1073/pnas.240305897.

Patrizi, A., Scelfo, B., Viltono, L., Briatore, F., Fukaya, M., Watanabe, M., Strata, P., Varoqueaux, F., Brose, N., Fritschy, J.M., and Sassoe-Pognetto, M. (2008). Synapse formation and clustering of neuroligin-2 in the absence of GABAA receptors. *Proc Natl Acad Sci U S A* 105**,** 13151-13156. doi: 10.1073/pnas.0802390105.

Pelkey, K.A., Barksdale, E., Craig, M.T., Yuan, X., Sukumaran, M., Vargish, G.A., Mitchell, R.M., Wyeth, M.S., Petralia, R.S., Chittajallu, R., Karlsson, R.M., Cameron, H.A., Murata, Y., Colonnese, M.T., Worley, P.F., and McBain, C.J. (2015). Pentraxins coordinate excitatory synapse maturation and circuit integration of parvalbumin interneurons. *Neuron* 85**,** 1257-1272. doi: 10.1016/j.neuron.2015.02.020.

Per Andersen, R.M., David Amaral, Tim Bliss, and John O'Keefe (2006). *The Hippocampus Book.* Oxford University Press.

Porjesz, B., and Rangaswamy, M. (2007). Neurophysiological endophenotypes, CNS disinhibition, and risk for alcohol dependence and related disorders. *ScientificWorldJournal* 7**,** 131-141. doi: 10.1100/tsw.2007.203.

Potter, G.B., Petryniak, M.A., Shevchenko, E., and McKinsey, G.L. (2009). Generation of Cre-transgenic mice using Dlx1/Dlx2 enhancers and their characterization in GABAergic interneurons. *Molecular and Cellular Neuroscience* 40**,** 167–186.

Povysheva, N.V., Zaitsev, A.V., Gonzalez-Burgos, G., and Lewis, D.A. (2013). Electrophysiological heterogeneity of fast-spiking interneurons: chandelier versus basket cells. *PLoS One* 8**,** e70553. doi: 10.1371/journal.pone.0070553.

Pozzi, L., Dorocic, I.P., Wang, X., Carlén, M., and Meletis, K. (2014). Mice Lacking NMDA Receptors in Parvalbumin Neurons Display Normal Depression-Related Behavior and Response to Antidepressant Action of NMDAR Antagonists *PLOS ONE* 9**,** 1-8.

Reiner, A., Shelby, E., Wang, H., Demarch, Z., Deng, Y., Guley, N.H., Hogg, V., Roxburgh, R., Tippett, L.J., Waldvogel, H.J., and Faull, R.L. (2013). Striatal parvalbuminergic neurons are lost in Huntington's disease: implications for dystonia. *Mov Disord* 28**,** 1691-1699. doi: 10.1002/mds.25624.

Reiss, J., Gross-Hardt, S., Christensen, E., Schmidt, P., Mendel, R.R., and Schwarz, G.n. (2001). A Mutation in the Gene for the Neurotransmitter Receptor–Clustering Protein Gephyrin Causes a Novel Form of Molybdenum Cofactor Deficiency. *Am J Hum Genet. Jan* 68**,** 208–213.

Rho, J.M., Sankar, R., and Stafstrom, C.E. (2010). "Epilepsy mechanisms, models, and translational perspectives". (Boca Raton: Taylor & Francis,).

Robbins, T.W. (2011). Cognition: the ultimate brain function. *Neuropsychopharmacology* 36**,** 1-2. doi: 10.1038/npp.2010.171.

Robbins, T.W., Gillan, C.M., Smith, D.G., de Wit, S., and Ersche, K.D. (2012). Neurocognitive endophenotypes of impulsivity and compulsivity: towards dimensional psychiatry. *Trends Cogn Sci* 16**,** 81-91. doi: 10.1016/j.tics.2011.11.009.

Rubinstein, M., Han, S., Tai, C., Westenbroek, R.E., Hunker, A., Scheuer, T., and Catterall, W.A. (2015). Dissecting the phenotypes of Dravet syndrome by gene deletion. *Brain* 138**,** 2219-2233. doi: 10.1093/brain/awv142.

Rubio, S.E., Vega-Flores, G., Martinez, A., Bosch, C., Perez-Mediavilla, A., del Rio, J., Gruart, A., Delgado-Garcia, J.M., Soriano, E., and Pascual, M. (2012). Accelerated aging of the GABAergic septohippocampal pathway and decreased hippocampal rhythms in a mouse model of Alzheimer's disease. *FASEB J* 26**,** 4458-4467. doi: 10.1096/fj.12-208413.

Sabri, M., Kawashima, A., Ai, J., and Macdonald, R.L. (2008). Neuronal and astrocytic apoptosis after subarachnoid hemorrhage: a possible cause for poor prognosis. *Brain Res* 1238**,** 163-171. doi: 10.1016/j.brainres.2008.08.031.

Sahakian, B.J., Bruhl, A.B., Cook, J., Killikelly, C., Savulich, G., Piercy, T., Hafizi, S., Perez, J., Fernandez-Egea, E., Suckling, J., and Jones, P.B. (2015). The impact of neuroscience on society: cognitive enhancement in neuropsychiatric disorders and in healthy people. *Philos Trans R Soc Lond B Biol Sci* 370**,** 20140214. doi: 10.1098/rstb.2014.0214.

Sassoè-Pognetto, M., and Fritschy, J.-M. (2001). gephyrin, a major postsynaptic protein of GABAergic synapses. *European Journal of Neuroscience***,** 2005-2010.

Satoh, Y., Endo, S., Ikeda, T., Yamada, K., Ito, M., Kuroki, M., Hiramoto, T., Imamura, O., Kobayashi, Y., Watanabe, Y., Itohara, S., and Takishima, K. (2007). Extracellular signal-regulated kinase 2 (ERK2) knockdown mice show deficits in long-term memory; ERK2 has a specific function in learning and memory. *J Neurosci* 27**,** 10765-10776. doi: 10.1523/JNEUROSCI.0117-07.2007.

Sauer, J.F., and Bartos, M. (2010). Recruitment of early postnatal parvalbumin-positive hippocampal interneurons by GABAergic excitation. *J Neurosci* 30**,** 110-115. doi: 10.1523/JNEUROSCI.4125-09.2010.

Saunders, A., Granger, A.J., and Sabatini, B.L. (2015). Corelease of acetylcholine and GABA from cholinergic forebrain neurons. *Elife* 4. doi: 10.7554/eLife.06412.

Saunders Iv, J.A. (2012). *NMDA receptor dysfunction and development of translational biomarkers for autism and schizophrenia.* Thesis (Ph D in Bioengineering), University of Pennsylvania.

Sawada, K., Barr, A.M., Nakamura, M., Arima, K., Young, C.E., Dwork, A.J., Falkai, P., Phillips, A.G., and Honer, W.G. (2005). Hippocampal complexin proteins and cognitive dysfunction in schizophrenia. *Arch Gen Psychiatry* 62**,** 263-272. doi: 10.1001/archpsyc.62.3.263.

Sawada, K., Young, C.E., Barr, A.M., Longworth, K., Takahashi, S., Arango, V., Mann, J.J., Dwork, A.J., Falkai, P., Phillips, A.G., and Honer, W.G. (2002). Altered immunoreactivity of complexin protein in prefrontal cortex in severe mental illness. *Mol Psychiatry* 7**,** 484-492. doi: 10.1038/sj.mp.4000978.

Scheff, S.W., Price, D.A., Schmitt, F.A., DeKosky, S.T., and Mufson, E.J. (2007). Synaptic alterations in CA1 in mild Alzheimer disease and mild cognitive impairment. *Neurology* 68**,** 1501-1508. doi: 10.1212/01.wnl.0000260698.46517.8f.

Scholz, J., Broom, D.C., Youn, D.H., Mills, C.D., Kohno, T., Suter, M.R., Moore, K.A., Decosterd, I., Coggeshall, R.E., and Woolf, C.J. (2005). Blocking caspase activity prevents transsynaptic neuronal apoptosis and the loss of inhibition in lamina II of the dorsal horn after peripheral nerve injury. *J Neurosci* 25**,** 7317-7323. doi: 10.1523/JNEUROSCI.1526-05.2005.

Schroll, C., Riemensperger, T., Bucher, D., Ehmer, J., Voller, T., Erbguth, K., Gerber, B., Hendel, T., Nagel, G., Buchner, E., and Fiala, A. (2006). Light-induced activation of distinct modulatory neurons triggers appetitive or aversive learning in Drosophila larvae. *Curr Biol* 16**,** 1741-1747. doi: 10.1016/j.cub.2006.07.023.

Schubert, T., Hoon, M., Euler, T., Lukasiewicz, P.D., and Wong, R.O. (2013). Developmental regulation and activity-dependent maintenance of GABAergic presynaptic inhibition onto rod bipolar cell axonal terminals. *Neuron* 78**,** 124-137. doi: 10.1016/j.neuron.2013.01.037.

Sebe, J.Y., and Baraban, S.C. (2011). The promise of an interneuron-based cell therapy for epilepsy. *Dev Neurobiol* 71**,** 107-117. doi: 10.1002/dneu.20813.

Seney, M.L., Chang, L.C., Oh, H., Wang, X., Tseng, G.C., Lewis, D.A., and Sibille, E. (2013). The Role of Genetic Sex in Affect Regulation and Expression of GABA-Related Genes Across Species. *Front Psychiatry* 4**,** 104. doi: 10.3389/fpsyt.2013.00104.

Seto-Ohshima, A., Emson, P.C., Berchtold, M.W., and Heizmann, C.W. (1989). Localization of parvalbumin mRNA in rat brain by in situ hybridization histochemistry. *Exp Brain Res* 75**,** 653-658.

Shah, A., and Lodge, D.J. (2013). A loss of hippocampal perineuronal nets produces deficits in dopamine system function: relevance to the positive symptoms of schizophrenia. *Transl Psychiatry* 3**,** e215. doi: 10.1038/tp.2012.145.

Shakkottai, V.G., Xiao, M., Xu, L., Wong, M., Nerbonne, J.M., Ornitz, D.M., and Yamada, K.A. (2009). FGF14 regulates the intrinsic excitability of cerebellar Purkinje neurons. *Neurobiol Dis* 33**,** 81-88.

Shavkunov, A., Panova, N., Prasai, A., Veselenak, R., Bourne, N., Stoilova-McPhie, S., and Laezza, F. (2012). Bioluminescence methodology for the detection of protein-protein interactions within the voltage-gated sodium channel macromolecular complex. *Assay Drug Dev Technol* 10**,** 148-160.

Shavkunov, A.S., Wildburger, N.C., Nenov, M.N., James, T.F., Buzhdygan, T.P., Panova-Elektronova, N.I., Green, T.A., Veselenak, R.L., Bourne, N., and Laezza, F. (2013). The fibroblast growth factor 14.voltage-gated sodium channel complex is a new target of glycogen synthase kinase 3 (GSK3). *J Biol Chem* 288**,** 19370-19385. doi: 10.1074/jbc.M112.445924.

Shulman, Y., and Tibbo, P. (2005). GABAergic Deficits in Schizophrenia: Evidence and Implications. *University of Alberta Health Sciences Journal* 2**,** 23-27.

Simerly, R.B. (2002). Wired for reproduction: organization and development of sexually dimorphic circuits in the mammalian forebrain. *Annu Rev Neurosci* 25**,** 507-536. doi: 10.1146/annurev.neuro.25.112701.142745.

Sindi, I., , T., RK, and Dodd, P. (2014). A role for the neurexin-neuroligin complex in Alzheimer's disease. *Neurobiol Aging* 35**,** 746-756.

Smith-Hicks, C.L. (2013). GABAergic dysfunction in pediatric neuro-developmental disorders. *Frontiers in Cellular Neuroscience* 7**,** 269. doi: 10.3389/fncel.2013.00269.

Sohal, V.S., Zhang, F., Yizhar, O., and Deisseroth, K. (2009). Parvalbumin neurons and gamma rhythms enhance cortical circuit performance. *Nature* 459**,** 698-702. doi: 10.1038/nature07991.

Somogyi, P. (1977). A specific 'axo-axonal' interneuron in the visual cortex of the rat. *Brain Res* 136**,** 345-350.

Spencer, J.R., Darbyshire, K.M., Boucher, A.A., Kashem, M.A., Long, L.E., McGregor, I.S., Karl, T., and Arnold, J.C. (2013). Novel molecular changes induced by Nrg1 hypomorphism and Nrg1-cannabinoid interaction in adolescence: a hippocampal proteomic study in mice. *Front Cell Neurosci* 7**,** 15. doi: 10.3389/fncel.2013.00015.

Spiegel, I., Mardinly, A.R., Gabel, H.W., Bazinet, J.E., Couch, C.H., Tzeng, C.P., Harmin, D.A., and Greenberg, M.E. (2014). Npas4 regulates excitatory-inhibitory balance within neural circuits through cell-type-specific gene programs. *Cell* 157**,** 1216-1229. doi: 10.1016/j.cell.2014.03.058.

Sun, J., Sun, J., Ming, G.L., and Song, H. (2011). Epigenetic regulation of neurogenesis in the adult mammalian brain. *Eur J Neurosci* 33**,** 1087-1093. doi: 10.1111/j.1460-9568.2011.07607.x.

Sun, X., Wu, Y., Gu, M., Liu, Z., Ma, Y., Li, J., and Zhang, Y. (2014). Selective filtering defect at the axon initial segment in Alzheimer's disease mouse models. *Proc Natl Acad Sci U S A* 111**,** 14271-14276. doi: 10.1073/pnas.1411837111.

Szabadics, J., Varga, C., Molnar, G., Olah, S., Barzo, P., and Tamas, G. (2006). Excitatory effect of GABAergic axo-axonic cells in cortical microcircuits. *Science* 311**,** 233-235. doi: 10.1126/science.1121325.

Szentagothai, J., and Arbib, M.A. (1974). Conceptual models of neural organization. *Neurosci Res Program Bull* 12**,** 305-510.

Szilagyi, T., Orban-Kis, K., Horvath, E., Metz, J., Pap, Z., and Pavai, Z. (2011). Morphological identification of neuron types in the rat hippocampus. *Rom J Morphol Embryol* 52**,** 15-20.

Taepavarapruk, P., Floresco, S.B., and Phillips, A.G. (2000). Hyperlocomotion and increased dopamine efflux in the rat nucleus accumbens evoked by electrical stimulation of the ventral subiculum: role of ionotropic glutamate and dopamine D1 receptors. *Psychopharmacology (Berl)* 151**,** 242-251.

Taupin, P. (2008). Adult neurogenesis pharmacology in neurological diseases and disorders. *Expert Rev Neurother* 8**,** 311-320. doi: 10.1586/14737175.8.2.311.

Teale, P., Collins, D., Maharajh, K., Rojas, D.C., Kronberg, E., and Reite, M. (2008). Cortical source estimates of gamma band amplitude and phase are different in schizophrenia. *Neuroimage* 42**,** 1481-1489. doi: 10.1016/j.neuroimage.2008.06.020.

Tempia, F., Hoxha, E., Negro, G., Alshammari, M.A., Alshammari, T., Panova-Elektronova, N., and Laezza, F. (2015). Parallel fiber to Purkinje cell synaptic impairment in a mouse model of spinocerebellar ataxia type 27. *Frontiers in Cellular Neuroscience* 9. doi: 10.3389/fncel.2015.00205.

Tepper, J.M., Tecuapetla, F., Koos, T., and Ibanez-Sandoval, O. (2010). Heterogeneity and diversity of striatal GABAergic interneurons. *Front Neuroanat* 4**,** 150. doi: 10.3389/fnana.2010.00150.

Terauchi, A., Johnson-Venkatesh, E.M., Toth, A.B., Javed, D., Sutton, M.A., and Umemori, H. (2010). Distinct FGFs promote differentiation of excitatory and inhibitory synapses. *Nature* 465**,** 783-787. doi: 10.1038/nature09041.

Terwisscha van Scheltinga, A.F., Bakker, S.C., and Kahn, R.S. (2010). Fibroblast growth factors in schizophrenia. *Schizophr Bull* 36**,** 1157-1166. doi: 10.1093/schbul/sbp033.

Thompson Ray, M., Weickert, C.S., Wyatt, E., and Webster, M.J. (2011). Decreased BDNF, trkB-TK+ and GAD67 mRNA expression in the hippocampus of individuals with schizophrenia and mood disorders. *J Psychiatry Neurosci* 36**,** 195-203. doi: 10.1503/jpn.100048.

Ting, A.K., Chen, Y., Wen, L., Yin, D.-M., Shen, C., Tao, Y., Liu, X., Xiong, W.-C., and Mei, L. (2011). Neuregulin 1 Promotes Excitatory Synapse Development and Function in GABAergic Interneurons. *The Journal of Neuroscience* 31**,** 15-25.

Tonnesen, J., Sorensen, A.T., Deisseroth, K., Lundberg, C., and Kokaia, M. (2009). Optogenetic control of epileptiform activity. *Proc Natl Acad Sci U S A* 106**,** 12162-12167. doi: 10.1073/pnas.0901915106.

Torrey, E.F., Barci, B.M., Webster, M.J., Bartko, J.J., Meador-Woodruff, J.H., and Knable, M.B. (2005). Neurochemical markers for schizophrenia, bipolar disorder, and major depression in postmortem brains. *Biol Psychiatry* 57**,** 252-260.

Turner, C.A., Watson, S.J., and Akil, H. (2012). The fibroblast growth factor family: neuromodulation of affective behavior. *Neuron* 76**,** 160-174. doi: 10.1016/j.neuron.2012.08.037.

Tyagarajan, S., and Fritschy, J. (2014). Gephyrin: a master regulator of neuronal function? *Nat Rev Neurosci* 15**,** 141-156.

Tye, K.M., Prakash, R., Kim, S.Y., Fenno, L.E., Grosenick, L., Zarabi, H., Thompson, K.R., Gradinaru, V., Ramakrishnan, C., and Deisseroth, K. (2011). Amygdala circuitry mediating reversible and bidirectional control of anxiety. *Nature* 471**,** 358-362. doi: 10.1038/nature09820.

Uchida, T., Furukawa, T., Iwata, S., Yanagawa, Y., and Fukuda, A. (2014). Selective loss of parvalbumin-positive GABAergic interneurons in the cerebral cortex of maternally stressed Gad1-heterozygous mouse offspring. *Transl Psychiatry*

Van Dam, D., D'Hooge, R., Staufenbiel, M., Van Ginneken, C., Van Meir, F., and De Deyn, P.P. (2003). Age-dependent cognitive decline in the APP23 model precedes amyloid deposition. *Eur J Neurosci* 17**,** 388-396.

Van Raamsdonk, J.M., Pearson, J., Slow, E.J., Hossain, S.M., Leavitt, B.R., and Hayden, M.R. (2005). Cognitive dysfunction precedes neuropathology and motor abnormalities in the YAC128 mouse model of Huntington's disease. *J Neurosci* 25**,** 4169-4180. doi: 10.1523/JNEUROSCI.0590-05.2005.

Van Swieten, J.C., Brusse, E., De Graaf, B.M., Krieger, E., Van De Graaf, R., De Koning, I., Maat-Kievit, A., Leegwater, P., Dooijes, D., Oostra, B.A., and Heutink, P. (2003). A mutation in the fibroblast growth factor 14 gene is associated with autosomal dominant cerebellar ataxia. *Am J Hum Genet* 72**,** 191-199.

Verbeek, E.C., Bakker, I.M., Bevova, M.R., Bochdanovits, Z., Rizzu, P., Sondervan, D., Willemsen, G., de Geus, E.J., Smit, J.H., Penninx, B.W., Boomsma, D.I., Hoogendijk, W.J., and Heutink, P. (2012). A fine-mapping study of 7 top scoring genes from a GWAS for major depressive disorder. *PLoS One* 7**,** e37384.

Verret, L., Mann, E.O., Hang, G.B., Barth, A.M., Cobos, I., Ho, K., Devidze, N., Masliah, E., Kreitzer, A.C., Mody, I., Mucke, L., and Palop, J.J. (2012). Inhibitory interneuron deficit links altered network activity and cognitive dysfunction in Alzheimer model. *Cell* 149**,** 708-721. doi: 10.1016/j.cell.2012.02.046.

Verte, S., Geurts, H.M., Roeyers, H., Oosterlaan, J., and Sergeant, J.A. (2005). Executive functioning in children with autism and Tourette syndrome. *Dev Psychopathol* 17**,** 415-445.

Vicario-Abejon, C., Collin, C., McKay, R.D., and Segal, M. (1998). Neurotrophins induce formation of functional excitatory and inhibitory synapses between cultured hippocampal neurons. *J Neurosci* 18**,** 7256-7271.

Vicario, A., Kisiswa, L., Tann, J.Y., Kelly, C.E., and Ibanez, C.F. (2015). Neuron-type-specific signaling by the p75NTR death receptor is regulated by differential proteolytic cleavage. *J Cell Sci* 128**,** 1507-1517. doi: 10.1242/jcs.161745.

Villeda, S.A., Plambeck, K.E., Middeldorp, J., Castellano, J.M., Mosher, K.I., Luo, J., Smith, L.K., Bieri, G., Lin, K., Berdnik, D., Wabl, R., Udeochu, J., Wheatley, E.G., Zou, B., Simmons, D.A., Xie, X.S., Longo, F.M., and Wyss-Coray, T. (2014). Young blood reverses age-related impairments in cognitive function and synaptic plasticity in mice. *Nat Med* 20**,** 659-663. doi: 10.1038/nm.3569.

Volk, D.W., and Lewis, D.A. (2010). Prefrontal cortical circuits in schizophrenia. *Curr Top Behav Neurosci* 4**,** 485-508.

Volk, D.W., Pierri, J.N., Fritschy, J.M., Auh, S., Sampson, A.R., and Lewis, D.A. (2002). Reciprocal alterations in pre- and postsynaptic inhibitory markers at chandelier cell inputs to pyramidal neurons in schizophrenia. *Cereb Cortex* 12**,** 1063-1070.

Vorstman, J.A., Breetvelt, E.J., Duijff, S.N., Eliez, S., Schneider, M., Jalbrzikowski, M., Armando, M., Vicari, S., Shashi, V., Hooper, S.R., Chow, E.W., Fung, W.L., Butcher, N.J., Young, D.A., McDonald-McGinn, D.M., Vogels, A., van Amelsvoort, T., Gothelf, D., Weinberger, R., Weizman, A., Klaassen, P.W., Koops, S., Kates, W.R., Antshel, K.M., Simon, T.J., Ousley, O.Y., Swillen, A., Gur, R.E., Bearden, C.E., Kahn, R.S., Bassett, A.S., International Consortium on, B., and Behavior in 22q11.2 Deletion, S. (2015). Cognitive decline preceding the onset of psychosis in patients with 22q11.2 deletion syndrome. *JAMA Psychiatry* 72**,** 377-385. doi: 10.1001/jamapsychiatry.2014.2671.

Waltz, J.A., and Gold, J.M. (2007). Probabilistic reversal learning impairments in schizophrenia: further evidence of orbitofrontal dysfunction. *Schizophr Res* 93**,** 296-303. doi: 10.1016/j.schres.2007.03.010.

Wang, A.Y., Lohmann, K.M., Yang, C.K., Zimmerman, E.I., Pantazopoulos, H., Herring, N., Berretta, S., Heckers, S., and Konradi, C. (2011a). Bipolar disorder type 1 and schizophrenia are accompanied by decreased density of parvalbumin- and somatostatin-positive interneurons in the parahippocampal region. *Acta Neuropathol* 122**,** 615-626. doi: 10.1007/s00401-011-0881-4.

Wang, Q., Bardgett, M.E., Wong, M., Wozniak, D.F., Lou, J., McNeil, B.D., Chen, C., Nardi, A., Reid, D.C., Yamada, K., and Ornitz, D.M. (2002). Ataxia and paroxysmal dyskinesia in mice lacking axonally transported FGF14. *Neuron* 35**,** 25-38.

Wang, W., Takashima, S., Segawa, Y., Itoh, M., Shi, X., Hwang, S.K., Nabeshima, K., Takeshita, M., and Hirose, S. (2011b). The developmental changes of Na(v)1.1 and Na(v)1.2 expression in the human hippocampus and temporal lobe. *Brain Res* 1389**,** 61-70. doi: 10.1016/j.brainres.2011.02.083.

Wiesel, T.N., and Hubel, D.H. (1963). SINGLE-CELL RESPONSES IN STRIATE CORTEX OF KITTENS DEPRIVED OF VISION IN ONE EYE. *J Neurophysiol* 26**,** 1003-1017.

Winterer, J. (2012). *Cell-Type-Specific Modulation of a Hippocampal Microcircuit by Serotonin* Dr. med, vorgelegt der Medizinischen Fakultät Charité – Universitätsmedizin Berlin

Woo, N.H., and Lu, B. (2006). Regulation of cortical interneurons by neurotrophins: from development to cognitive disorders. *Neuroscientist* 12**,** 43-56.

Woo, T.U., Walsh, J.P., and Benes, F.M. (2004). Density of glutamic acid decarboxylase 67 messenger RNA-containing neurons that express the N-methyl-D-aspartate receptor subunit NR2A in the anterior cingulate cortex in schizophrenia and bipolar disorder. *Arch Gen Psychiatry* 61**,** 649-657. doi: 10.1001/archpsyc.61.7.649.

Woodruff, A.R., Anderson, S.A., and Yuste, R. (2010). The enigmatic function of chandelier cells. *Front Neurosci* 4**,** 201. doi: 10.3389/fnins.2010.00201.

Wozniak, D.F., Xiao, M., Xu, L., Yamada, K.A., and Ornitz, D.M. (2007). Impaired Spatial Learning and Defective Theta Burst Induced LTP in Mice Lacking Fibroblast Growth Factor 14. *Neurobiol Dis* 1**,** 14-26.

Xiao, M., Xu, L., Laezza, F., Yamada, K., Feng, S., and Ornitz, D.M. (2007). Impaired hippocampal synaptic transmission and plasticity in mice lacking fibroblast growth factor 14. *Mol. Cell. Neurosci.* 34**,** 366- 377.

Yamamoto, J., Suh, J., Takeuchi, D., and Tonegawa, S. (2014). Successful execution of working memory linked to synchronized high-frequency gamma oscillations. *Cell* 157**,** 845-857. doi: 10.1016/j.cell.2014.04.009.

Yamasaki, N., Maekawa, M., Kobayashi, K., Kajii, Y., Maeda, J., Soma, M., Takao, K., Tanda, K., Ohira, K., Toyama, K., Kanzaki, K., Fukunaga, K., Sudo, Y., Ichinose, H., Ikeda, M.,

Iwata, N., Ozaki, N., Suzuki, H., Higuchi, M., Suhara, T., Yuasa, S., and Miyakawa, T. (2008). Alpha-CaMKII deficiency causes immature dentate gyrus, a novel candidate endophenotype of psychiatric disorders. *Molecular Brain* 1**,** 1-21. doi: 10.1186/1756-6606-1-6.

Yan, H., Pablo, J.L., and Pitt, G.S. (2013). FGF14 regulates presynaptic Ca2+ channels and synaptic transmission. *Cell Rep* 4**,** 66-75. doi: 10.1016/j.celrep.2013.06.012.

Yang, Y., Ogawa, Y., Hedstrom, K.L., and Rasband, M.N. (2007). βIV spectrin is recruited to axon initial segments and nodes of Ranvier by ankyrinG. *The Journal of Cell Biology* 176**,** 509-519. doi: 10.1083/jcb.200610128.

Yizhar, O., Fenno, L.E., Prigge, M., Schneider, F., Davidson, T.J., O/'Shea, D.J., Sohal, V.S., Goshen, I., Finkelstein, J., Paz, J.T., Stehfest, K., Fudim, R., Ramakrishnan, C., Huguenard, J.R., Hegemann, P., and Deisseroth, K. (2011). Neocortical excitation/inhibition balance in information processing and social dysfunction. *Nature* 477**,** 171-178. doi: http://www.nature.com/nature/journal/v477/n7363/abs/nature10360.html#supplementary-information.

Yu, F.H., Mantegazza, M., Westenbroek, R.E., Robbins, C.A., Kalume, F., Burton, K.A., Spain, W.J., McKnight, G.S., Scheuer, T., and Catterall, W.A. (2006). Reduced sodium current in GABAergic interneurons in a mouse model of severe myoclonic epilepsy in infancy. *Nat Neurosci* 9**,** 1142-1149. doi: http://www.nature.com/neuro/journal/v9/n9/suppinfo/nn1754_S1.html.

Yu, W., and De Blas, A.L. (2008). Gephyrin expression and clustering affects the size of glutamatergic synaptic contacts. *J Neurochem* 104**,** 830-845. doi: 10.1111/j.1471-4159.2007.05014.x.

Zhang, F., Gradinaru, V., Adamantidis, A.R., Durand, R., Airan, R.D., de Lecea, L., and Deisseroth, K. (2010). Optogenetic interrogation of neural circuits: technology for probing mammalian brain structures. *Nat Protoc* 5**,** 439-456. doi: 10.1038/nprot.2009.226.

Zhang, Z.J., and Reynolds, G.P. (2002). A selective decrease in the relative density of parvalbumin-immunoreactive neurons in the hippocampus in schizophrenia. *Schizophr Res* 55**,** 1-10.

Zierhut, K.C., Grassmann, R., Kaufmann, J., Steiner, J., Bogerts, B., and Schiltz, K. (2013). Hippocampal CA1 deformity is related to symptom severity and antipsychotic dosage in schizophrenia. *Brain* 136**,** 804-814. doi: 10.1093/brain/aws335.

VITA

Tahani Khulaif Alshammari was born on July 18th 1982 in Saudi Arabia. She is the daughter of Khulaif Alshammari and Nouf Alshammari. She obtained a Bachelor Degree in Pharmaceutical Sciences from King Saud University College of Pharmacy in February of 2006. In August 2011 she enrolled in the Pharmacology and Toxicology Graduate Program at the University of Texas Medical Branch Galveston to begin her doctoral research. Tahani received The Society for Neuroscience Trainee Professional Development Award.

EDUCATION

Aug. 2000-Feb. 2006	Bachelor's Degree in Pharmaceutical Sciences, College of Pharmacy, King Saud University, Riyadh, Saudi Arabia.

PUBLICATIONS

1- Tempia, F, Hoxha, E., Negro, G., Alshammari, M., **Alshammari, T.,** Panova-Elektronova, N., Laezza, F. Parallel fiber to Purkinje cell synaptic impairment in a mouse model of spinocerebellar ataxia type 27. *Frontiers in Cellular Neuroscience*, 2015.

2- * Alshammari, M., * **Alshammari, T.,** Nenov, Miroslav N., Scala, Federico, Laezza, F. Fibroblast Growth Factor 14 Modulates the Neurogenesis of Granule Neurons in the Adult Dentate Gyrus. *Molecular Neurobiology*, 2015.

3- * Alshammari, M., * **Alshammari, T.,** Laezza, F. Improved methods for fluorescence microscopy detection of macromolecules at the axon initial segment. *Frontiers in Cellular Neuroscience*, 2016.

4- **Alshammari, T.,** Musaad A. Alshammari, Miroslav N. Nenov, Eriola Hoxha, Marco Cambiaghi, Andrea Marcinno`, Thomas F. James, Pankaj Singh, Demetrio Labate, Jiang Li, Herbert Y. Meltzer, Benedetto Sacchetti, Filippo Tempia, and Fernanda Laezza. (2015). Genetic deletion of fibroblast growth factor 14 recapitulates phenotypic alterations underlying cognitive impairment associated with schizophrenia. *Submitted Translational Psychiatry*, 2015 [in press].

* Equally contributed.